INTERNATIONAL ATOMIC ENERGY AGENCY
UNITED NATIONS EDUCATIONAL, SCIENTIFIC AND CULTURAL ORGANIZATION

INTERNATIONAL CENTRE FOR THEORETICAL PHYSICS
34100 TRIESTE (ITALY) - P.O.B. 586 - MIRAMARE - STRADA COSTIERA 11 - TELEPHONE: 2240-1
CABLE: CENTRATOM - TELEX 460392-1

H4.SMR/285 - 3

WINTER COLLEGE ON
LASER PHYSICS: SEMICONDUCTOR LASERS
AND INTEGRATED OPTICS

(22 February - 11 March 1988)

QUANTUM WELL DEVICES:
STRUCTURES AND APPLICATIONS

A. Christou
Institute of Electronic Sturcture & Laser
Research Centre of Crete
Crete, Greece

OUTLINE

I. III-V SEMICONDUCTOR QUANTUM WELLS AND OPTO-ELECTRONIC DEVICES

1. Molecular Beam Epitaxial Growth
2. Absorption and Electroabsorption in Strained QW
3. Photodiodes: Impact Ionization Phenomena in QW
4. Detectors
5. Guided Wave Devices

II. III-V SEMICONDUCTOR QUANTUM WELLS IN HIGH FREQUENCY DEVICES

1. HEMTs
2. HBTs
3. Reliability Science of QW and HEMTs

6830.05.2

III. THEORETICAL ISSUES IN QUANTUM WELLS FOR HIGH SPEED OPTICAL AND ELECTRONIC DEVICES

1. Optical Devices
2. Electronic Devices
3. Free Carrier Transport in Heterostructures
4. Pseudomorphic Superlattices and Quantum Wells

IV. DEVICE PERFORMANCE OF STRAINED QUANTUM WELLS IN HETEROSTRUCTURE TRANSISTORS

1. Figures of Merit of Device Performance
2. Strained Layer Pseudomorphic Structures

V. DEVICE PERFORMANCE OF PSEUDOMORPHIC FETs AND PHOTODETECTORS

1. Pseudomorphic Devices
2. Photodetectors with Quantum Wells

VI. MOLECULAR BEAM EPITAXIAL GROWTH OF MULTI-QUANTUM WELLS FOR DEVICE APPLICATIONS

1. GROWTH ISSUES
2. MULTI-QUANTUM WELL STRUCTURES

6850.05.5

Contents of Presentation

1. Molecular Beam Epitaxial Growth
   – Perfection of Heterointerfaces
2. Absorption and Electroabsorption in Strained QW
3. Photodiodes: Impact Ionization Phenomena in QW
4. High-Gain Detection Devices
5. Guided-Wave Devices

Electronic Materials and Growth Techniques

Liquid Phase Epitaxy

- Near-Equilibrium Growth
- Very-pure, uncompensated material
- High-resistivity material possible with controlled Fe addition
- Applications -Lasers and Detectors

Molecular Beam Epitaxy

- Far-from-Equilibrium Growth
  -growth occurs by physisorption and chemisorption
- Only very pure GaAs, (AlGa)As has been achieved
- Applications - Heterostructures and MQW Devices
- Integrated Optics - Shadow masking and regrowth possible

THE MOLECULAR BEAM EPITAXY SYSTEM

- BASIC SYSTEM REQUIREMENTS
  - An ultra high vacuum chamber
  - Substrate heater block
  - individually shuttered and liquid nitrogen shrouded molecular beam effusion cells
  - Substrate exchange load lock system
- ADVANTAGES OF MBE
  - Low growth rate
  - Low growth temperature
  - Ability of abrupt cessation or initiation of growth
  - A smoothing of the surface of the growing crystal during growth down to atomic steps
  - Facility for in situ analysis
- SURFACE DIAGNOSTICS
  - Auger Electron Spectroscopy (AES)
  - Reflection High Energy Electron Diffraction (RHEE]
  - Secondary Ion Mass Spectroscopy (SIMS)

Cation	Anion
Impingement from vapor	Impingement
⇓	⇓
Chemisorption	Physisorption
⇓	⇓
Surface evaporation	Surface migration/evaporation
⇓	⇓
Surface migration (in-plane; inter-plane)	Dissociative chemisorption
⇓	⇓
Incorporation	Surface migration/evaporation
	⇓
	Incorporation

Table 1: Conceptual Picture of MBE Growth

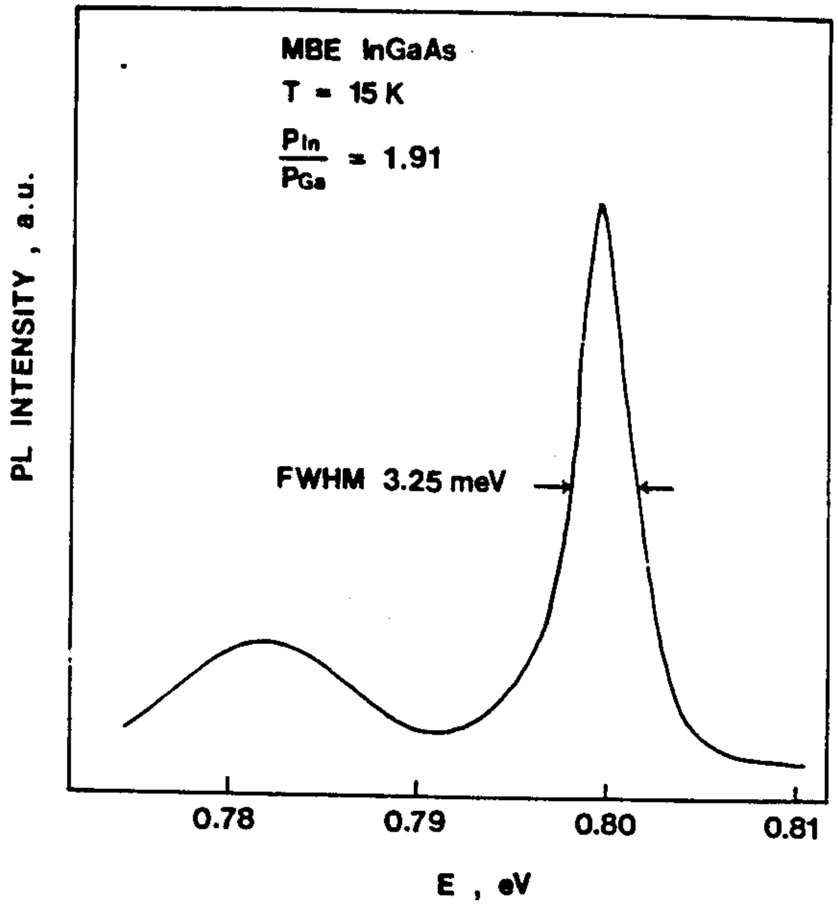

u_{300K} = 10,000 $cm^2/V\cdot s$

n_{300K} = 5E15 cm^{-3}

thickness = 1.5 μm

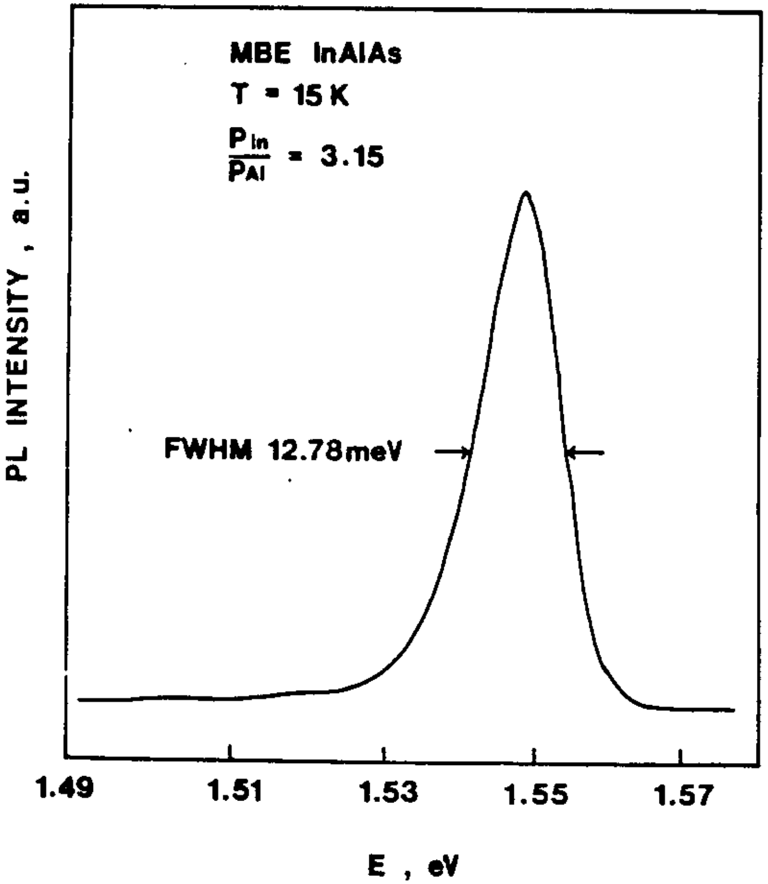

FOR A FIXED GROWTH RATE :

AMORPHOUS HIGH INTRINSIC DEFECTS	FILM WITH ROUGH SURFACE/ INTERFACE	FILM WITH SHARP INTERFACE	BULK DIFF… HIGH DEFE… DENSITY

T_{c1} T_{c2} T_{c3}

FREE ENERGY = U- T.S

KINETICS ⟶ APPROACH TO FREE ENERGY MINIMUM

EXTREMELY KINETICS LIMITED	PARTIALLY KINETICS LIMITED	SUFFICIENT SURFACE KINETICS	ENTROPY CONTROLLED GROWTH

T_{c1} T_{c2} T_{c3}

HETEROSTRUCTURES FROM 'A' AND 'B' SEMICONDUCTORS
TEMPERATURE 'WINDOW' FOR 'A' MUST COINCIDE WITH WINDOW FOR 'B'
---PROBLEMS.

InAlAs/InGaAs SQW

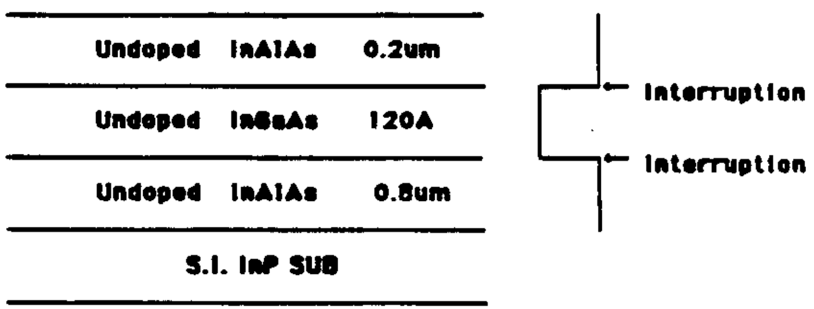

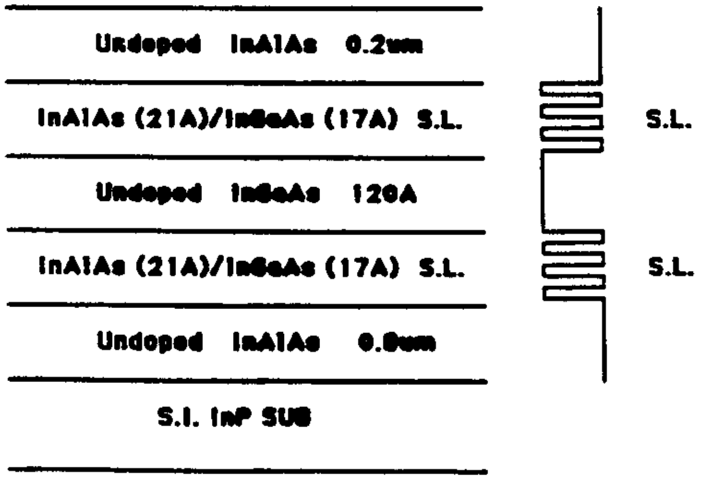

13

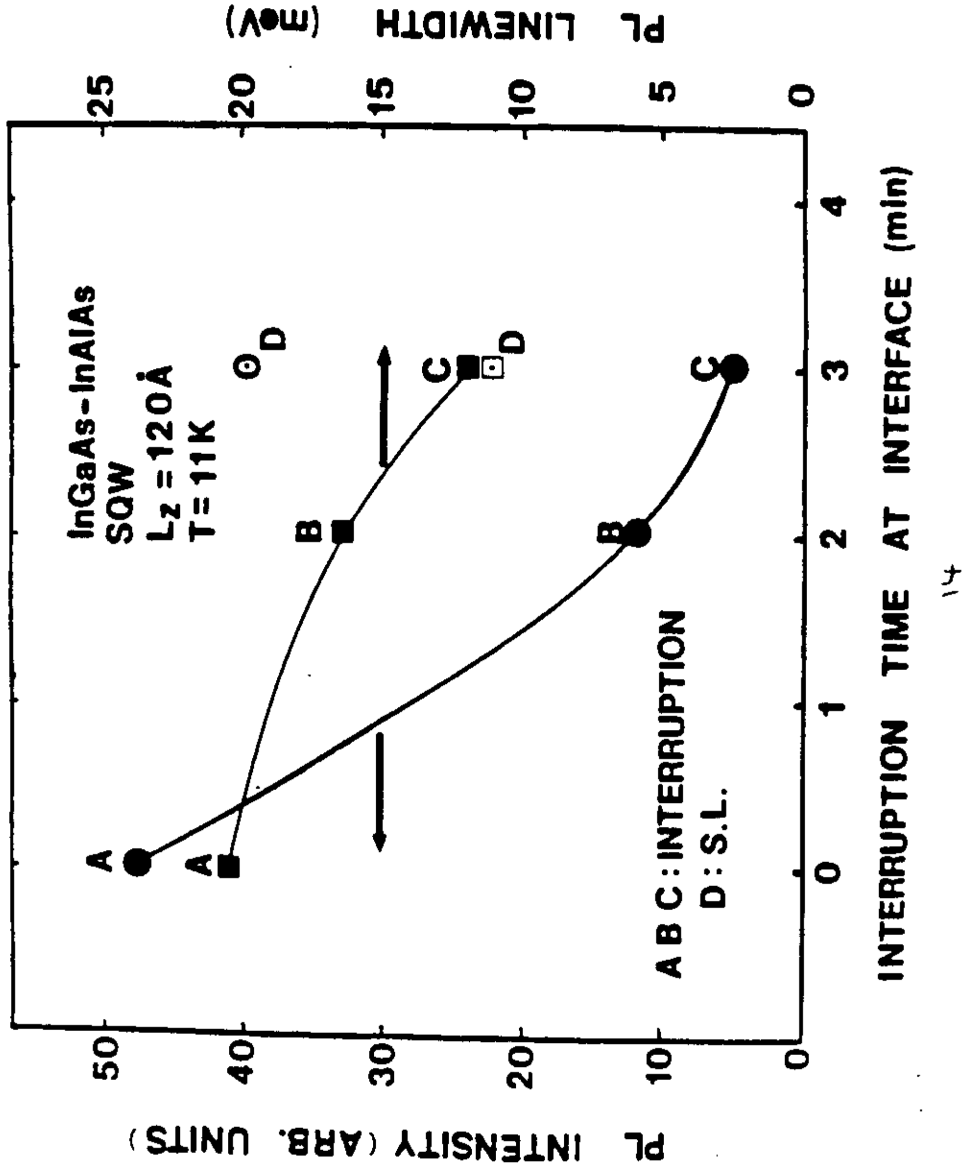

14

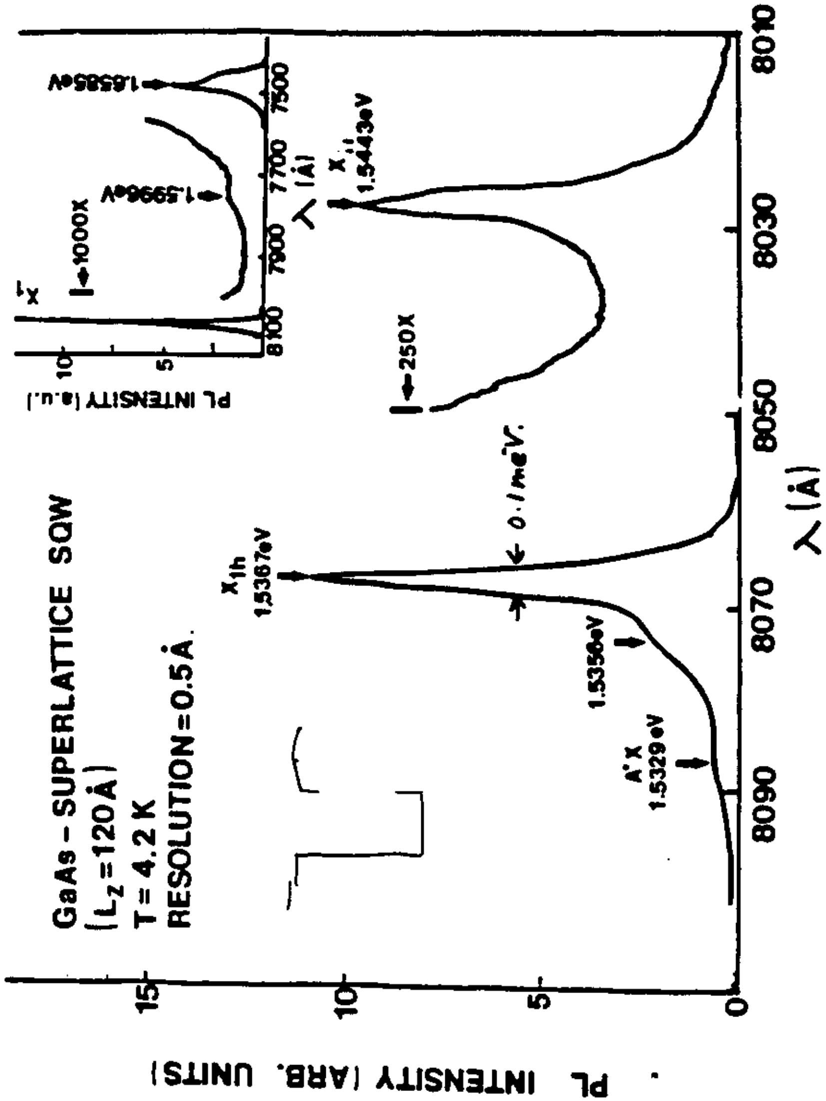

Figure 3 Photoluminescence in 120 Å GaAs single quantum well with superlattice barriers. The superlattice is composed of 30 Å GaAs and 43 Å $Al_{0.3}Ga_{0.7}As$ wells and barriers, respectively

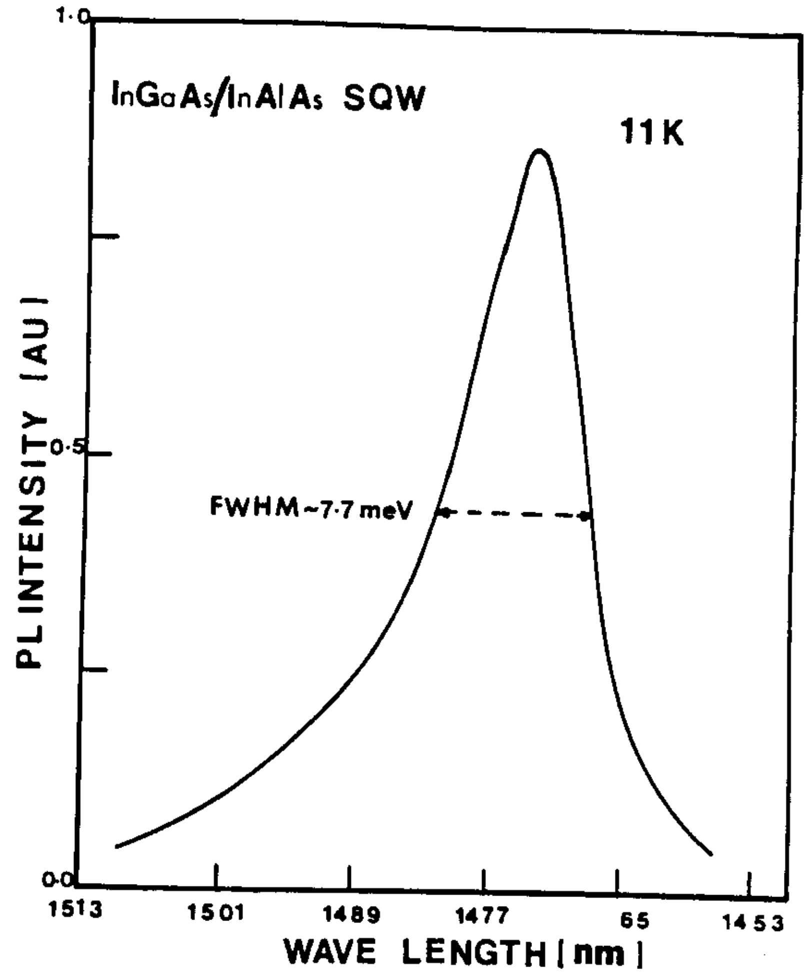

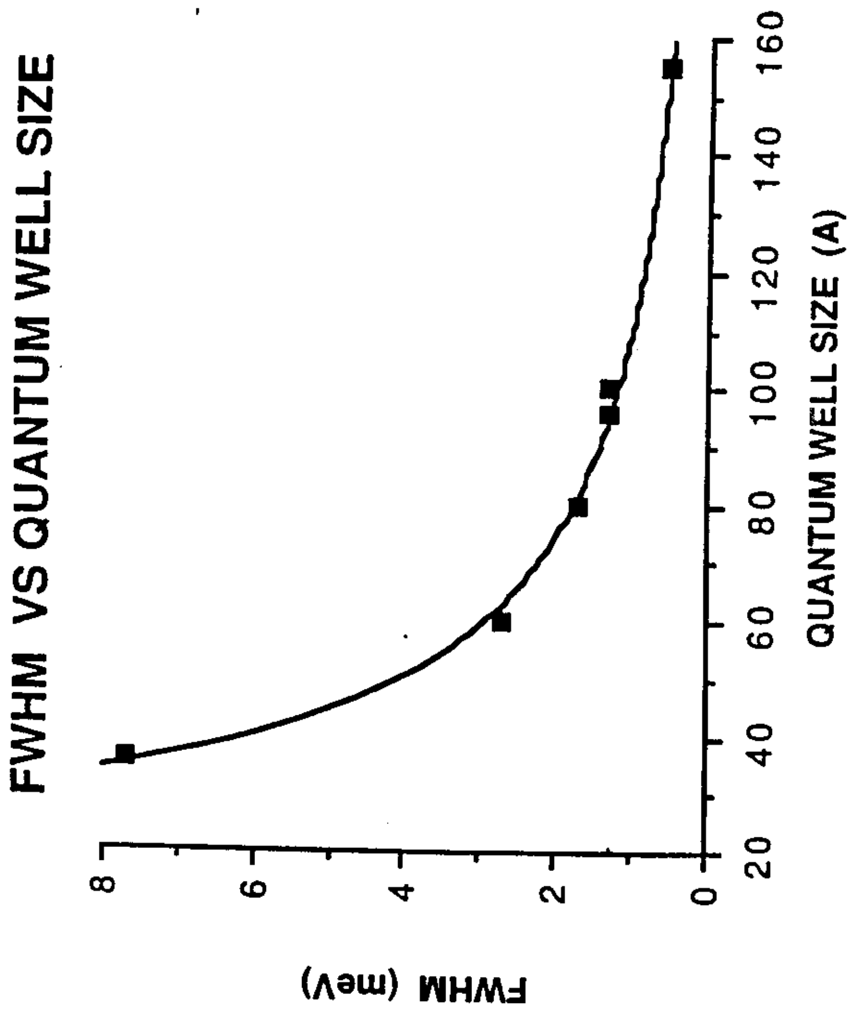

IMPORTANT ISSUES IN OPTICAL MODULATORS;

- **High speed modulation:**
  - **Fast absorption of photons**
  - **Fast extraction of e-h pairs**
    - **Radiative recombination ~ ns**
    - **Tunneling (Field dependent)**
- **High ON/OFF ratio - (Modulation depth):**
  - **Spectral width of incoming light**
  - **Switching fields employed**
  - **Material quality**
- **High temperature operation:**
  - **Strong exciton binding energy**
  - **High quality heterostructures**

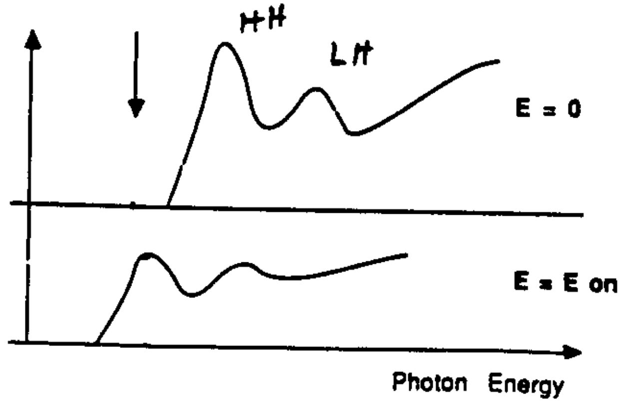

CONTRIBUTIONS TO EXCITON LINEWIDTHS

. Phonon broadening

$$\sigma_{tot} = \sigma_0 + \alpha T + \frac{\beta}{exp(\frac{\hbar\omega_0}{k_B T}) - 1}$$

. Lifetime broadening due to tunneling

- Negligible at low switching fields

(E < 80 kV/cm)

. Lifting of Kramer's Degenerance

(1 - 2 meV > Field dependent)

. Alloy Broadening (InGaAs/InAlAs system)

. Interface roughness

. Well to well size fluctuations in the MQW.

STRAINED QUANTUM WELLS : TENSILE STRAIN

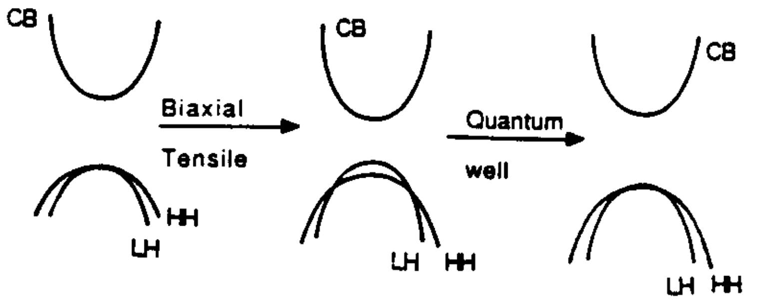

BULK

LH STATE ABOVE HH STATE

DEGENERACY RESTORED

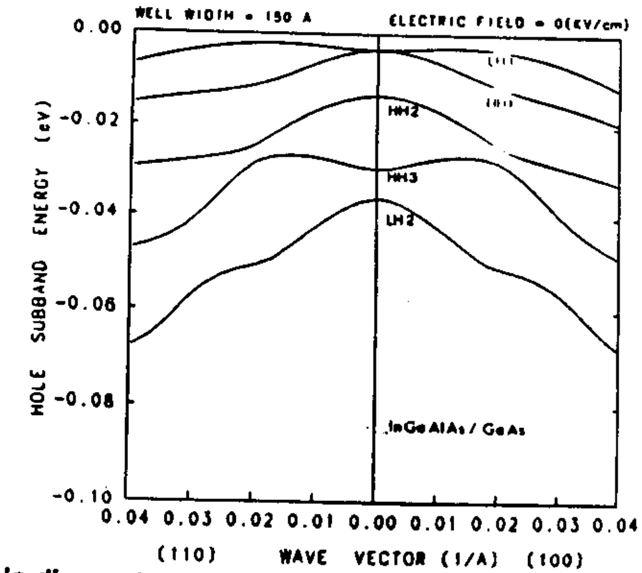

Hole dispersion relation for 150 Å $GaAs/In_{0.06}Ga_{0.57}Al_{0.37}As$ QW with degenerate LH, HH states

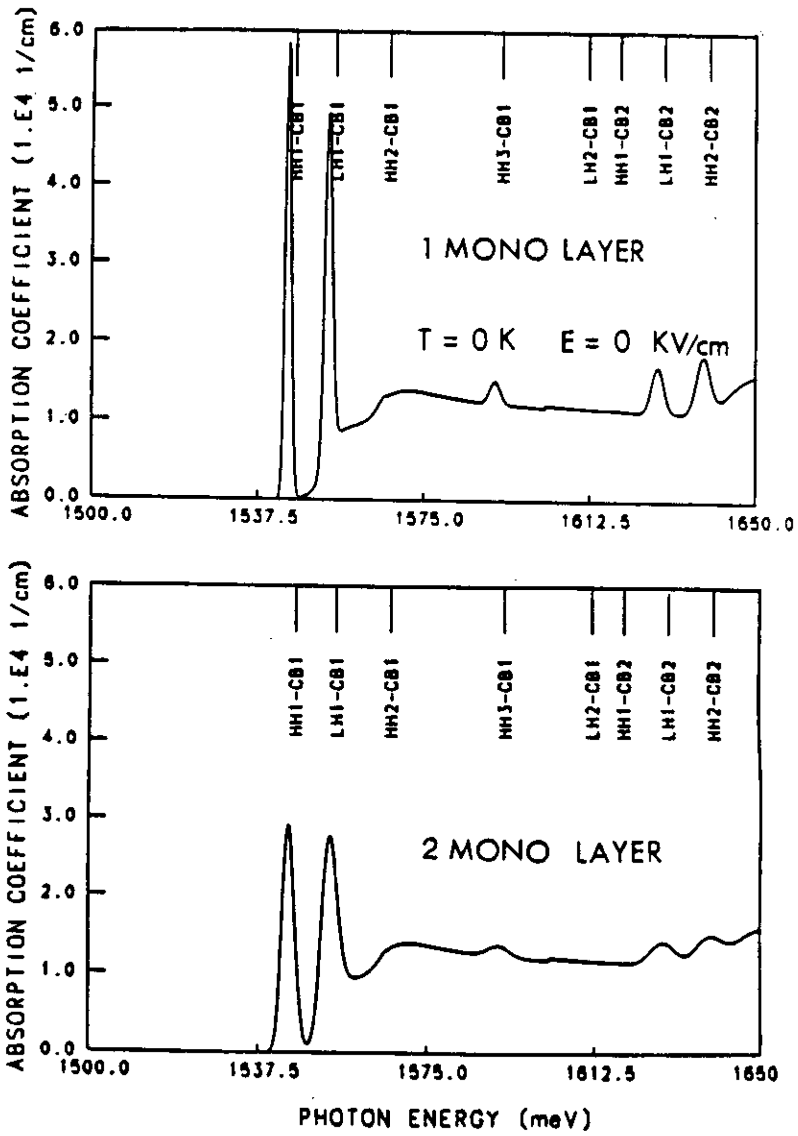

ABSORPTION SPECTRA OF GaAs/$In_{0.06}Ga_{0.57}Al_{0.37}As$

MQW

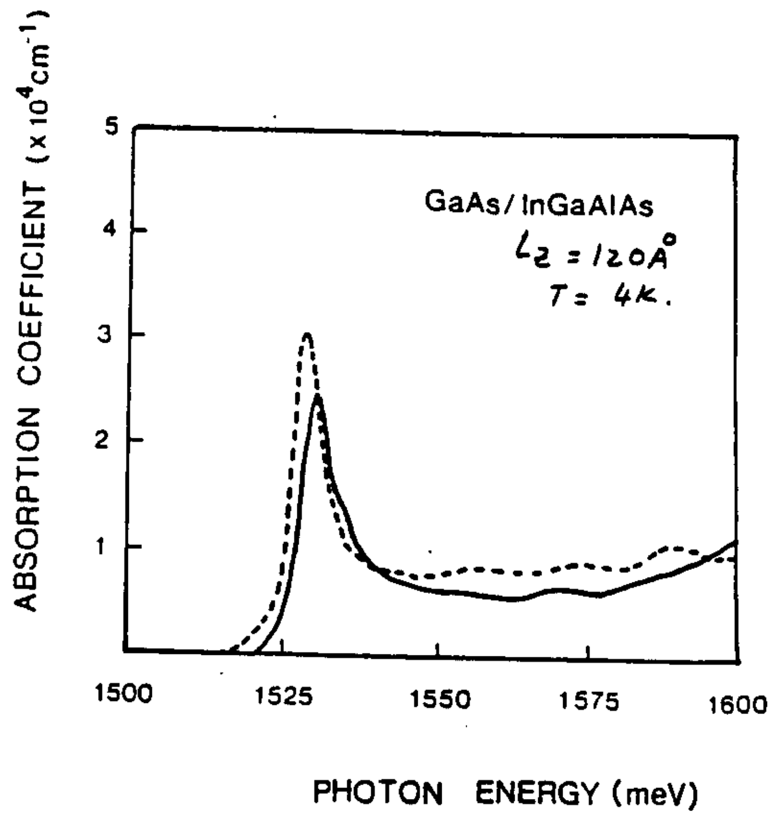

Noise in Photodetectors

Photoconductor

Thermal noise
G-R noise (shot noise)

PIN Diode

Shot noise

Avalanche Photodiode

Shot noise
Avalanche noise

IMPACT IONIZATION COEFFICIENTS IN III-V SEMICONDUCTORS

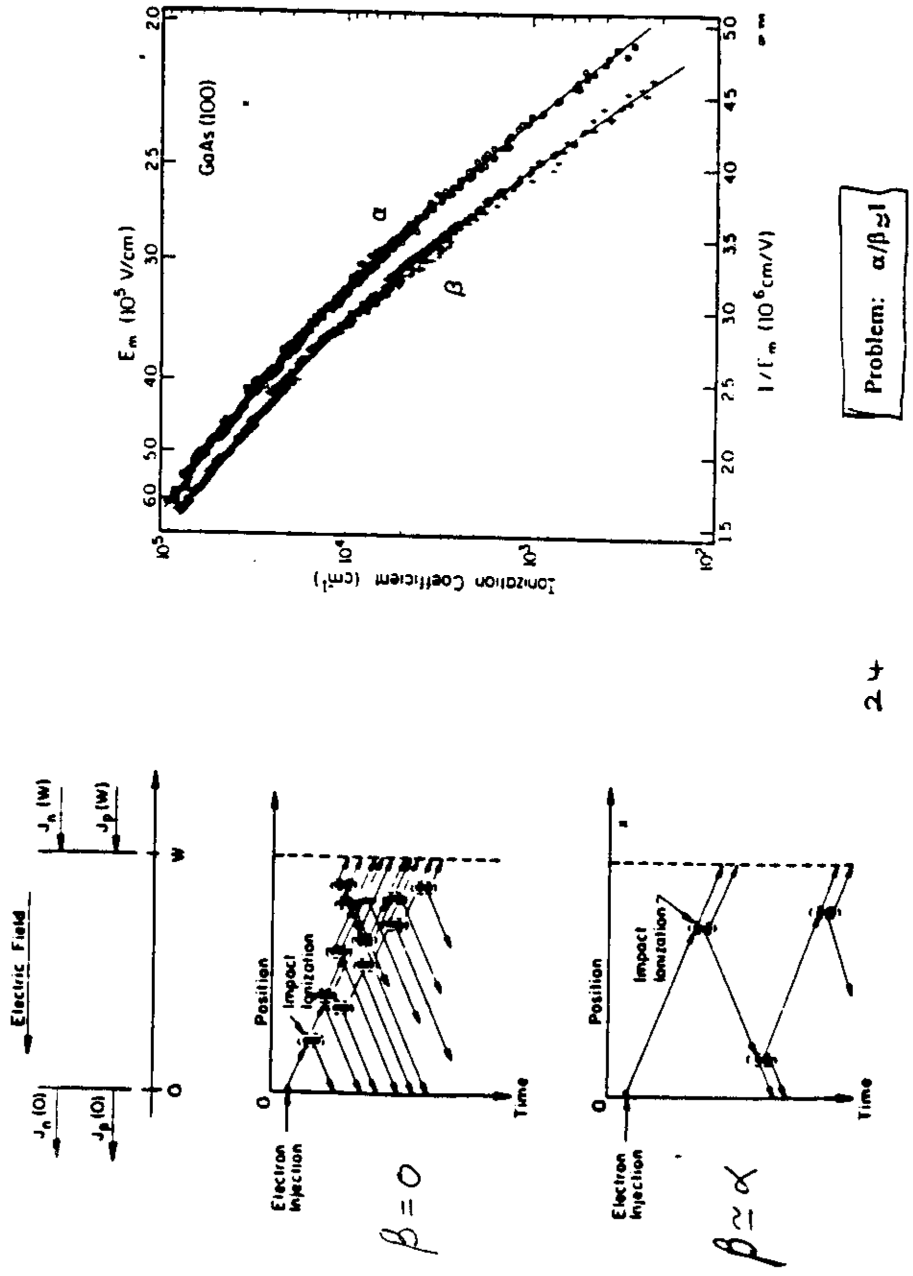

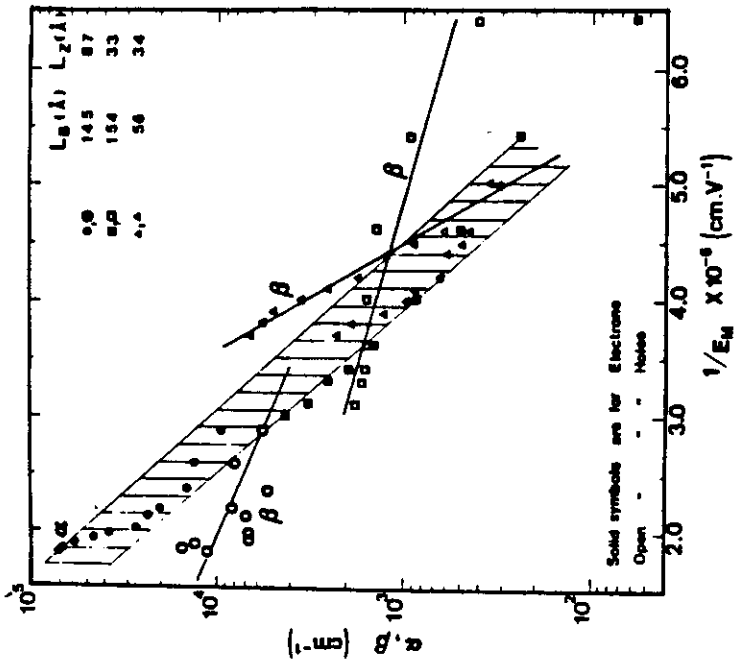

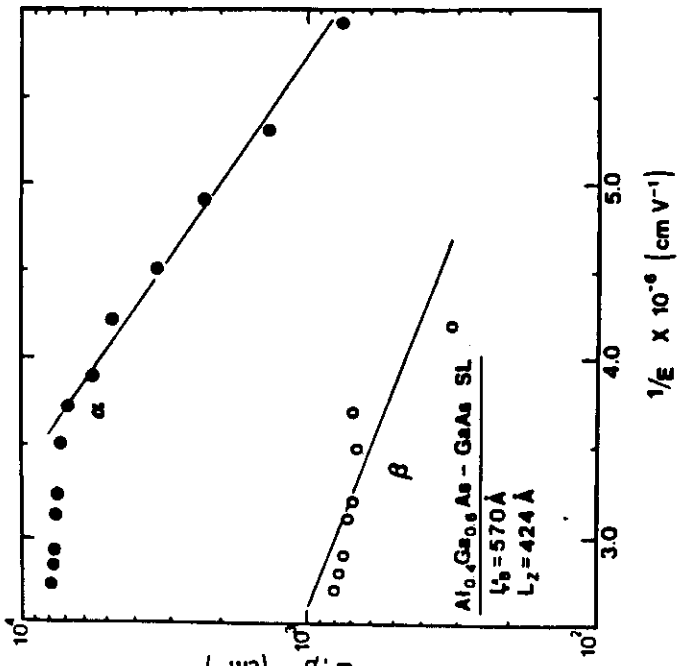

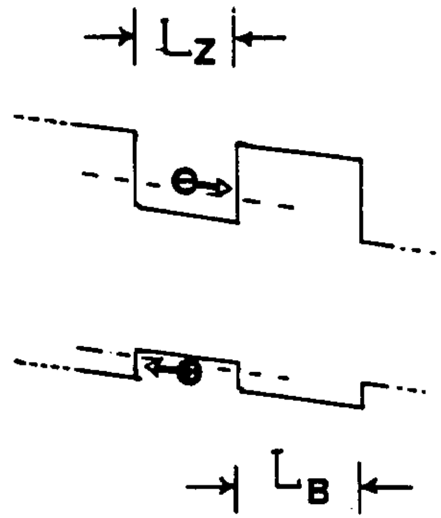

1) Increasing well size increases carrier confinement and scattering, predominantly for holes. Thereby β changes

2) In graded bandgap APD, decrease of β may be due to:

(i) Quasi-field opposing holes.

(ii) Large wells in the GaAs side coupled with small barriers.

3) For very large wells and barriers, β is similar to that in GaAs, α is greatly enhanced.

Key Results from Monte Carlo Simulations:

- High (low) values of $\Delta E_c / \Delta E_v$ can produce high (low) α/β ratio.

- Dispersive barrier can significantly alter the impact ionization rates.

- High α/β (or β/α) ratio can be produced by choosing barriers which are selectively dissipative for holes (or electrons).

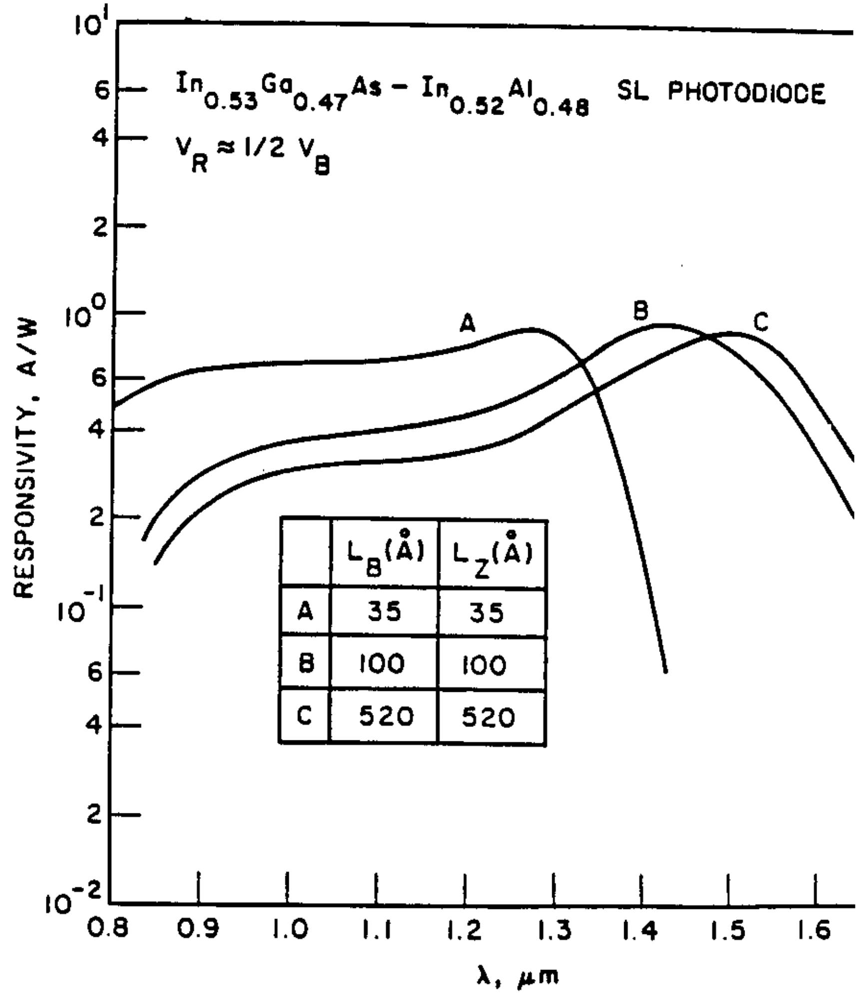

	L_B(Å)	L_Z(Å)
A	35	35
B	100	100
C	520	520

GAIN AND BANDWIDTH OF SL APD

3dB roll-off ~ 12 GHz

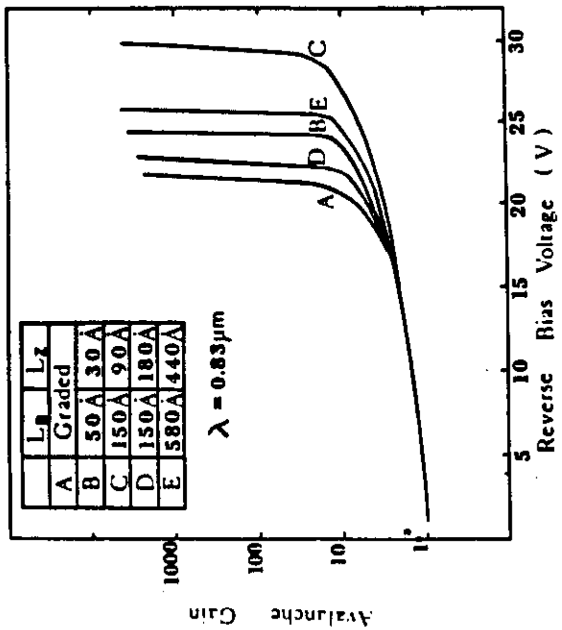

29

InGaAs/InAlAs PIN Detector

50 Å	p^+	GaAs	2 E 18 cm^{-3}
0.3 µm	p^+	$In_{0.52}Al_{0.48}As$	2 E 18 cm^{-3}
0.75 µm	n^-	$In_{0.53}Ga_{0.47}As$	2 E 15 cm^{-3}
0.5 µm	n^+	$In_{0.52}Al_{0.48}As$	2 E 18 cm^{-3}

Fe - doped InP substrate

[a]

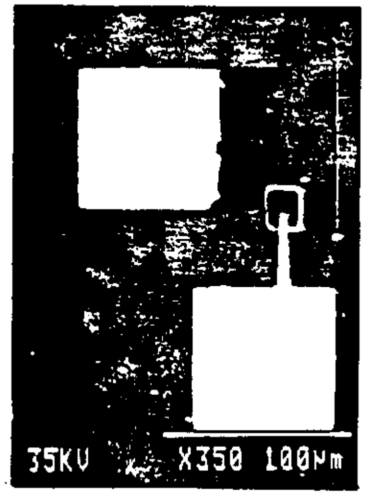

[b]

30

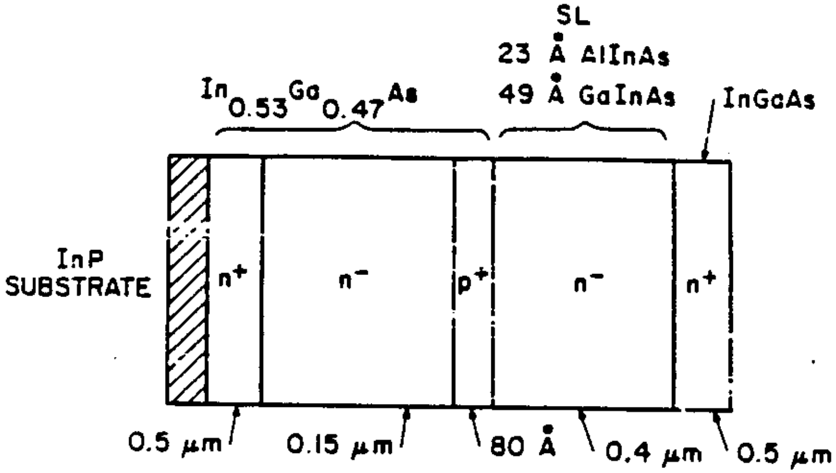

MODULATED-BARRIER EFFECTIVE

MASS FILTER

A NOVEL LOW NOISE, HIGH-GAIN DETECTOR INCORPORATING MASS FILTERING

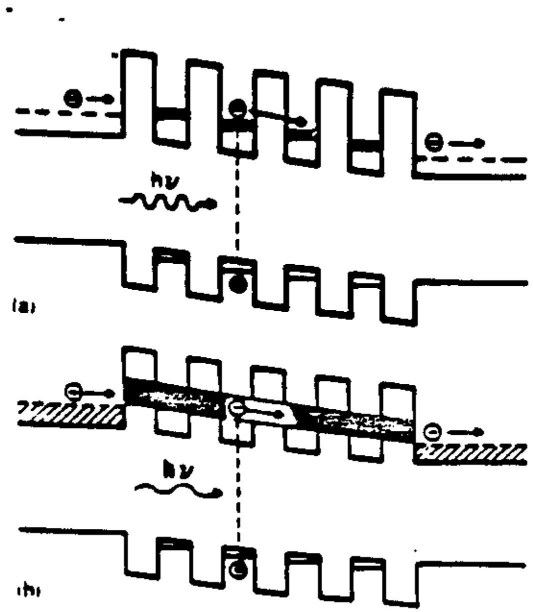

PRINCIPLE OF EMF

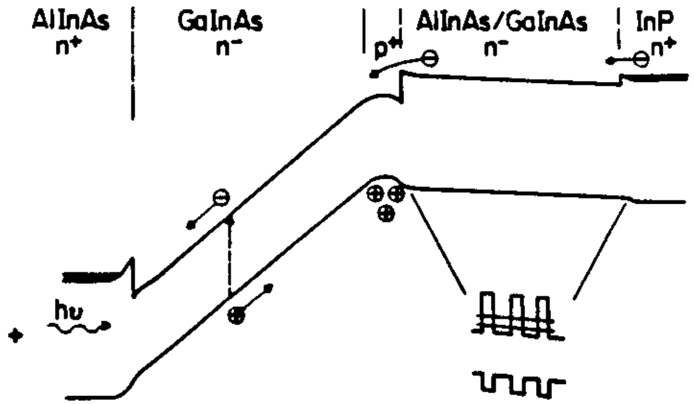

BAND DIAGRAM

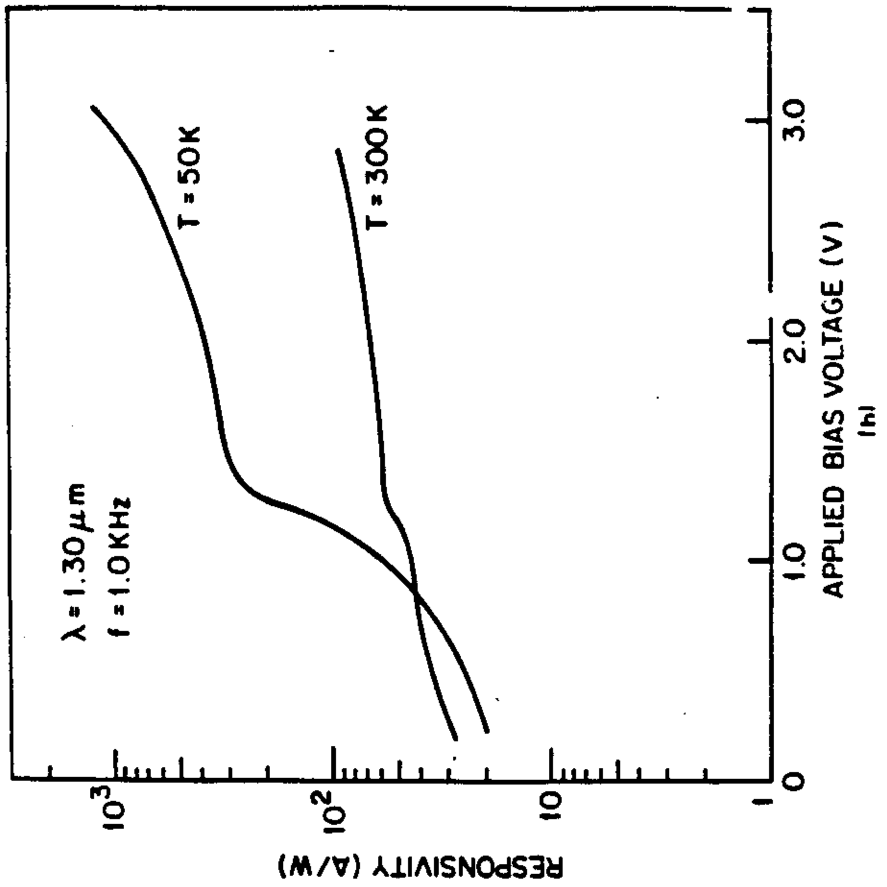

λ = 1.30 μm
f = 1.0 KHz
T = 50K
T = 300K
APPLIED BIAS VOLTAGE (V)
RESPONSIVITY (A/W)
0
1.0
2.0
3.0
1
10
10^2
10^3
(b)

33

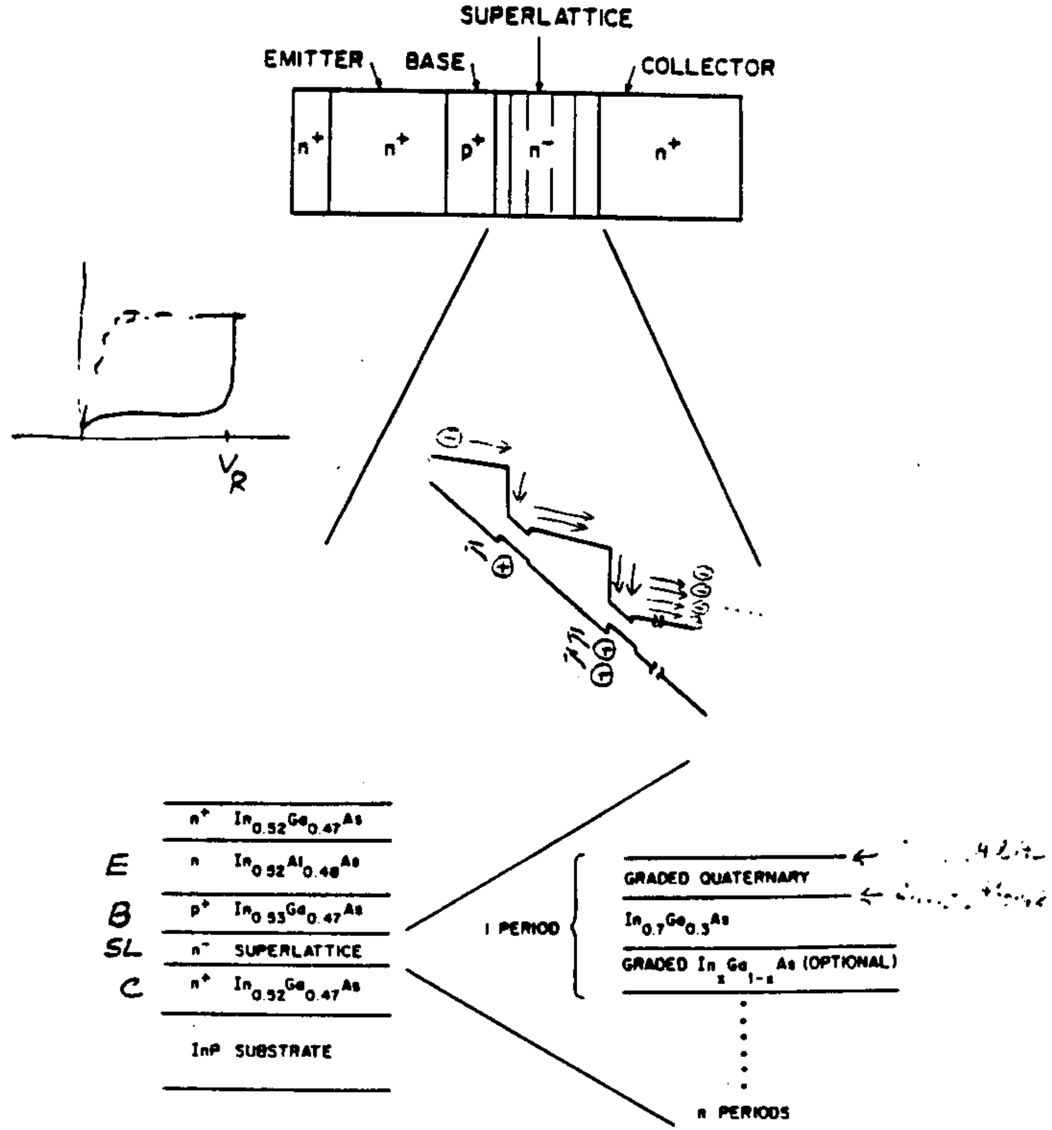

SUPERLATTICE
EMITTER
BASE
COLLECTOR
n+
n+
p+
n-
n+
V_R
E
B
SL
C
n+ In0.52Ga0.47As
n In0.52Al0.48As
p+ In0.53Ga0.47As
n- SUPERLATTICE
n+ In0.52Ga0.47As
InP SUBSTRATE
1 PERIOD
GRADED QUATERNARY
In0.7Ga0.3As
GRADED InxGa1-xAs (OPTIONAL)
n PERIODS

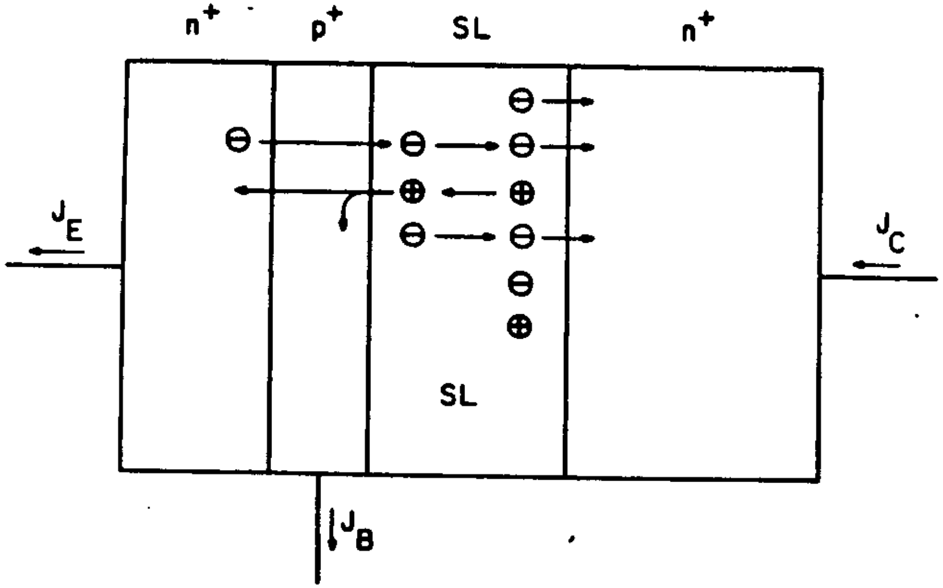

$$\alpha = \alpha_{\cdot} \cdot M_e = \left[1 + \frac{D_{hE} N_A x_B}{D_{eB} N_D x_E}\left(\frac{m^*_{eE} m^*_{hE}}{m^*_{eB} m^*_{hB}}\right)^{3/2} \cdot \exp(-\Delta E_g/kT)\right]\left(1-\frac{x_B^2}{2L_n^2}\right) M_e. \quad (2)$$

$$J_c = q\,\frac{n_{iB}^2 D_{eB}}{N_A x_B}\left(\exp[qV_{BE}/kT]-1\right)M_e \quad (3)$$

where $M_e = (1+\gamma)^N$. The ionization yield γ is given by [7]

$$\gamma = 1 + \left[1 - e^{E_p/kT_e}\left\{\left[1-\left(1-\frac{\sigma_i}{\sigma_T}\right)e^{-E_p/kT_e}\right]^{-1}-1\right\}\right. . \quad (4)$$

Here E_p is the optical phonon energy, T_e is the electron temperature, and

$$\sigma_T = \sigma_i + \sigma_{ph} \quad (5)$$

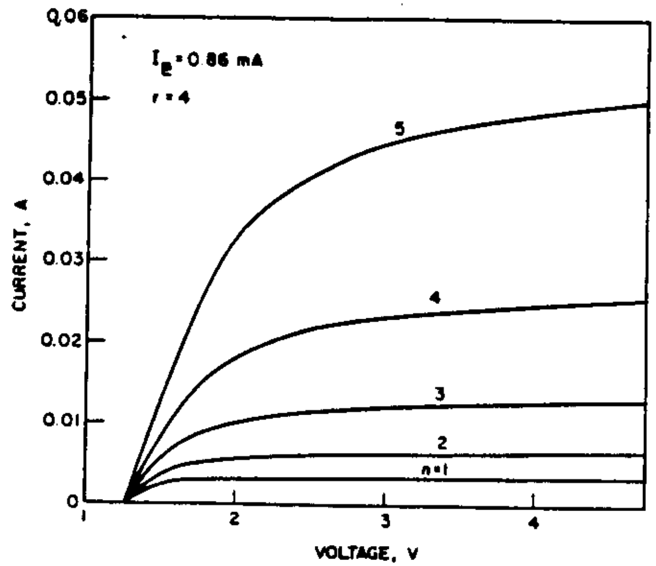

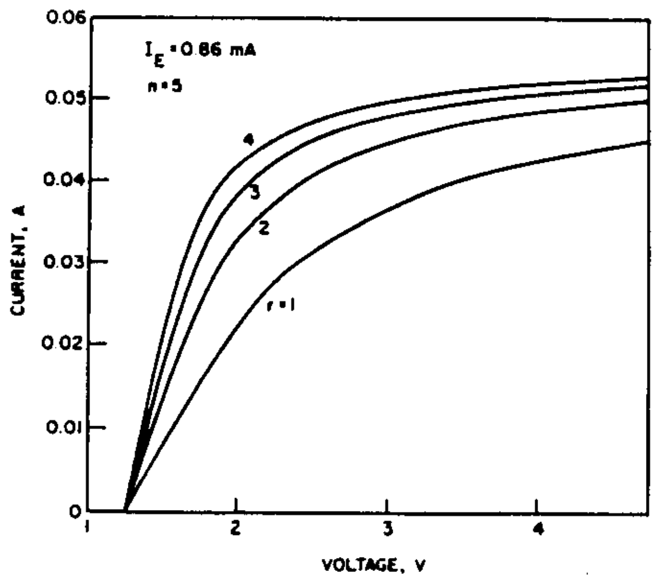

Overview of Device and Circuit Activities

HEMTs

* Large Signal properties and study of **Saturation Mechanisms** for improved device performance
* Multichannel Devices with undoped **i-layer** gates
* Strained **InAlAs/In$_{0.53+x}$ Ga$_{0.47-x}$ As** transistors

HBTs

* **Technology** Development
* Modeling and **Parameter Optimization**
* Experimental **Device Characterization**
* The **Double Base** Transistor

Microwave Monolithic Integrated Circuits

* Heterojuction **Attenuator**
* Heterojunction **Phase Shifter**
* **Passive Component Modeling** at millimeter-wavelengths

LARGE SIGNAL PROPERTIES OF HEMTs

* Understand Saturation Mechanisms
* Estimate the influence of Harmonic Signal Components
* Improve Power Characteristics

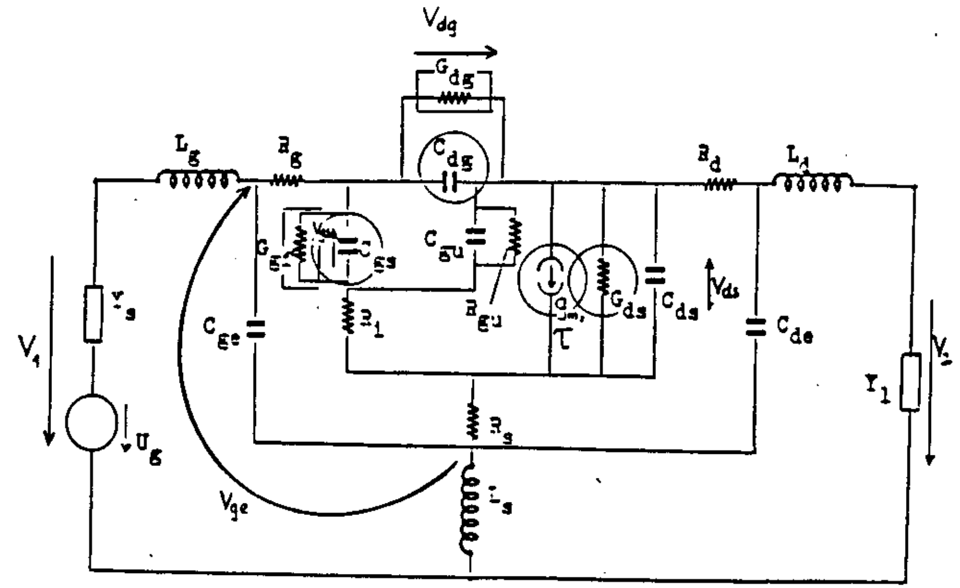

Large-Signal Equivalent Circuit

Improving Power Characteristics using i-layers under the gate

G_{gf} SATURATION MECHANISM

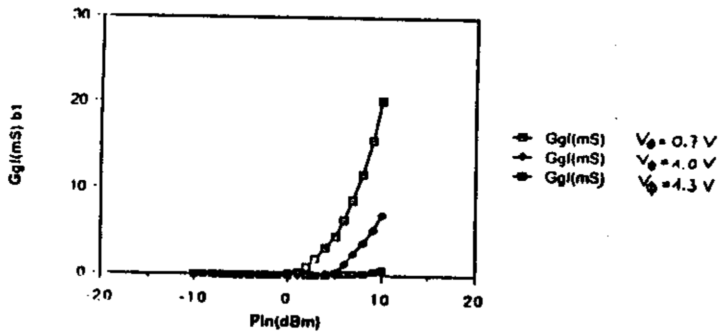

Power Saturation occuring due to Gate-Source forward conduction

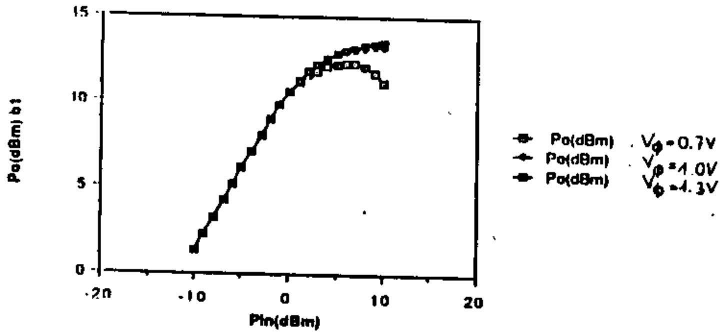

- Larger input power levels are necessary for G_{gf} conduction when i-layer included under the gate.

- Power improves but saturates for $V_T > 1.0V$
  G_{gf} turn-on delayed in i-HEMTs ==> Smaller Operating G_{gf}
  ==> device failure reduction

Increasing Current Density using Double-channel High-Electron Mobility Tansistors

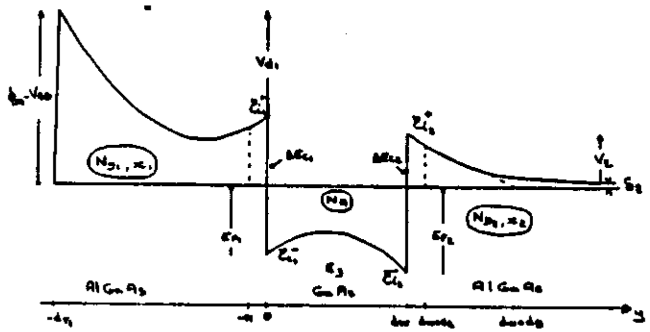

Band diagram used for analytic model

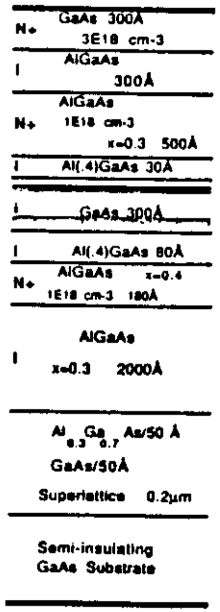

Cross Section of device grown by MBE

I-V Characteristics of 1µm x 75µm HEMT with i-layer under the gate

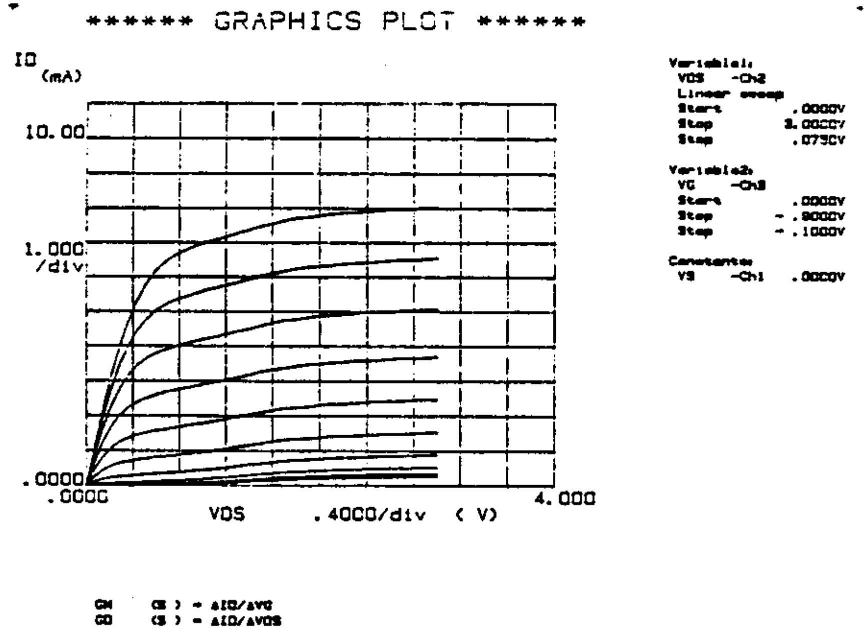

Single Channel

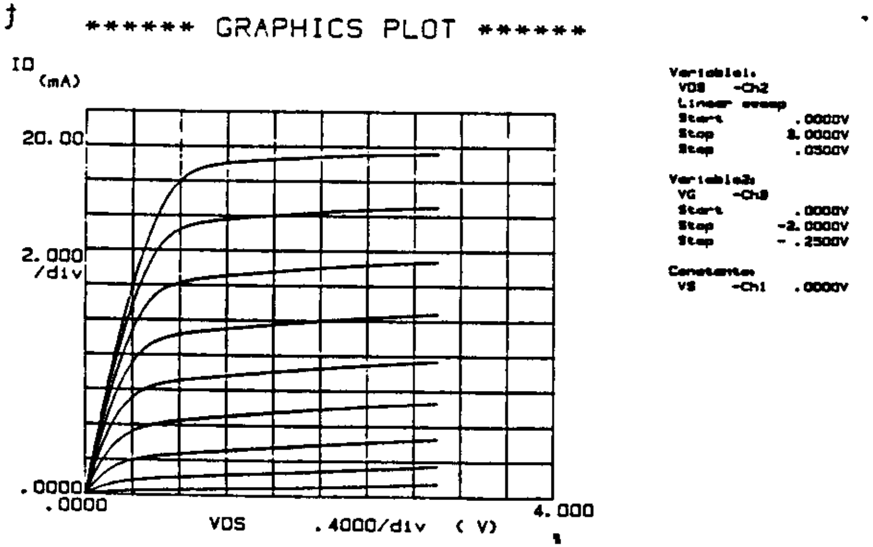

Double Channel

Improving Device Characteristics Using Strained Channels

Motivation of Study :

1. Pseudomorphic AlGaAs/InGaAs/GaAs MODFETs

   - Reduce persistent photoconductivity and uncontrolled threshold-voltage shifts at cryogenic temperature by decreasing Al mole fraction.

   - > 495 mS/mm with 0.25µm devices
     Acceptable measured gain at > 60GHz

2. Strained $In_{0.52}Al_{0.48}As/In_{0.53+x}Ga_{0.47-x}As$ MODFETs

   - High InAs composition and therefore full use of superior InGaAs transport properties.

   - Confinement advantages (large conduction band discontinuity).

Variation of high frequency equivalent circuit parameters of a MODFET in the presence of strain (1.5μmx150μm)

Parameters	In-composition	
	53%	60%
Cgs	0.48 pF	0.53pF
g_m	28.6 mS	48.1 mS
Rds	480 Ω	480 Ω
f_T	9 GHz	14 GHz

Strained InAlAs/InGaAs HEMTs

– Small decrease of electron mass
but
mobility enhancement primarily due to better confinement.

- Mobility enhancement at 16⁰K
  from 36500 $cm^2/V\text{-}s$ with no excess In
  to 55100 $cm^2/V\text{-}s$ with 7% excess In

- No significant Ns variation with strain and thus no important change in C-V characteristics.

- Intrinsic transconductance change of 1.5μm long MODFETs
  from 211 mS/mm lattice matched
  to 348 mS/mm with 7% excess In

- f_T improvement but no substantial microwave gain variation with strain.

– P-channel device study (large mobility improvement by dramatic decrease in hole masses).

Heterojunction Bipolar Transistor(HBT) Studies

Research Subjects

- Establish bipolar transistor fabrication capability
- Study Ion Implantation Compatibility
- Optimize technology for:
  - MBE growth temperature
  - Dopant types
  - Base, Collector Gradients
  - Layer composition
- Study ways of decreasing resistance by
  - Metal - contact systems
  - MBE - contact layers
  - Highly conducting base layers
- Improve electrical characteristics by optimizing operating conditions
- Evaluate novel HBT structures

HBT Device Advantages

- High current drive and power density
- Reproducible threshold voltage (dictated by B-E junction characteristics) ΔV_{be} = 7.6 mV over 3 inch wafer
- No substrate leakage
- High output resistance (Output isolated from input junction(E-B) through base)
- Breakdown voltage controlled by collector layer doping and thickness ($V_{br} \geq$ 15 volts)
- Low 1/f noise and reduced current lagging f_c < 1MHz - only recently obtained by best FETs; but high noise figure (NF=8dB at 35GHz !)
- Easy to integrate with optical devices
- Relaxed (conventional) lithography for mm-wave performance

HBT - EQUIVALENT CIRCUIT and CROSS-SECTION

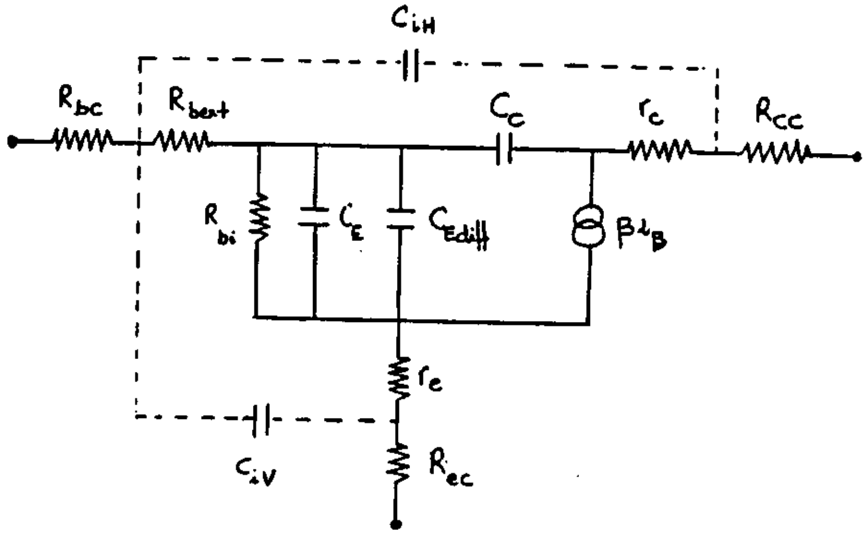

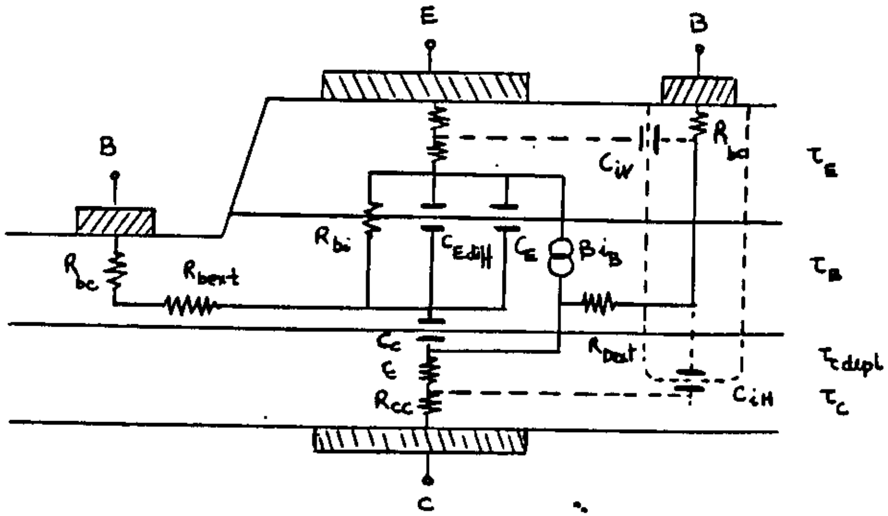

HBT - Device Considerations

$1/2\pi f_T = \tau_{E,C} + \tau_B + \tau_C + \tau_{Cdepl}$ = total emitter-collector transit time (τ_{EC})

66 GHz => 0.6 + 0.8 + 0.3 + 0.7 = 2.5 psecs

$\tau_{E,C} = (r_e + V_{th}/I_C)(C_E + C_{Ediff} + C_C)$

E-series resist.	Junction Intr. (R_{bi})	E-depl. Cap.	E-diff. Cap.	C-depl. Cap.

$V_{th} = kT/q$

$\tau_B = W_B^2/2D_B$ (Assume Fick's law for minority carrier diffusion -- no scattering)

$W_B = W_{bnom} - W_{bE} - W_{bc}$

$C_{Ediff} = \tau_B I_c/V_{th}$

$\tau_C = r_c C_c$

$\tau_{cdepl} = W_C/2vs$

where v_S(scattering limited carrier velocity)$=D_C W_C$

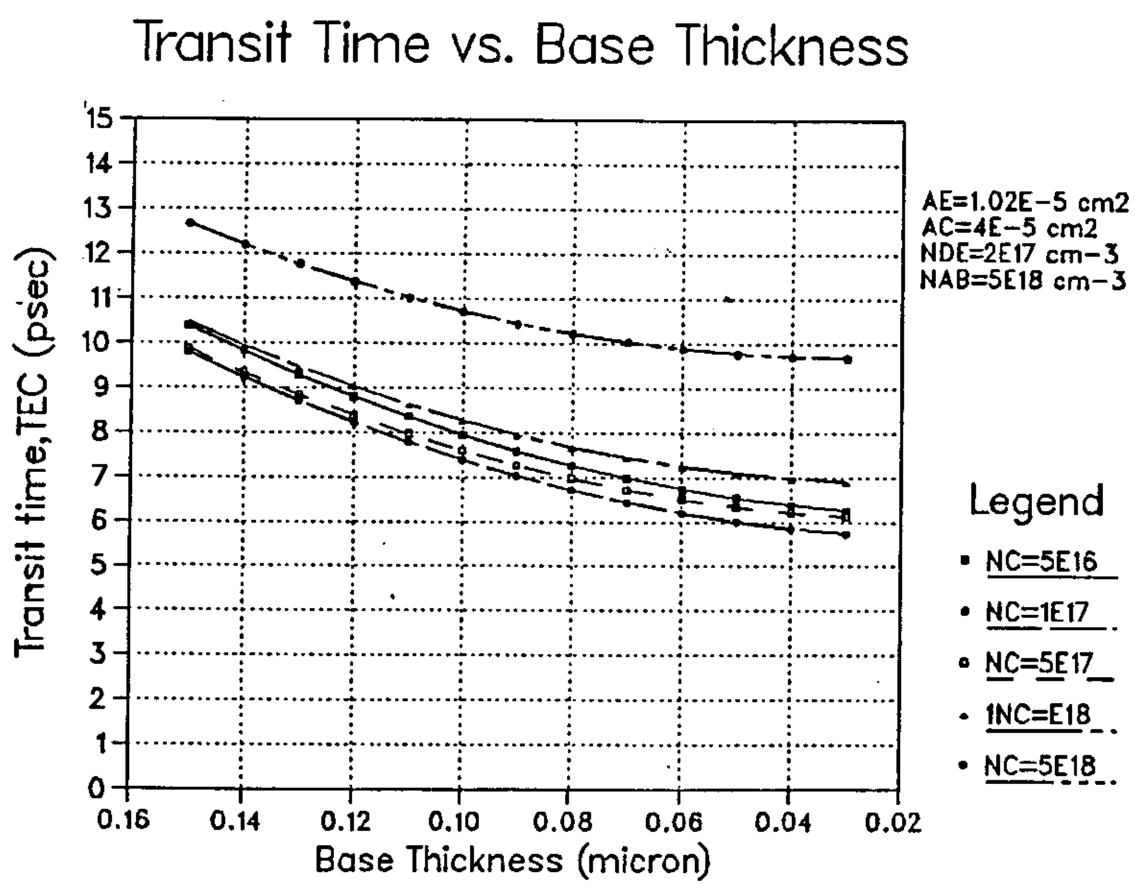
Transit Time vs. Base Thickness
Transit time,TEC (psec)
Base Thickness (micron)
AE=1.02E-5 cm2
AC=4E-5 cm2
NDE=2E17 cm-3
NAB=5E18 cm-3
Legend
NC=5E16
NC=1E17
NC=5E17
1NC=E18
NC=5E18

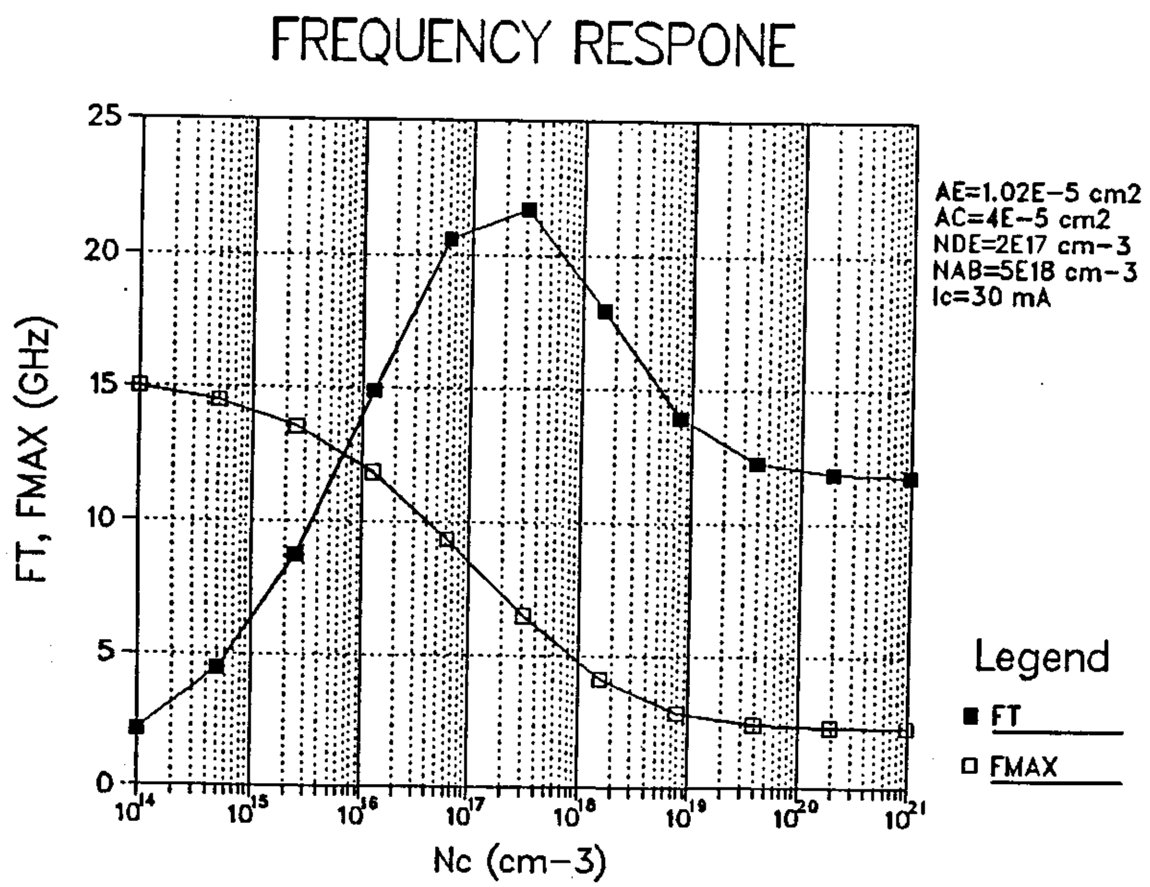
FREQUENCY RESPONE
FT, FMAX (GHz)
Nc (cm-3)
AE=1.02E-5 cm2
AC=4E-5 cm2
NDE=2E17 cm-3
NAB=5E18 cm-3
Ic=30 mA
Legend
FT
FMAX

Ongoing Research

- Comparison MOCVD vs MBE HBT's (spacer need?)
- Ion Implantation for base contacts (Be,Mg,Mg+P,Zn+As)
- Proton Implantation for Collector Capacitance Reduction (lateral - vetical diffusion control)
- Base Grading
- ballistic launchers and base grading
- Collector transit time optimization/velocity overshoot effects
- High frequency characterizations (normal, double-base transistor)
- New structures (Superlattice-base transistor)

RELIABILITY SCIENCE OF MODFET TEST STRUCTURES

GENERIC ISSUES

- CONFINEMENT OF THE HIGH ELECTRON DENSITY TWO DIMENSIONAL ELECTRON GAS

  PHYSICAL PHENOMENON:

  1. CHANGES IN BAND GAP OFFSET ΔE_C DUE TO Al DIFFUSION
  2. CHANGES IN BAND-BENDING AT THE AlGaAs-GaAs INTERFACE
  3. INCREASE IN IMPURITY SCATTERING IN THE 2 DEG-REGION

- GENERATION OF ELECTRON AND HOLE TRAP CENTERS IN THE BULK/HETERO-INTERFACES AND THE MIGRATION OF SUCH TRAPS IN A HIGH TEMPERATURE/RADIATION ENVIRONMENT

  PHYSICAL PHENOMENON:

  1. TRAP ASSISTED TUNNELING
  2. RECOMBINATION — EMISSION PHENOMENON
  3. DEFECT GENERATION (I.E., DISLOCATIONS AND VACANCIES)

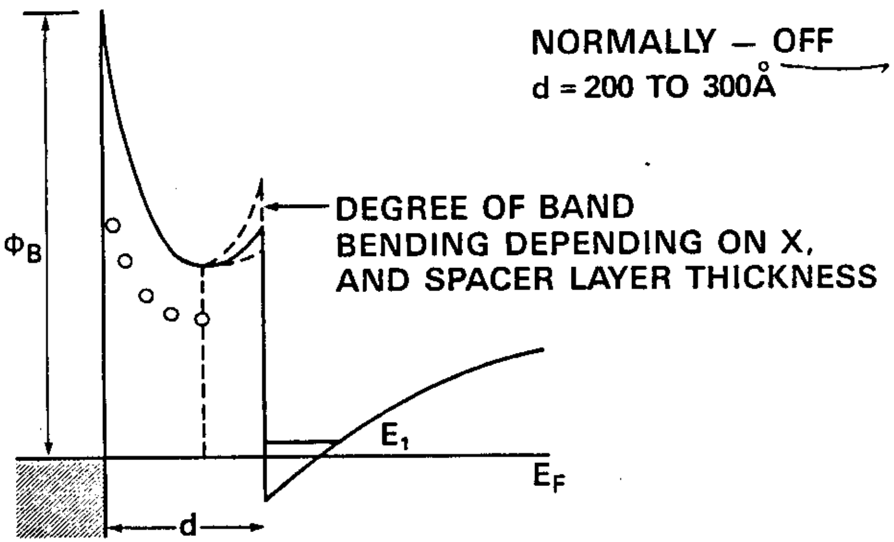

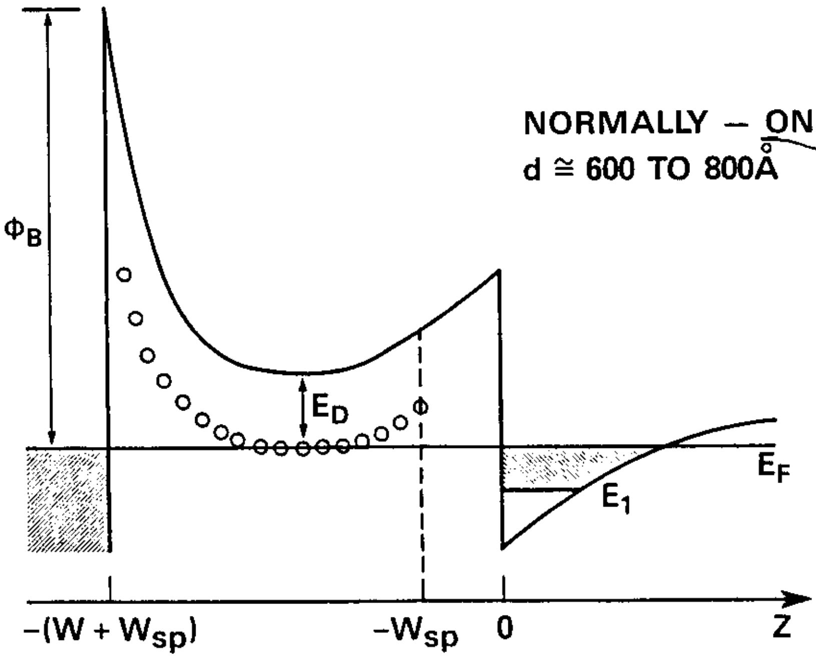

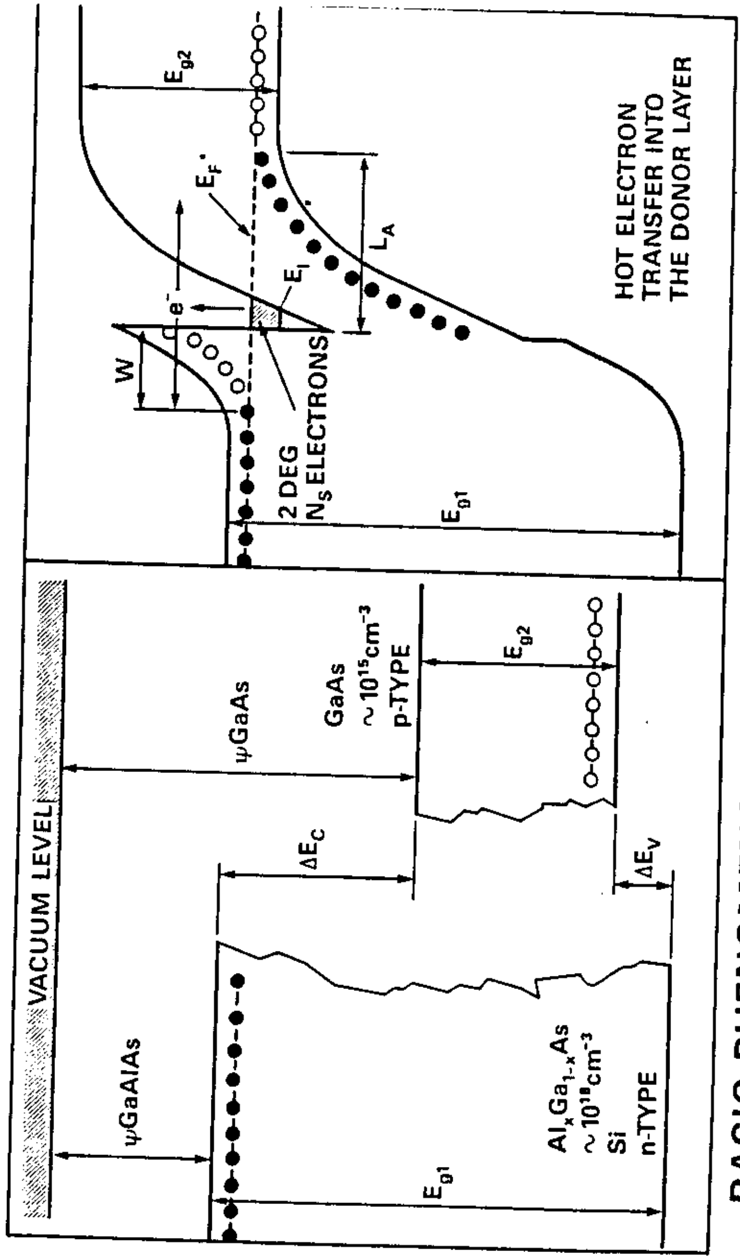

BASIC PHENOMENON AFFECTING RELIABILITY

1. ΔE_C, AND CHANGES IN ΔE_C WITH TEMP, time
2. IMPURITY AND ALLOY SCATTERING
3. DEFECT MIGRATION, FROM SUBSTRATE, DEEP LEVELS IN AlGaAs
4. FIXED CHARGE BUILD-UP

OBSERVATIONS ON HEMTS

- E-MODE DISCRETE HEMTS ARE 10× LESS RELIABLE (MTF) THAN D-MODE HEMTS
- RAPID DEGRADATION OF BOTH D-MODE AND E-MODE HEMTS OCCURS AT T > 200°C
- HEMT I.C.s (E/D MODE DESIGN) FOLLOW E-MODE HEMT MTF PROJECTIONS
- BASIC DIFFERENCE IN MTF OF FETS AND HEMTS PROCESSED UNDER CONTROLLED CONDITIONS
- RELIABILITY ANALYSIS OF HEMT DISCRETES AND I.C.s MUST ADDRESS GENERIC ISSUES

DISCRETE FET RELIABILITY LIFE TESTS

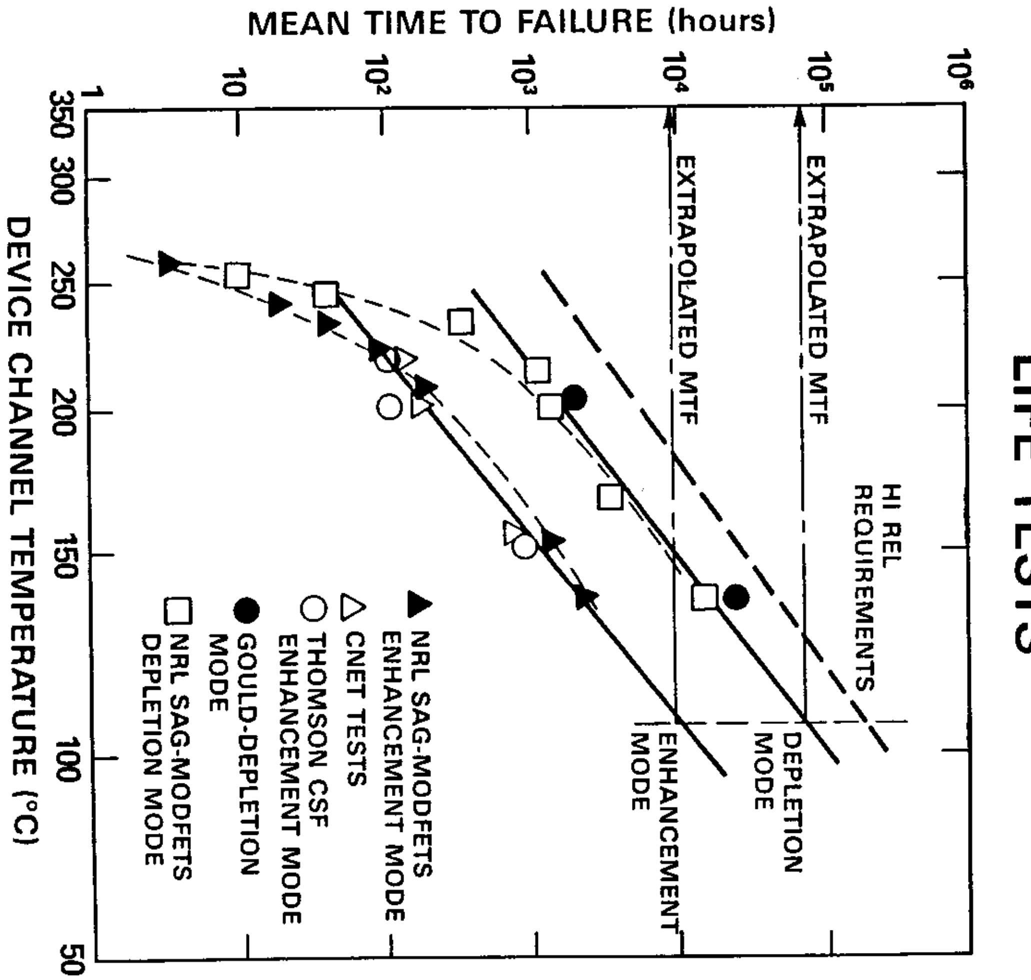

COMPARISON OF FET I.C.s WITH HEMT I.C.s

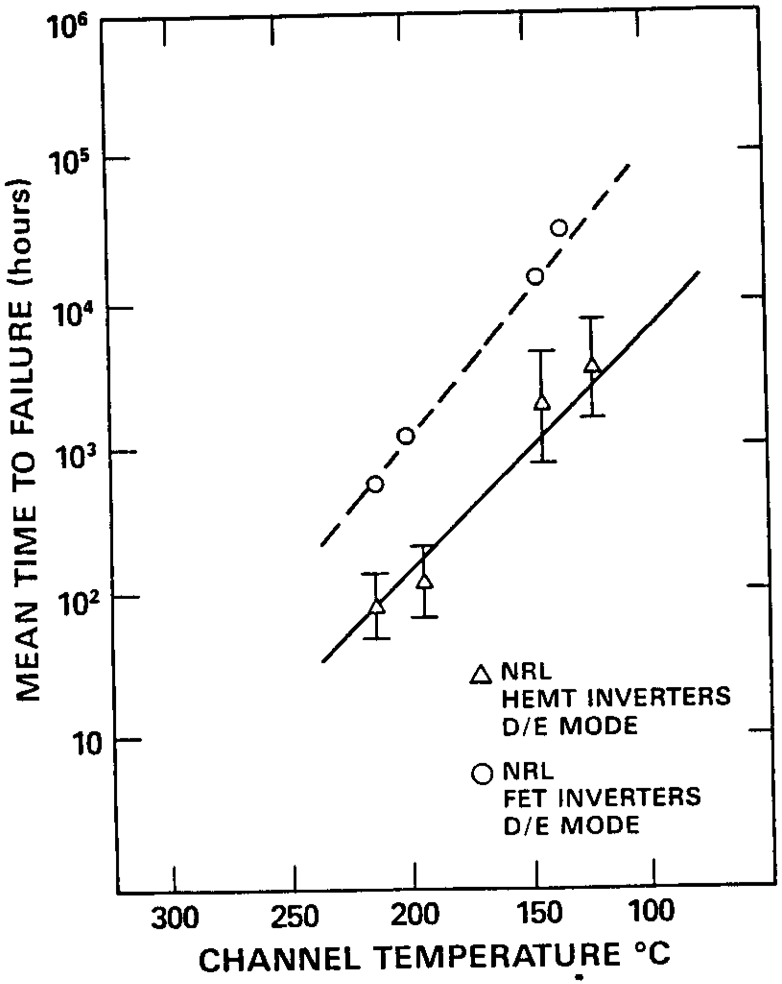

59

COMPARISON OF HEMT WITH FET DYNAMIC SHIFT REGISTER RELIABILITY DATA

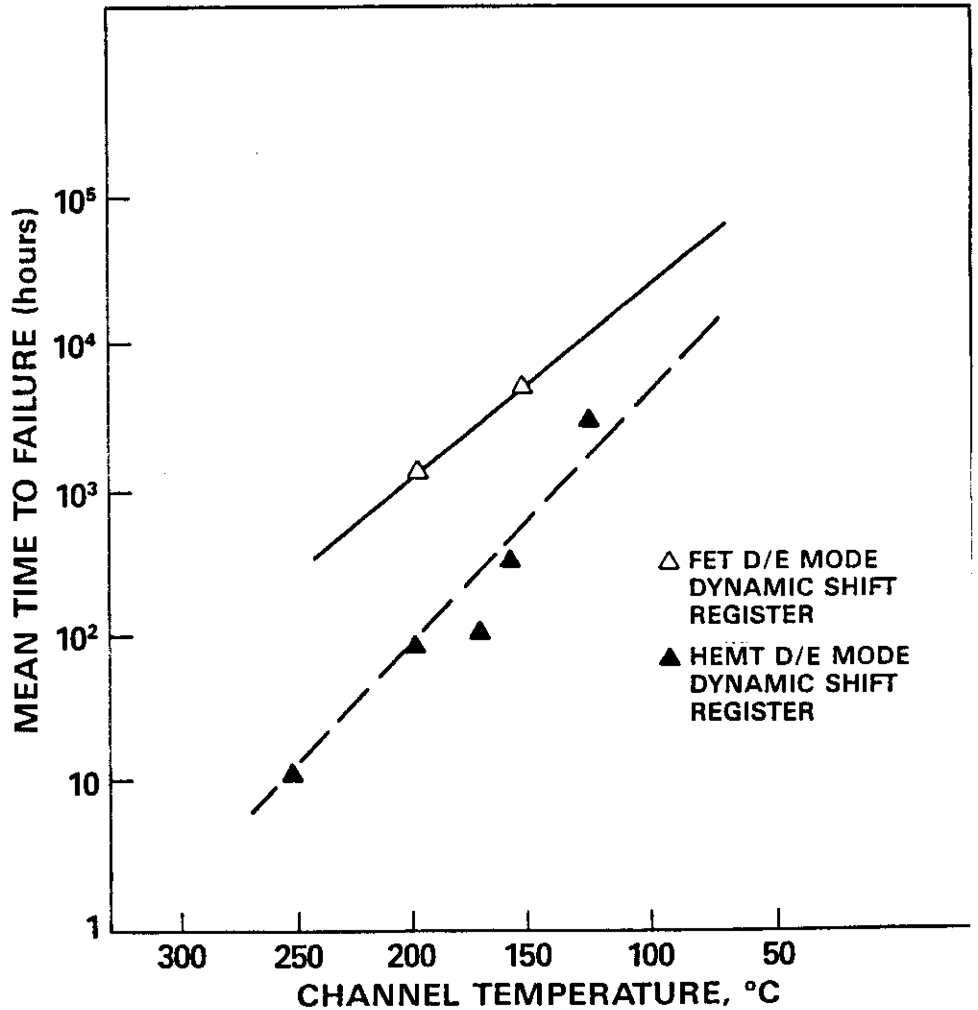

60

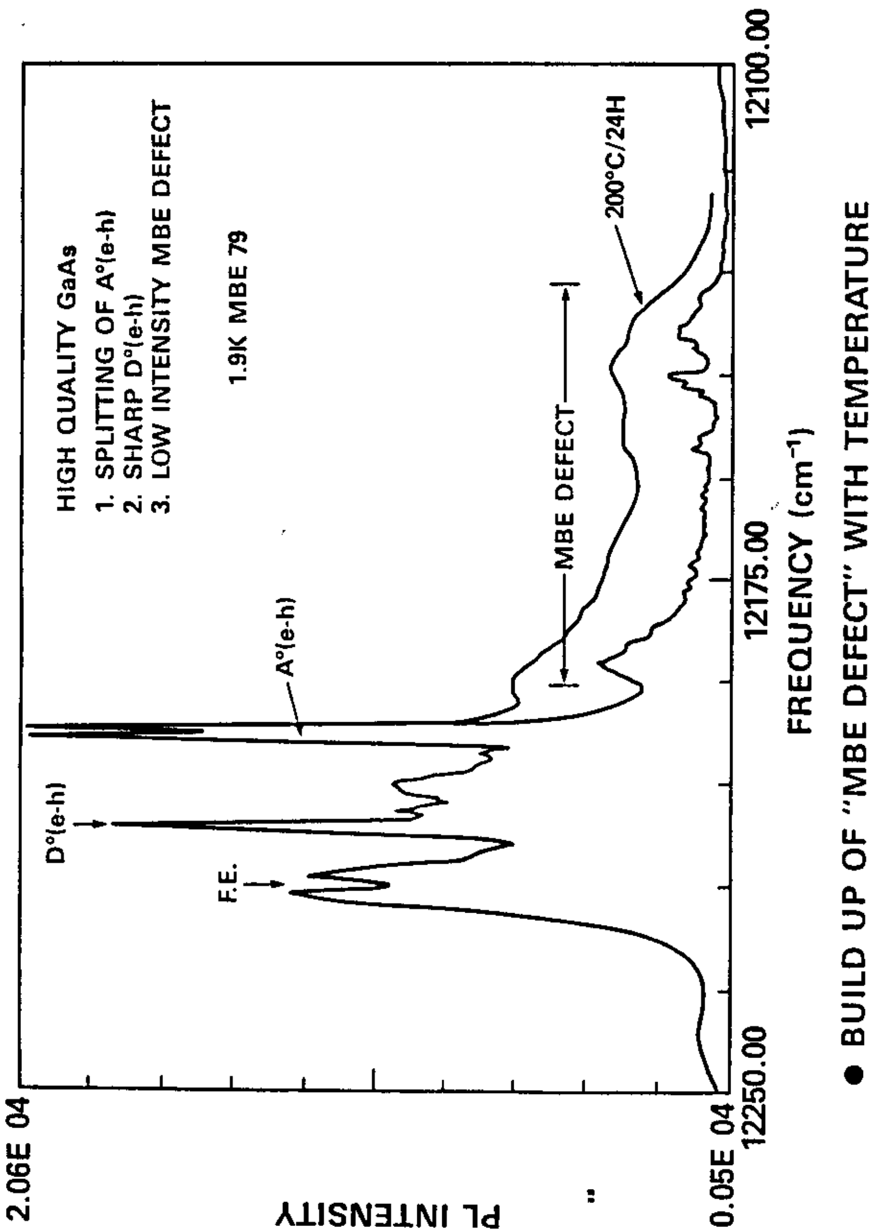

- BUILD UP OF "MBE DEFECT" WITH TEMPERATURE AND TIME
- BROADENING OF P.L. SPECTRA

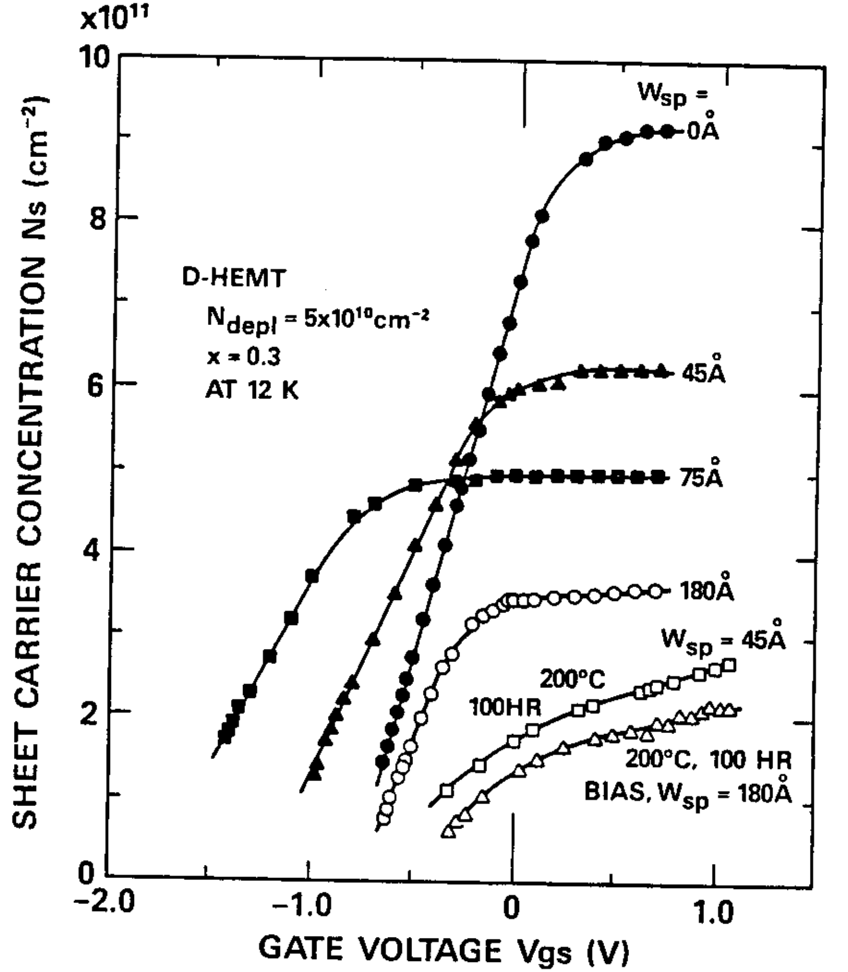

- SPACER LAYER THICKNESS DEPENDENCE
- EFFECT OF ΔE_C DEGRADATION OF SHEET CARRIER CONCENTRATION

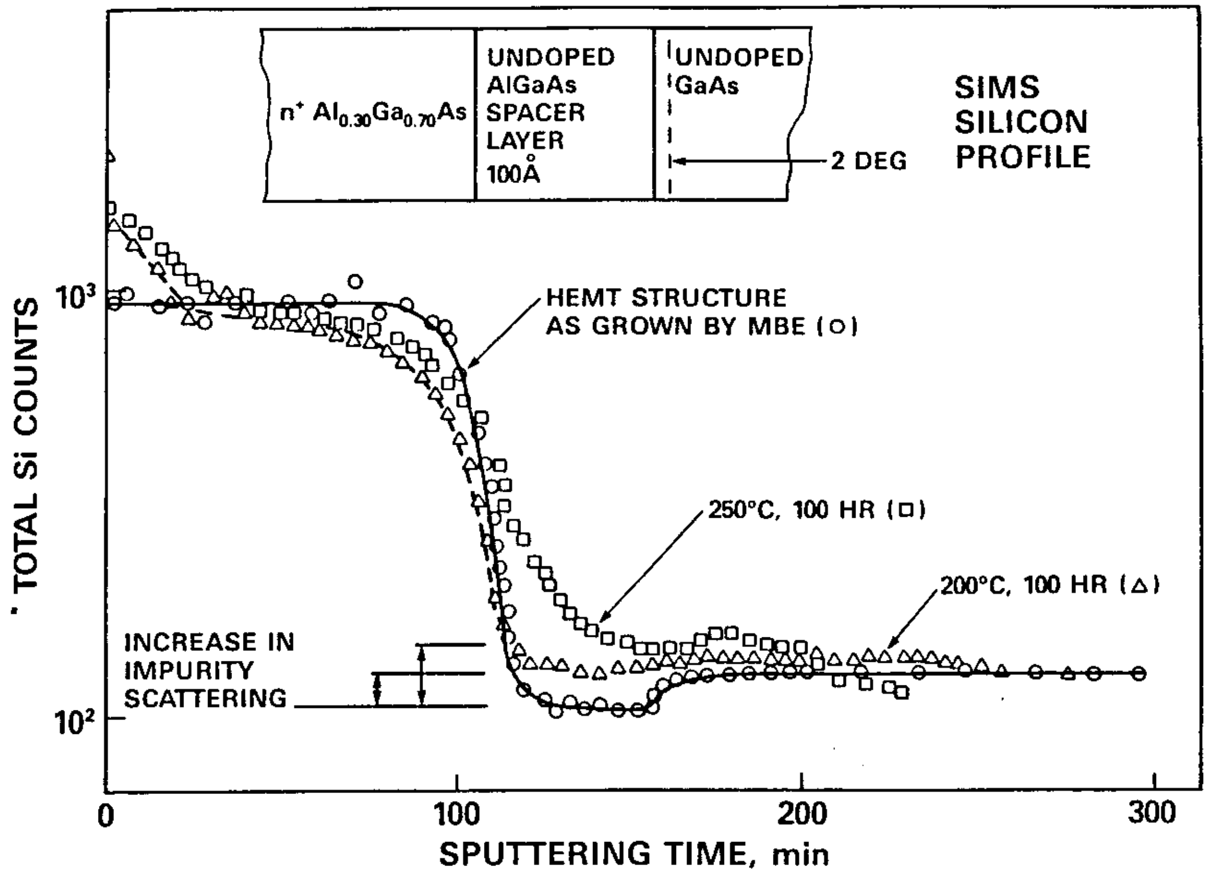
n+ Al0.30Ga0.70As
UNDOPED AlGaAs SPACER LAYER 100Å
UNDOPED GaAs
2 DEG
SIMS SILICON PROFILE
HEMT STRUCTURE AS GROWN BY MBE (○)
250°C, 100 HR (□)
200°C, 100 HR (△)
INCREASE IN IMPURITY SCATTERING
TOTAL Si COUNTS
10^3
10^2
0
100
200
300
SPUTTERING TIME, min

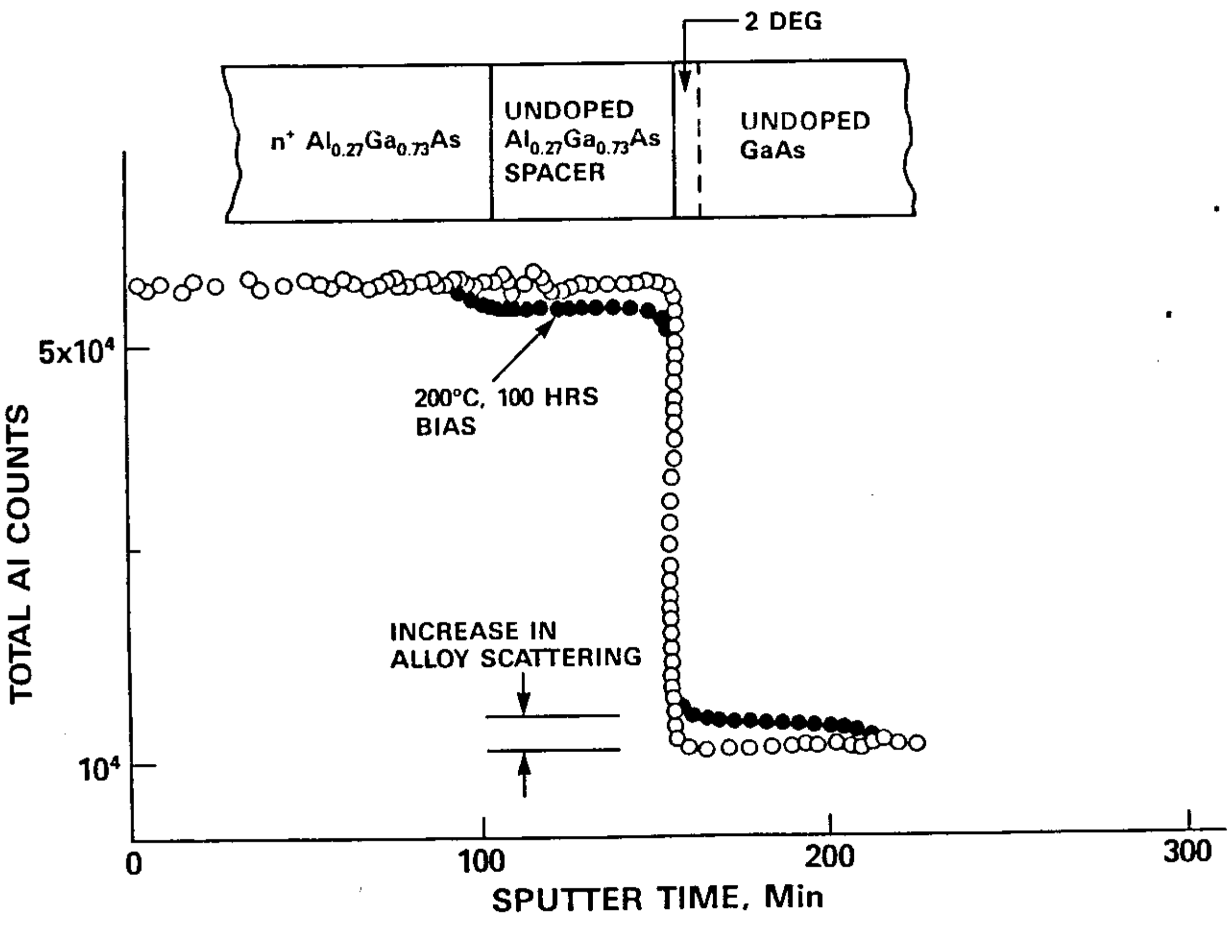
2 DEG
n+ Al0.27Ga0.73As
UNDOPED Al0.27Ga0.73As SPACER
UNDOPED GaAs
200°C, 100 HRS BIAS
INCREASE IN ALLOY SCATTERING
TOTAL Al COUNTS
5x10^4
10^4
0
100
200
300
SPUTTER TIME, Min

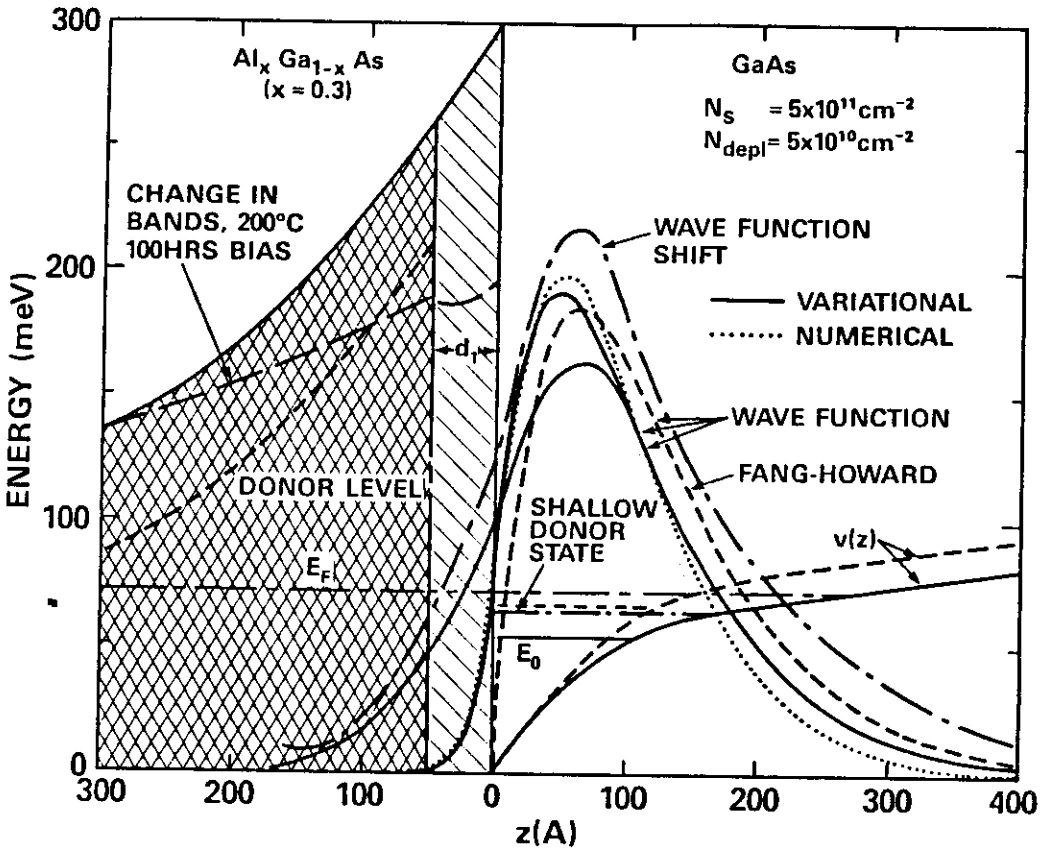

1. ENERGY BANDS IN AlGaAs ARE LOWERED
2. SHALLOW DONOR STATES MUST BE INCLUDED IN GaAs
3. WAVE FUNCTION PENETRATION INCREASES

EFFECT OF LATERAL DIFFUSION ON HEMT RELIABILITY

- Au FROM OHMIC CONTACTS INTO GATE CHANNEL
- ALUMINUM MIGRATION: FIRST TO THE OHMIC CONTACT; THEN ACROSS CHANNEL

LATERAL MIGRATION EFFECTS IN HEMTS

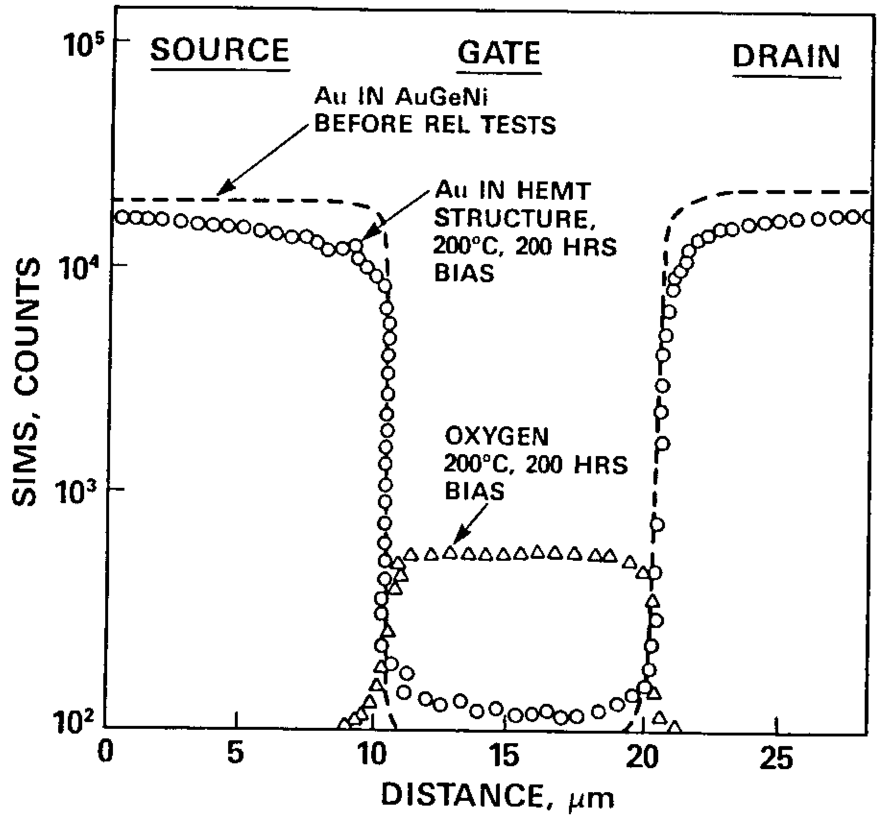

LATERAL MIGRATION OF ALUMINUM DETERMINED BY SIMS

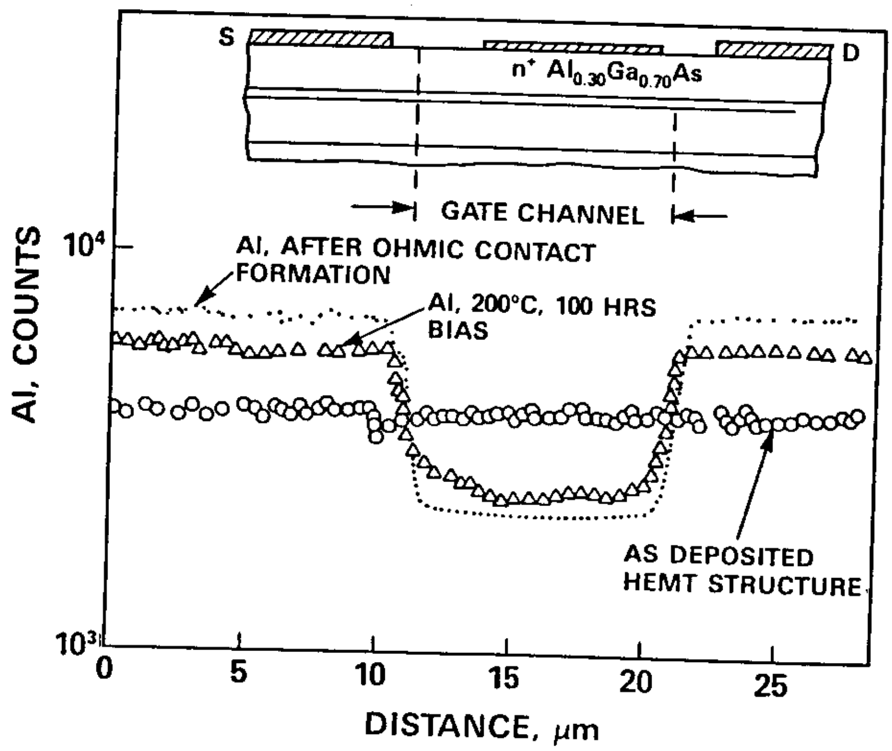

RELIABILITY OF DUAL CHANNEL HEMTS

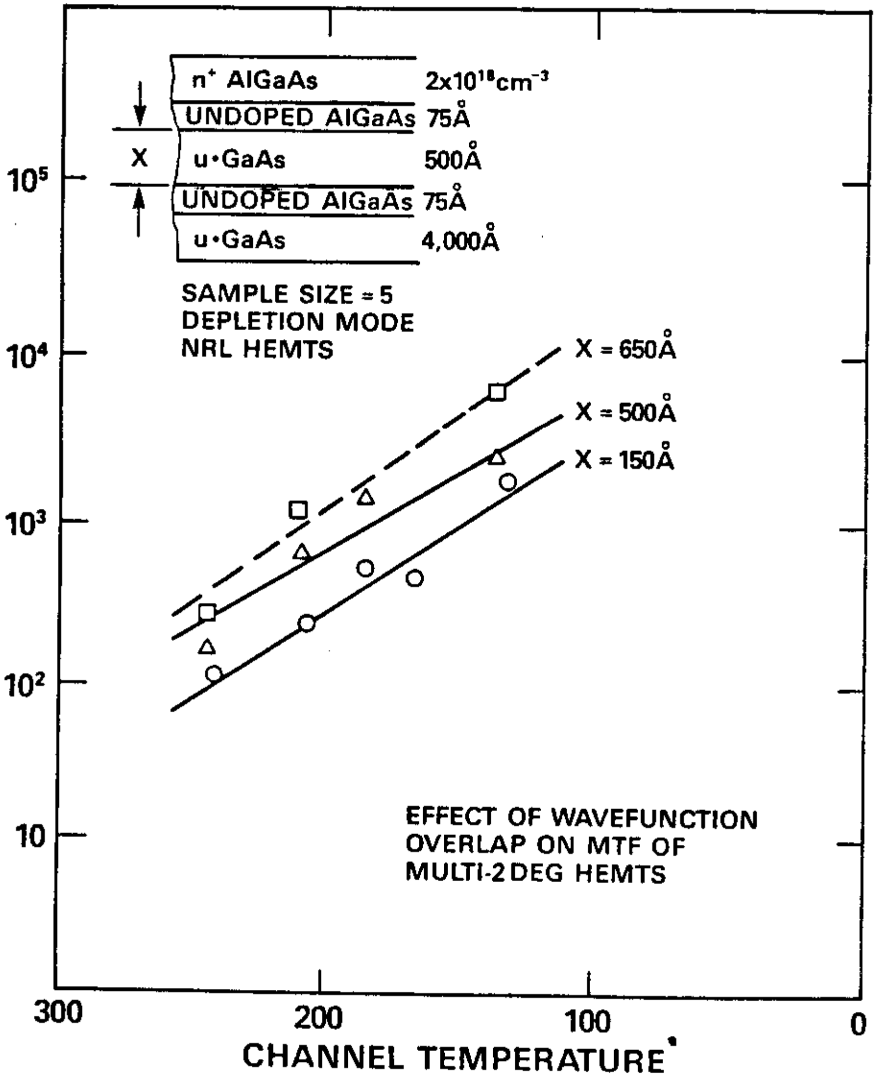

MULTI - 2DEG - HEMTS

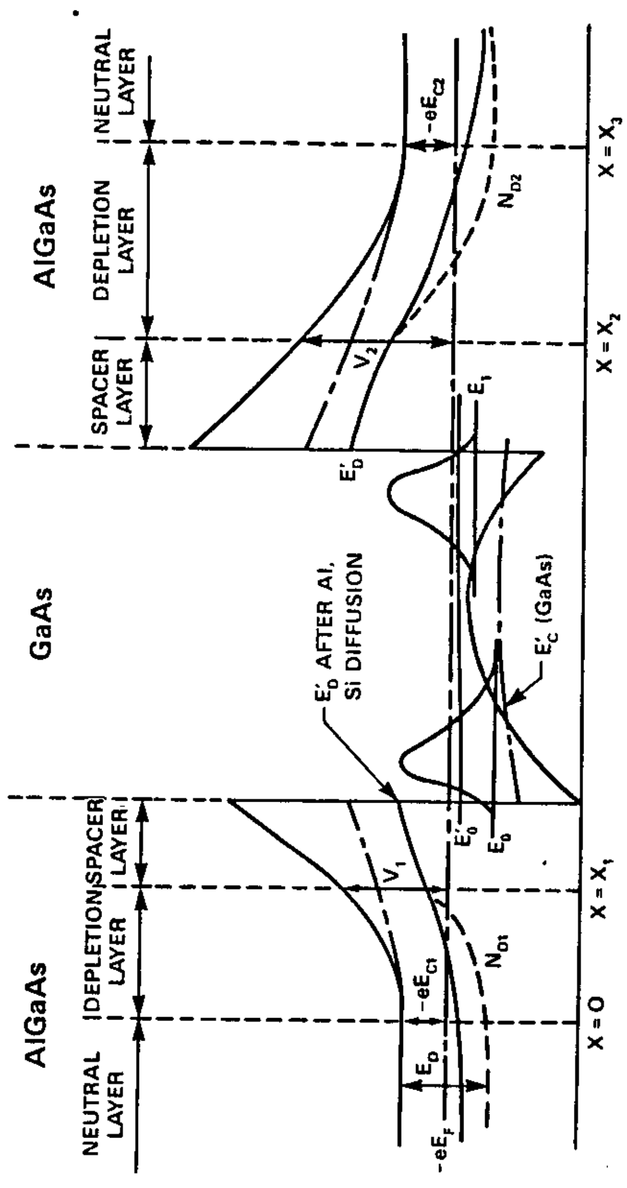

E_0' = BOUND STATE AFTER 200°C/100HR Al, Si DIFFUSION

E_D' = DONOR LEVEL IN SPACER LAYERS

E_C' = GaAs CONDUCTION BAND AFTER 200°C/100HR Al, Si DIFFUSION

EFFECT OF ALUMINUM MOLE FRACTION ON DEEP DONOR IONIZATION

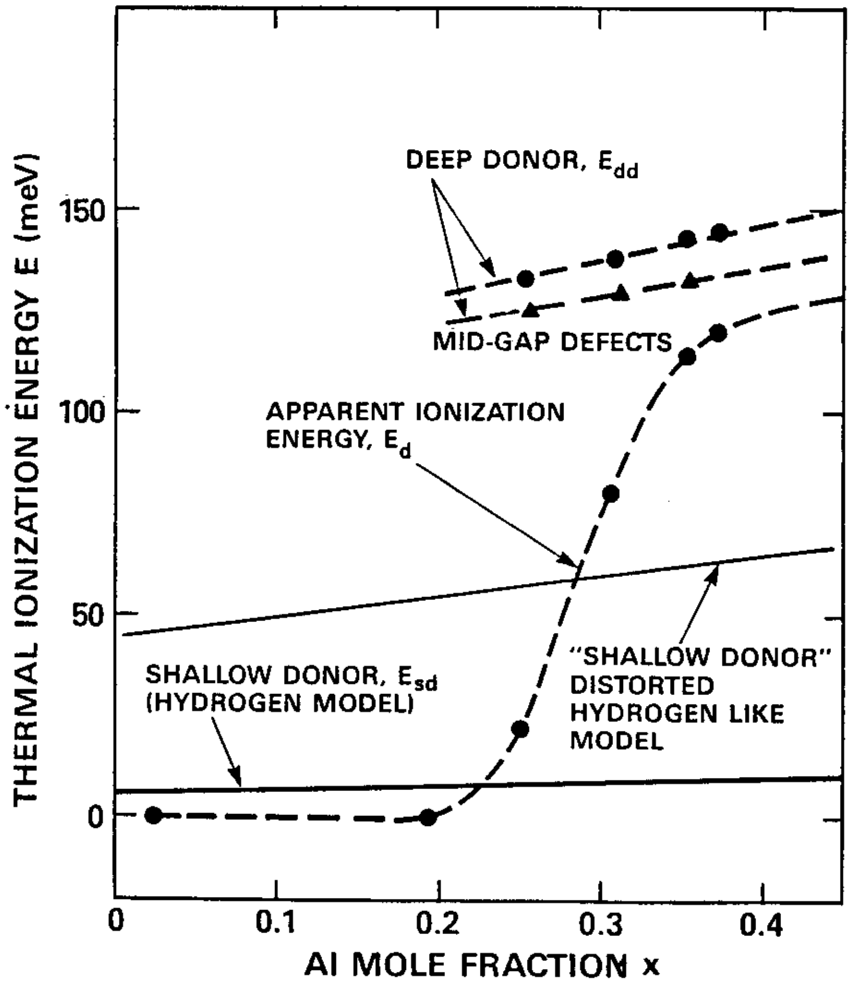

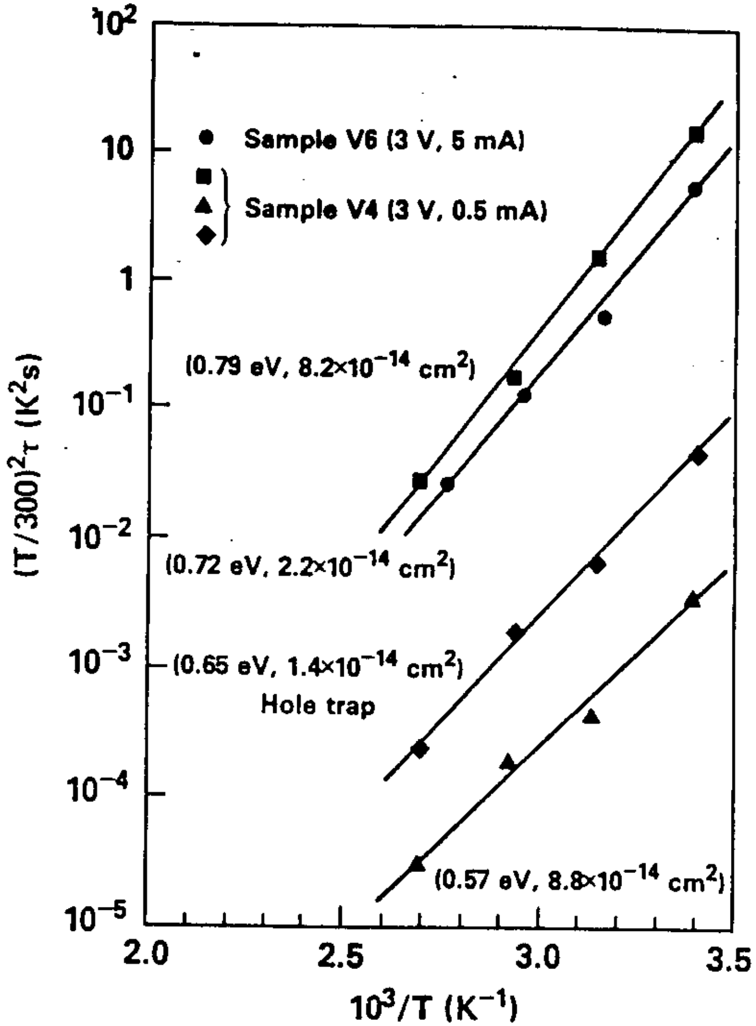

– Reciprocal temperature data for type B MODFETs exposed to 60-80 r FXR pulses while biased at $V_D = 3V$.

THRESHOLD VOLTAGE SHIFT AND SCATTER AFTER 200°C/24HR WITH BIAS TEST → TWO ORDERS OF MAGNITUDE INCREASE IN TRAP DENSITY

$N_T = 10^{19} cm^{-3}$
AFTER 200°C
24 HR.

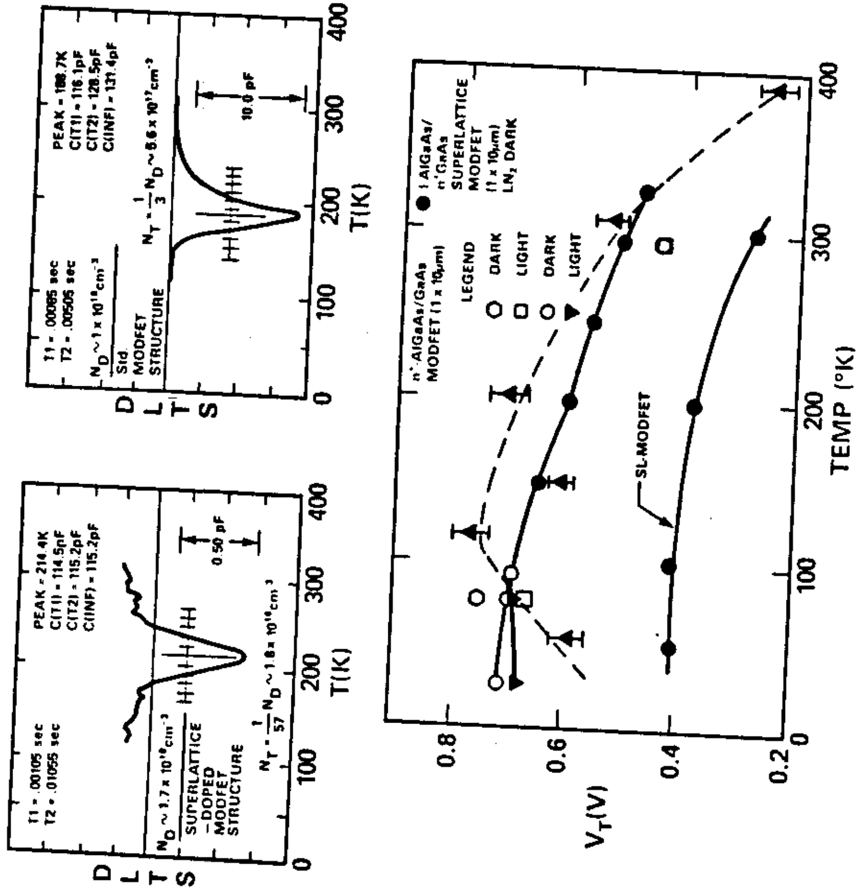

RELIABILITY OF HEMTs WITH SUPERLATTICE DONOR LAYER

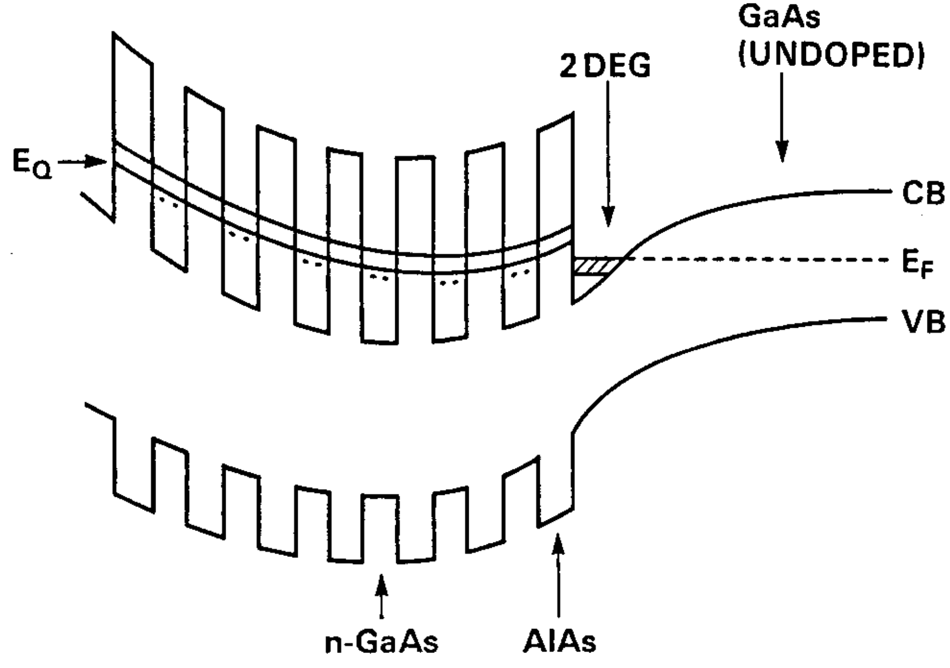

1. INCREASE IN V_{TH} SCATTER
2. INCREASE IN PHOTOCURRENTS AND LIGHT SENSITIVITY
3. INCREASE IN SURFACE AND INTERFACE TRAPPING
4. SUPERLATTICE PERIODIC POTENTIAL BECOMES WAVEY LIKE

75

RELIABILITY PROBLEMS OF HEMTS

HOT ELECTRONS ENTER DEPLETED AlGaAs AREAS CAUSING DEVICE PERFORMANCE TO DEGRADE OVER TIME

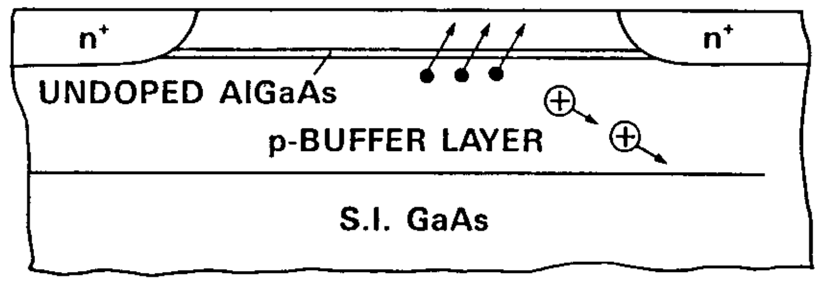

76

HOT ELECTRONS IN HEMTS
[ASSUME BEHAVIOR IS SIMILAR TO MOS]

DISTRIBUTION FUNCTION MUST BE DERIVED

⇨ NUMBER OF ELECTRONS AVAILABLE FOR
- GATE LEAKAGE CURRENT
- SUBSTRATE CURRENT

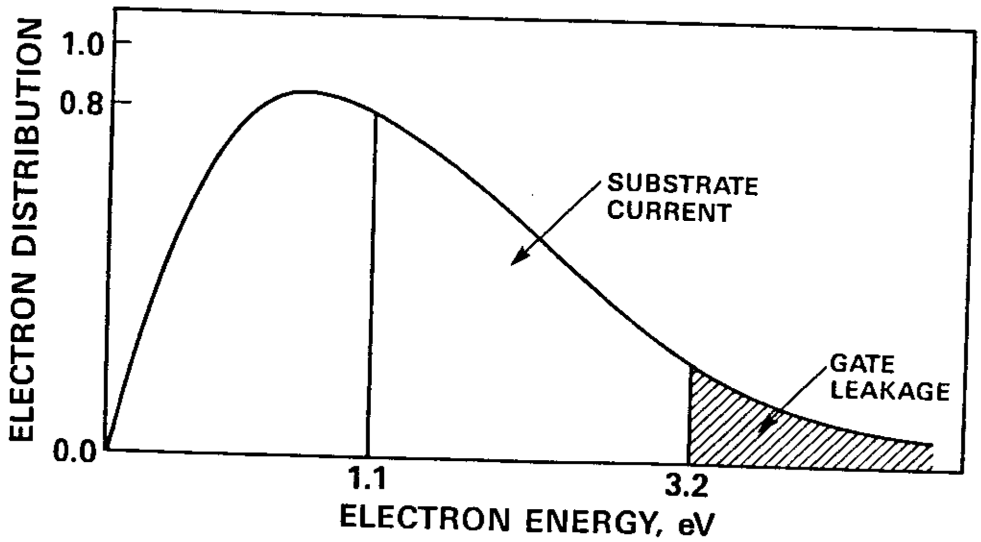

HOT ELECTRONS IN HEMTS

1. OBTAIN HOT ELECTRON DISTRIBUTION FUNCTION FROM
   A) ENERGY TRANSPORT EQUATION
   B) BOLTZMAN TRANSPORT EQUATION

1) BOLTZMANN TRANSPORT EQUATION:

$$\frac{eE}{h}\frac{\partial f(k)}{\partial k} + \left\{\frac{\partial f(k)}{\partial t}\right\}_{coll} = 0$$

a) COLLISION TERM QUANTIFIES THE EFFECT OF ELECTRONS INTERACTING WITH ATOMS AND OTHER ELECTRONS

b) FIELD TERM QUANTIFIES THE EFFECT OF THE ELECTRIC FIELD ON ELECTRONS

(INTEGRATE BOLTZMANN EQUATION TO FIND)

ENERGY TRANSPORT EQUATION:
QUANTIFIES THE AVERAGE ELECTRON ENERGY AT EACH DEVICE COORDINATE

$$\frac{\partial\langle\omega\rangle}{\partial x} = \frac{3}{5}\left[eE(x) - \frac{\langle\omega\rangle - \omega_0}{\lambda(\langle\omega\rangle)}\right]$$

$\langle\omega\rangle$ = AVERAGE ELECTRON ENERGY

$E(x)$ = ELECTRIC FIELD

$\lambda(\langle\omega\rangle)$ = ENERGY RELAXATION LENGTH, MEASURES AMOUNT OF ENERGY ELECTRON LOSES IN A COLLISION

GATE LEAKAGE CURRENT

- SOLVE BOLTZMANN AND ENERGY TRANSPORT EQUATIONS SIMULTANEOUSLY FOR ELECTRON TEMPERATURE T_e, AND HOT ELECTRON DISTRIBUTION FUNCTION:

$$f_o(\omega) = A\, e^{-\alpha\left[\frac{\omega}{KT_e} + \frac{\gamma\omega^2}{KT_e}\right]}$$

A = NORMALIZATION FACTOR

γ = RATIO OF ACOUSTIC TO INTERVALLEY PHONON COUPLING FACTORS

α = FUNCTION OF ELECTRON TEMPERATURE WHICH ENSURES SOLUTION IS CONSISTENT

GATE LEAKAGE CURRENT

- USE HOT ELECTRON DISTRIBUTION FUNCTION TO DERIVE RICHARDSON-LIKE EQUATION FOR INJECTION OVER AlGaAs BARRIER AND GATE LEAKAGE CURRENT

$$J_g(x) = qA(x)N(x) \langle \nu_z \rangle \int_{\psi}^{\infty} \omega^{\frac{3}{2}} e^{-a(x)\left[\frac{\omega}{KT_e(x)} + \frac{\gamma\omega^2}{KT_e(x)}\right]} d\omega$$

a) $J_g(x)$ = GATE CURRENT DENSITY

b) $N(x)$ = AVERAGE ELECTRON CONCENTRATION

c) ν_z = ELECTRON VELOCITY TOWARDS OXIDE

d) ψ = AlGaAs BARRIER HEIGHT

79

ENERGY TRANSPORT EQUATION CALCULATION OF HEMT CHANNEL ELECTRON TEMPERATURE

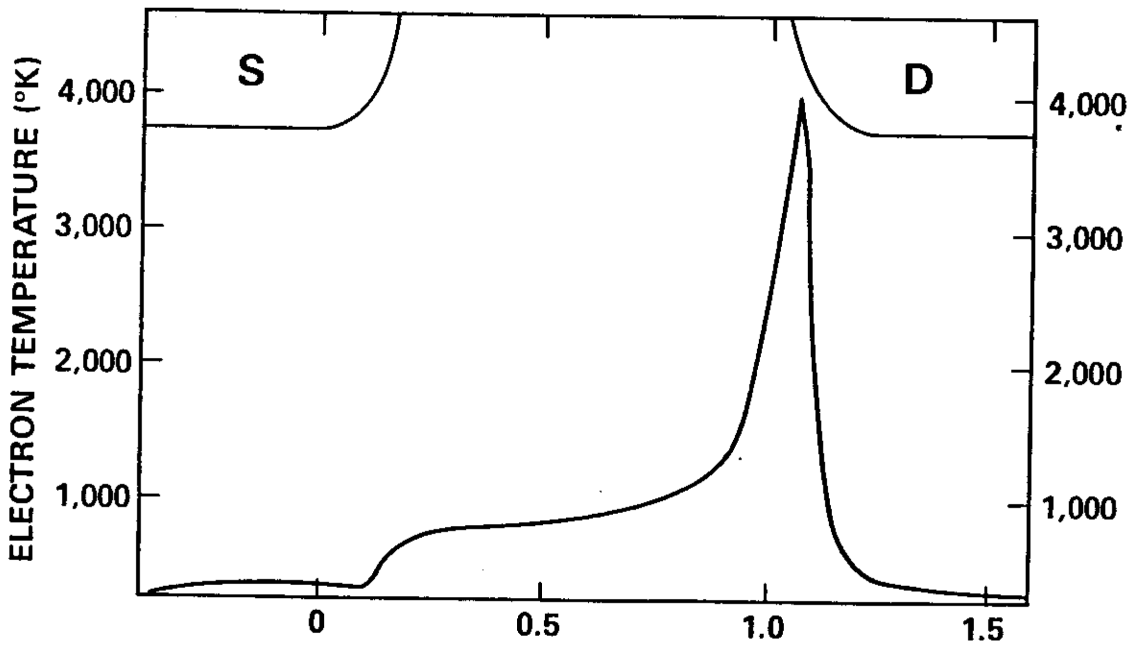

(REF: J. FREY)

$$\frac{d\omega}{dx} = \frac{3}{5}\left[eE(x) - \frac{\omega - \omega_0}{\lambda(\omega)}\right]$$

80

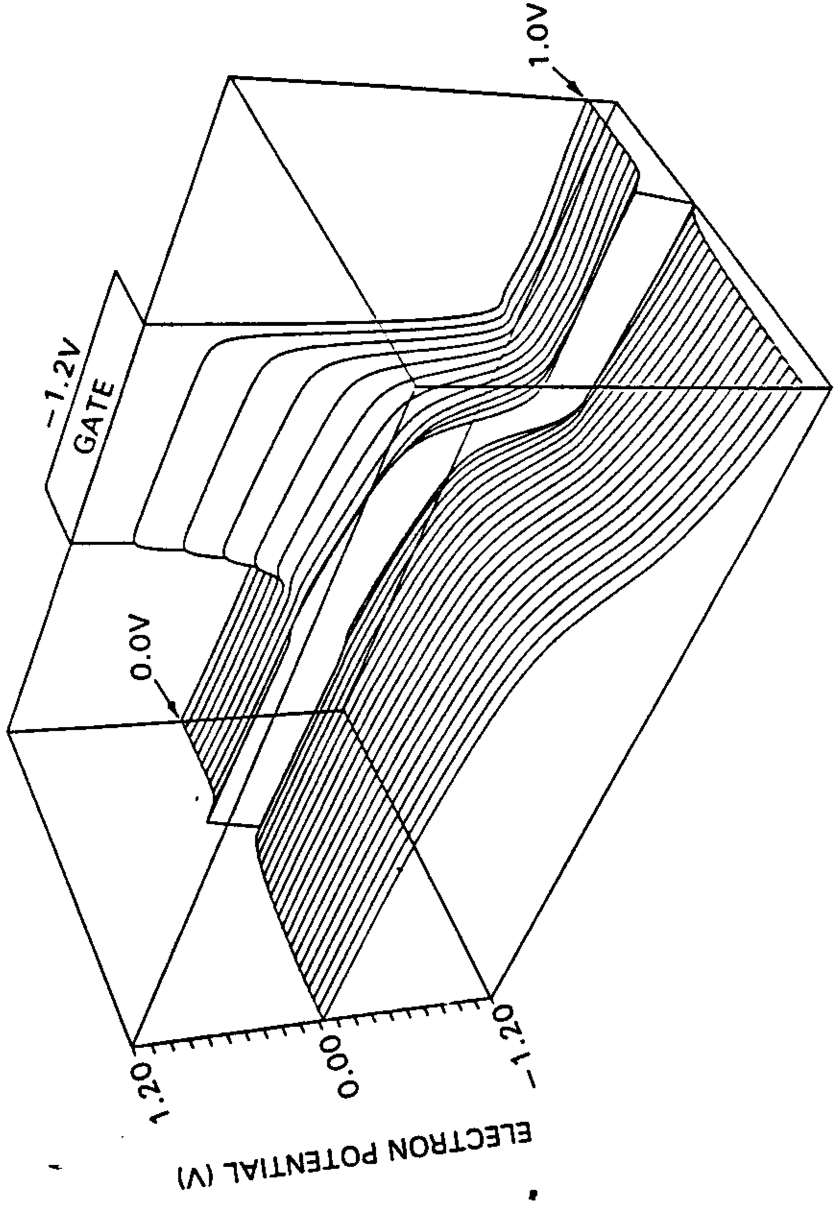

Optical Devices

- Optical Modulators

  Electro-optic switches

  All Optical switches

  ⇓

  Based on Strained and Unstrained III-V Quantum Well Structures

Electronic Devices

- Strained Channel MODFETs - n-type, p-type
- Transport in Semiconductor Alloys

  Role of Alloy Clustering
- Thin Period Superlattice Based Devices.

Issues

Electronic	Optical	Transport
Bandstructure of lattice matched and strained heterostructures	oscillator strengths in arbitrary shaped quantum wells	Free carrier transport in heterostructures

PROGRAMMABLE SLM DEVELOPMENT

SC3

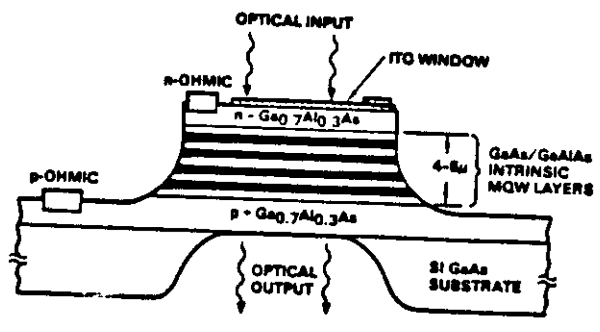

(a) MQW ABSORPTION CELL

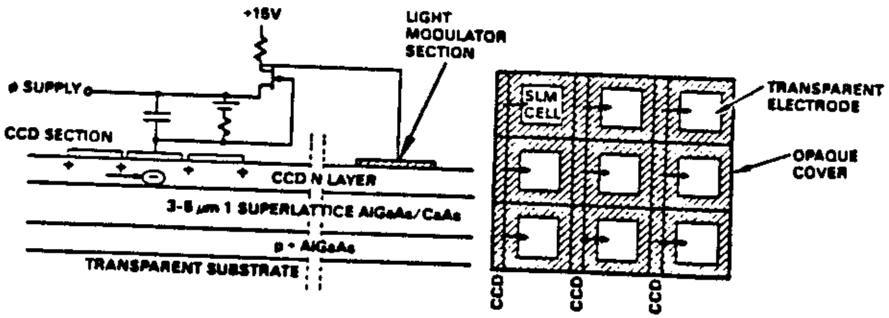

(b) SCHEMATIC FOR THE 2-D PSLM CHIP LAYOUT

Issues in Modulators and Detectors using III-V Heterostructures-
Relationship to Systems Considerations for Optical Processing

Why optical processing?

- -Highly parallel processing possible
- -Use of devices with special logic functions (other than 0,1)
  - Fourier optics
  - (neural networks?)

Successes in optical processing:

- -1- & 2-d spectral analysis
- -multichannel spectral analysis
- -frequency plane matched filtering
- -correlation, convolutions

Parallelism + special purpose logic

10^{13} - 10^{14} bits/sec.

- Stark effect based
- Optical non-linearity due to high intensity
- Promising for low power applications
- Modulation/Switching can be done electronically or optically

Maybe easy to apply in a number of systems

Issues in SLMS:

- Potential contrast ratio
- Energy requirements
- Dynamic range
- Storage density possible
- Uniformity/Reliability

Dynamic range $\geq 10^3$

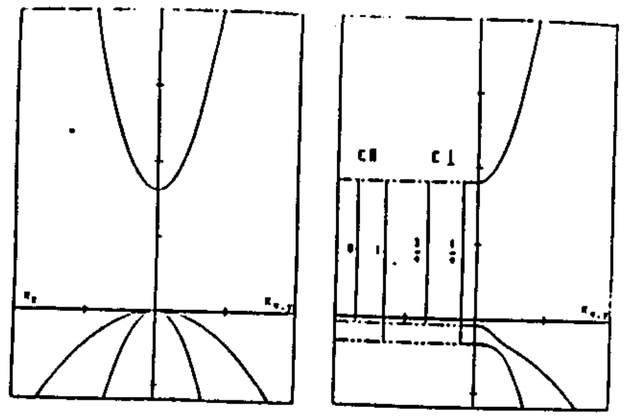

ADDITIONAL CHANGES:

- Exciton volume decreases as well size is decreased. (W > 50 Å)
- Binding energy increases as well size decreases.(W < 50 Å)
- Absorption constant increases

· Exciton binding energy can increase by a factor of 2.5 over bulk value.

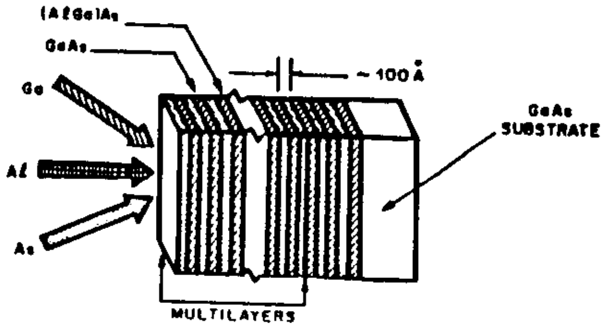

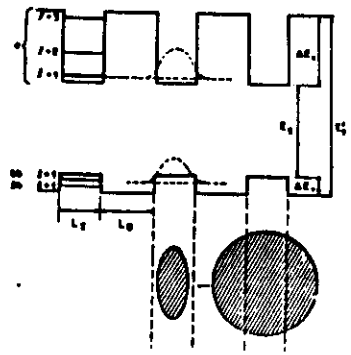

IMPORTANT ISSUES IN OPTICAL MODULATORS;

- **High speed modulation:**
  - **Fast absorption of photons**
  - **Fast extraction of e-h pairs**
    - **Radiative recombination ~ ns**
    - **Tunneling (Field dependent)**
- **High ON/OFF ratio - (Modulation depth):**
  - **Spectral width of incoming light**
  - **Switching fields employed**
  - **Material quality**
- **High temperature operation:**
  - **Strong exciton binding energy**
  - **High quality heterostructures**

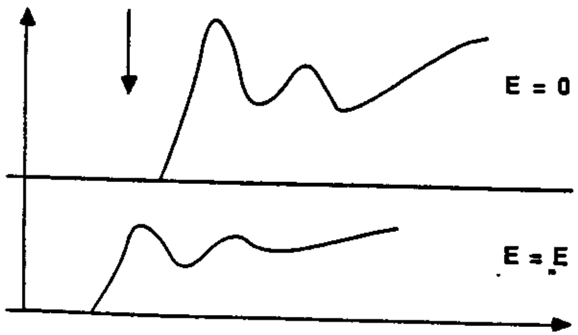

THE EXCITON PROBLEM : ABSORPTION SPECTRA

. ELECTRON PROBLEM

$$-\frac{\hbar^2}{2m}\nabla^2\Psi(\mathbf{k},z) + V(z)\Psi(\mathbf{k},z) = E\Psi(\mathbf{k},z)$$

$$\Psi^n_{el}(\mathbf{k},z) = f^n(z)U_0(r)e^{i\mathbf{k}_\parallel\cdot\rho}$$

. HOLE PROBLEM

HEAVY HOLE,	LIGHT HOLE STATES
3/2, 3/2 >	3/2, 1/2 >
3/2, - 3/2 >	3/2, - 1/2 >

HOLE STATES DEFINED BY THE KOHN-LUTTINGER HAMILTONIAL

$$\begin{bmatrix} H_{hh} & c & b & 0 \\ c^* & H_{lh} & 0 & -b \\ b^* & 0 & H_{lh} & c \\ 0 & -b^* & c^* & H_{hh} \end{bmatrix} \begin{bmatrix} \Phi_{\frac{3}{2}\frac{3}{2}} \\ \Phi_{\frac{3}{2}\frac{1}{2}} \\ \Phi_{\frac{3}{2}\frac{-1}{2}} \\ \Phi_{\frac{3}{2}\frac{-3}{2}} \end{bmatrix} = E \begin{bmatrix} \Phi_{\frac{3}{2}\frac{3}{2}} \\ \Phi_{\frac{3}{2}\frac{1}{2}} \\ \Phi_{\frac{3}{2}\frac{-1}{2}} \\ \Phi_{\frac{3}{2}\frac{-3}{2}} \end{bmatrix}$$

where

$$H_{hh} = -\frac{\hbar^2}{2m_o}\left[(k_x^2+k_y^2)(\gamma_1+\gamma_2) - (\gamma_1-2\gamma_2)\frac{\partial^2}{\partial^2 z}\right] + V_p($$

$$H_{lh} = -\frac{\hbar^2}{2m_o}\left[(k_x^2+k_y^2)(\gamma_1-\gamma_2) - (\gamma_1+2\gamma_2)\frac{\partial^2}{\partial^2 z}\right] + V_p($$

$$c = \frac{\sqrt{3}\hbar^2}{2m_o}\left[\gamma_2(k_x^2-k_y^2) - 2i\gamma_3 k_x k_y\right]$$

$$b = \frac{\sqrt{3}\hbar^2}{m_o}(-k_y - ik_x)\gamma_3\frac{\partial}{\partial z}$$

Optical Absorption in Quantum Wells

$$\alpha(\hbar\omega) = \frac{4\pi^2 e^2 \hbar}{\eta c m^2 \hbar\omega} \sum_{k_\parallel} \sum_{n,m} \left| \hat{\epsilon} \cdot p_{nm}(k_\parallel) \right|^2 \delta(E^h_m(k_\parallel) - E^e_n(k_\parallel) + \hbar\omega)$$

$$\mathrm{p}_{nm}(k_\parallel) = < \Psi^h_m(k_\parallel) \mid \mathrm{p} \mid \Psi^e_n(k_\parallel) >$$

$$\mathrm{p}_{nm}(k_\parallel) = \sum_{\nu,\mu} \int dr U_0^{\nu *}(r) \mathrm{p} U_0^{\mu}(r) \int dz f^{\mu}_n(z) g^{\nu *}_m(k_\parallel, z)$$

$$\alpha(\hbar\omega) \propto \sum_{n,m} |\hat{\epsilon} \cdot p_{nm}(0)|^2 \delta_{nm} \rho_{nm}(\hbar\omega)$$

$$\rho_{nm}(\hbar\omega) = \sum_{nm} \frac{\mu_{nm}}{\pi\hbar^2} \Theta_{nm}(\hbar\omega)$$

$$\alpha_{nm} = \frac{4\pi^2 e^2 \hbar}{\eta m_0 c W} \frac{1}{\hbar\omega} \left| \sum_{k_\parallel} G_{nm}(k_\parallel) \hat{\epsilon} \cdot p_{nm}(k_\parallel) \right|^2 \delta(\hbar\omega - E_{nm})$$

$$\delta(\hbar\omega - E_{nm}) = \frac{1}{\sqrt{1.44\pi\sigma}} exp(\frac{-(\hbar\omega - E_{nm})^2}{1.44\sigma^2})$$

Linewidth is extremely important.

CONTRIBUTIONS TO EXCITON LINEWIDTHS

. Phonon broadening

$$\sigma_{tot} = \sigma_0 + \alpha T + \frac{\beta}{exp(\frac{\hbar\omega_0}{k_B T}) - 1}$$

. Lifetime broadening due to tunneling

- Negligible at low switching fields

(E < 80 kV/cm)

. Lifting of Kramer's Degenerance

(1 - 2 meV > Field dependent)

. Alloy Broadening (InGaAs/InAlAs system)

. Interface roughness

. Well to well size fluctuations in the MQW.

The Exciton Problem

$$H = -\frac{\hbar^2}{2\mu}\left(\frac{1}{\rho}\frac{\partial}{\partial\rho}\rho\frac{\partial}{\partial\rho} + \frac{1}{\rho^2}\frac{\partial^2}{\partial\phi^2}\right) - \frac{\hbar^2}{2m_e}\frac{\partial^2}{\partial z_e^2} - \frac{\hbar^2}{2m_h}\frac{\partial^2}{\partial z_h^2}$$
$$- \frac{e^2}{\epsilon\,|\,r_e - r_h\,|} + V_{ew}(z_e) + V_{hw}(z_h) + eEz_e - eEz_h \qquad (27)$$

$$E^{ex}_{K.E.}(k_\parallel) = E^e(k_\parallel) + E^h(k_\parallel)$$

$$E = \frac{\int\int\int \Psi^* H \Psi dz_e dz_h \rho d\rho}{\int\int\int \Psi^* \Psi dz_e dz_h \rho d\rho}$$

$$E^e(k_\parallel) = \frac{\hbar^2}{2m_e^*}k_\parallel^2$$
$$E^h(k_\parallel) = \alpha k_\parallel^2 + \beta k_\parallel^4$$

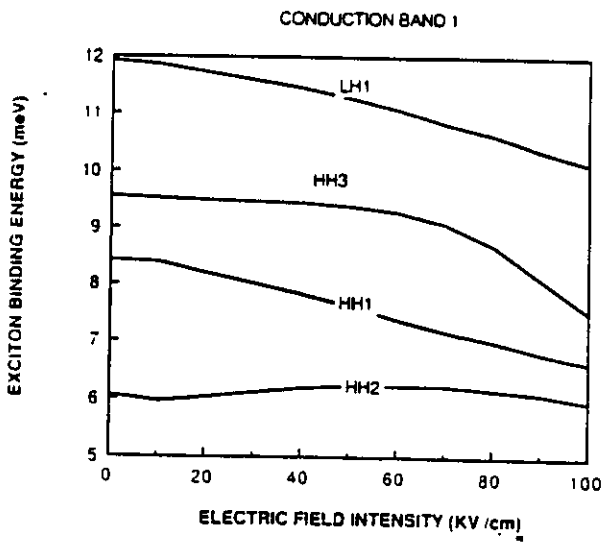

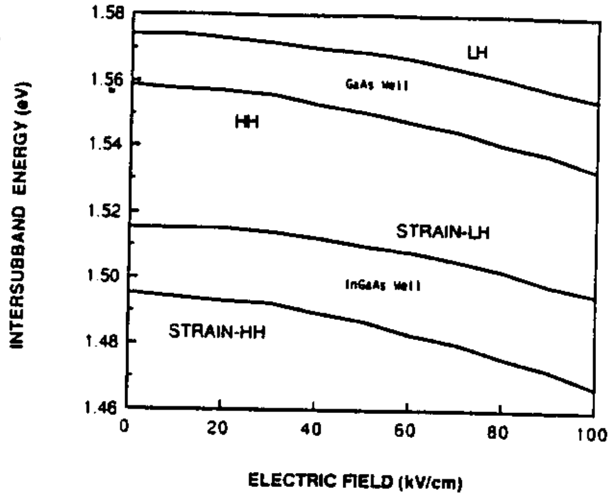

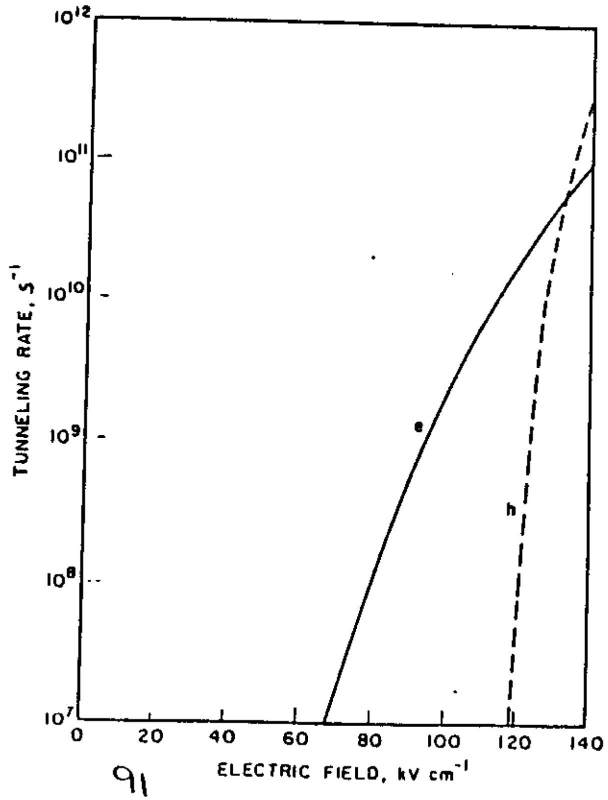

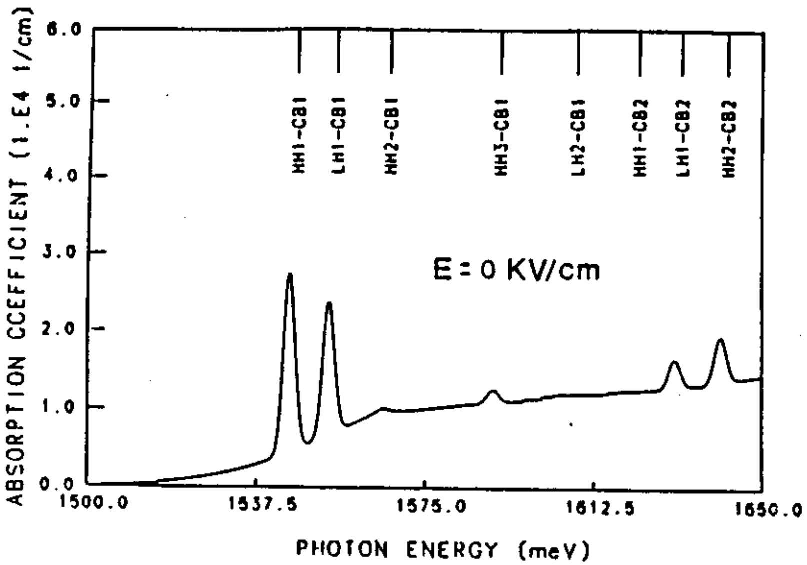

a

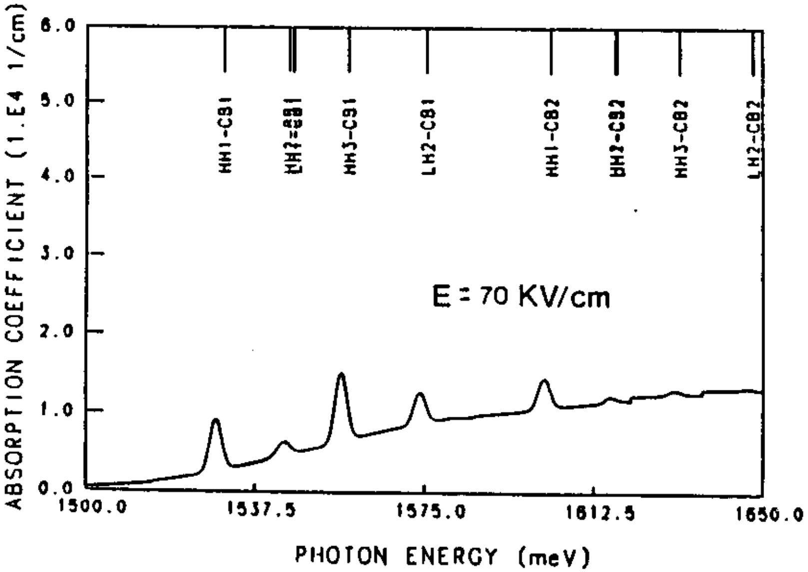

b

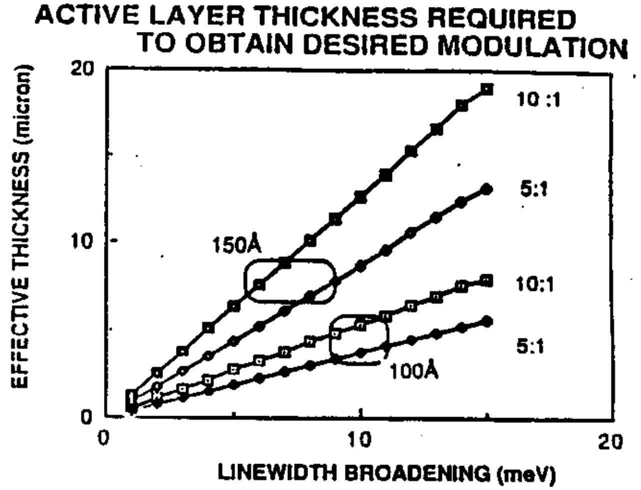

Figure 1. Results of calculations showing the amount of active region required to obtain the desired contrast ratio in a 1.0 μm 100 Å and 150 Å MQW structure as a function of exciton linewidth. The results are for a modulator where the maximum transmittance is at zero field and minimum transmittance is at 75 kV/cm for the 100 Å MQW and 50 kV/cm for the 150 Å structure. Note that the phonon broadening at room temperature is 3 meV and a one monolayer rms fluctuation in well size for the 100 A structure produces a linewidth of 3 meV at the maximum field.

STRAINED QUANTUM WELLS : TENSILE STRAIN

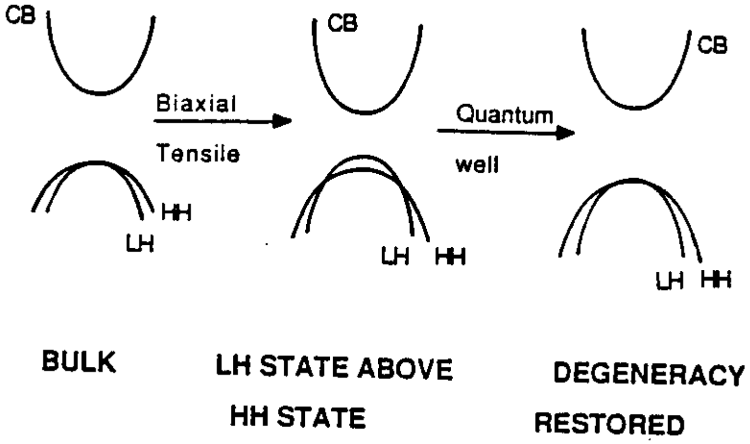

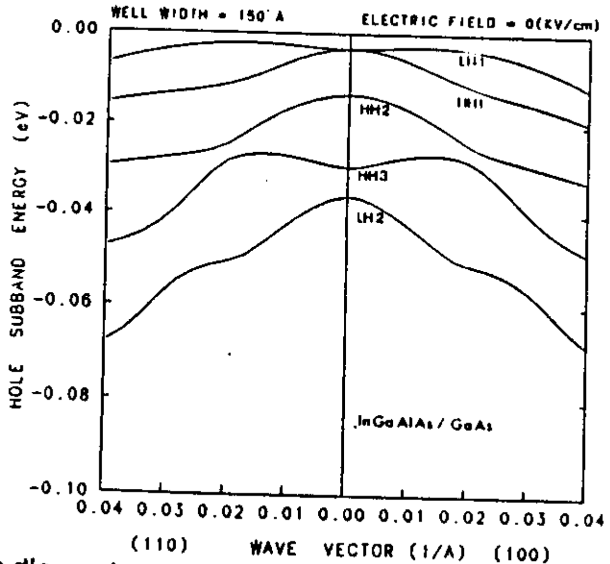

Hole dispersion relation for 150 Å $GaAs/In_{0.06}Ga_{0.57}Al_{0.37}As$ QW with degenerate LH, HH states

Summary: Optical Devices

- Detailed formalism for electric field dependent op absorption in lattice matched and strained quantum well
- Enhanced absorption in biaxially tensive quantum wells
- New schemes for electro-optic and all optical devices.

Ongoing Work:

- Detailed understanding of photo current in MQW modulato
- Optical devices for specific optical systems.
  - Rubic architecture
  - Hopfield neural networks

15

MATERIAL ISSUES IN THE InAlAs / InGaAs HETEROSTRUCTURES

CONSEQUENCES FOR DEVICES

ABILITY TO GROW HIGH QUALITY InAlAs/InGaAs HETEROSTRUCTURES IS ALLOWING FABRICATION OF POTENTIALLY VERY HIGH PERFORMANCE ELECTRONIC AND OPTICAL DEVICES

MODFETs

OPTICAL MODULATORS

SHOULD ONE EXPECT ANY SERIOUS PROBLEMS IN THIS MATERIAL SYSTEM?

InGaAs

InAlAs

InAlAs/InGaAs

WHAT ARE THE CONSEQUENCES OF THESE PROBLEMS ?

WHAT ARE THE POSSIBLE SOLUTIONS TO THE PROBLEMS ?

IMPORTANCE OF THE InAlAs/InGaAs SYSTEM:

HIGH CHANNEL VELOCITY

HIGH BAND DISCONTINUITY

HIGH PEAK VELOCITY

EXCELLENT MATCHING FOR OPTICAL MODULATORS AND OTHER OPTICAL DEVICES

REFERENCES

1. T. P. Pearsall, G. Beuchet, J. P. Hirtz, N. Visentin, and M. Bonnet, "Electron and hole mobilities in $Ga_{0.47}In_{0.53}As$" in *GaAs and Related Compounds, Institute of Physics Confrence Ser. No. 56*, 1980, p.639.
2. K. Seo, P. K. Bhattacharya and K. R. Gleason, "DC and microwave characteristics of an $In_{0.53}Ga_{0.47}As/In_{0.52}Al_{0.48}As$ modulation doped quasi MISFET", submitted to *Electronics Letters.*
3. C. Peng, M. I. Aksun, A. A. Kelterson, H. Morkoc and K. R. Gleason, "Microwave performance of InAlAs/InGaAs /InP MODFETs," *IEEE Electron Device Letters*, vol. EDL-8, pp.24-26, 1987.
4. T. Itoh, A. S. Brown, L. H. Gammitz, G. W. Wicks, J. D. Berry and L. F. Eastman, "Delpetion and enhancement mode $Al_{0.48}In_{0.52}As/Ga_{0.47}In_{0.53}As$ modulation doped field effect transistors with recessed gate structure," Proceedings of the 12_{th} International Symposium on GaAs and Related Compounds, pp. 571-576, 1986.

... alloy clustering observed in MBE grown InAlAs system

...inescence linewidth in perfect $In_{0.52}Al_{0.48}As \rightarrow 3$ meV

...bserved linewidth $\rightarrow$ 11 meV

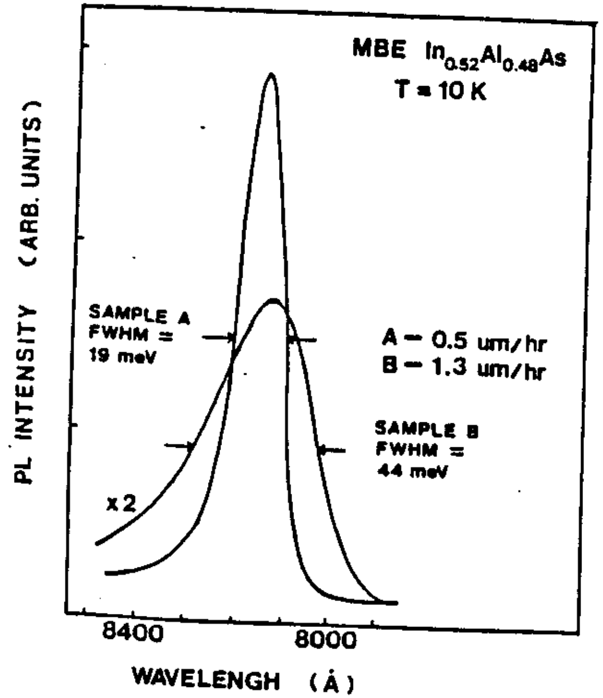

- THEORETICAL LINEWIDTH (limit ~ 3 meV)
  (ALLOY QUALITY)

$$\sigma_B = 2\left(\frac{1.4 C_A^* C_B^* r_c^3}{R_{ex}^3}\right)\Delta_1$$

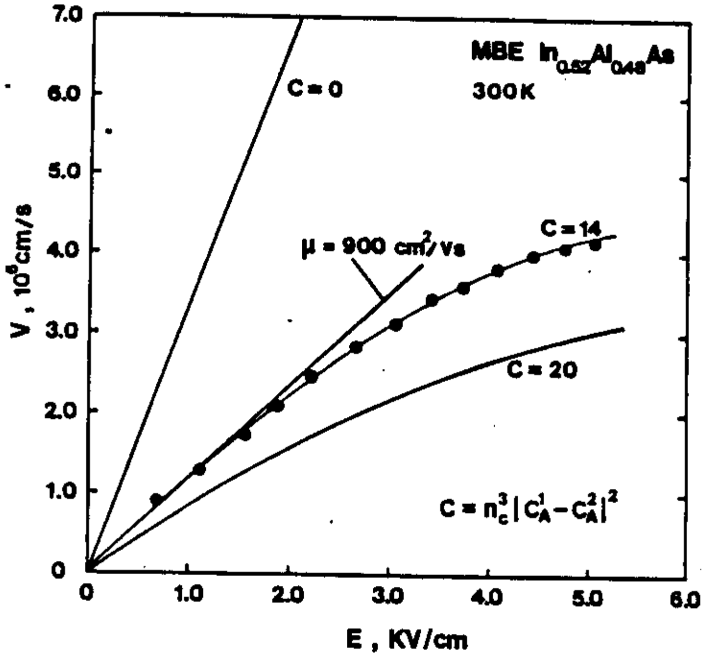

EFFECT OF ALLOY CLUSTERING ON VELOCITY- FIELD CHARACTERIS

C —— CLUSTERING PARAMETER

Semiconductor alloys vs. thin superlattices.

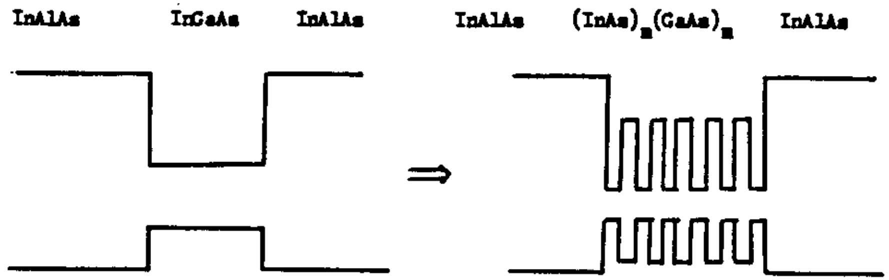

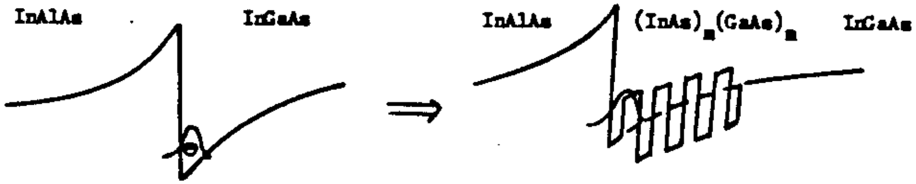

ADVANTAGES OF THIN SUPERLATTICES ⟹ LONG RANGE ORDER

- HIGH MOBILITY
- SHARPER EXCITONIC LINES

DISADVANTAGES ?

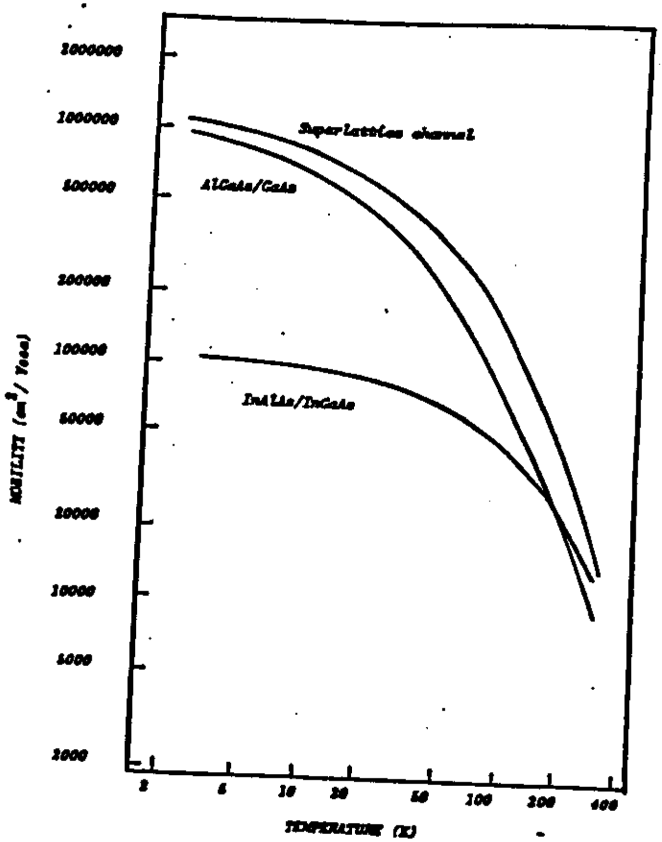

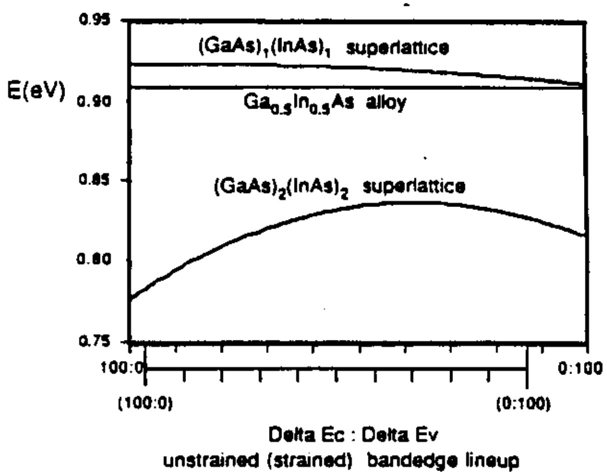

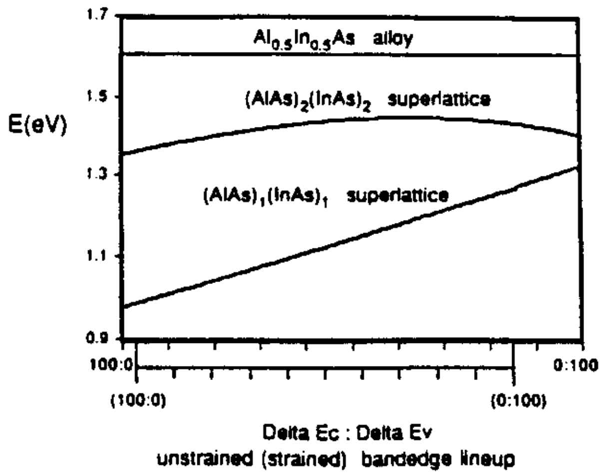

Summary:

- InAlAs grown by MBE expected to have In-rich and Ae-r regions ⟶ Alloy clustering
  ⇓
  Serious effects on μ, V-E relations, exciton linew in narrow quantum wells (< 100 A)
- Thin period superlattices may have strong potentia: active regions of optical and electronic devices.

Ongoing Work:

- Transport in heterostructures -- parallel and perpendicu:
- Role of strain on transport
- Transport studies for Optical switches and detectors.

QUANTUM TRANSPORT MODELING OF THE

RESONANT TUNNELING DIODE

METHOD OF SOLUTION AND APPROXIMATIONS USED

1). Internal state of device described by Wigner distribution function.

2). Irreversibility from interaction with external reservoir is introduced through contact boundary conditions.

3). Quantum effects are included in one dimension only.

4). Effective mass approximation is used.

5). Phonon scattering is introduced to first order (Golden Rule expressions are used for bulk phonon modes).

6). Electron-electron interactions are not included.

SIMULATION METHOD USING THE WIGNER FUNCTION

system state ψ is taken as an incoherent superposition of states :

$$\psi = \sum_j \sqrt{p_j}\psi_j \; ;$$

where ψ_j are pure states with associated probabilities p_j , determined according to quantum statistical mechanics.

Wigner funcion is a transform of states ψ_j :

$$f(x,k) = \frac{1}{\pi}\sum_j p_j \int_{-\infty}^{\infty} dy \psi_j^*(x+y)\psi_j(x-y)e^{2iky}$$

taking time derivative and substituting the Schrödinger equation yields equation for time evolution of f :

$$\frac{\partial f}{\partial t} = -\frac{\hbar k}{m^*} + \frac{1}{\hbar}\int_{-\infty}^{\infty}\frac{dk'}{2\pi}VK(x,k'-k)f(x,k')$$

where : $VK(x,k'-k) =$

$$2\int_0^{\infty} dy \sin([k'-k]y)\,[V(x+y/2) - V(x-y/2)]$$

where $V(x)$ is the potential energy of electrons. Wigner function is the quantum analog of the classical distribution function.

IN DISCRETIZED FORM :

$$\frac{f^f(x,k) - f(x,k)}{\Delta t} =$$

$$-\frac{\hbar k}{m^*}\frac{f^f(x,k) - f^f(x-\Delta x,k)}{\Delta x} + \frac{1}{\hbar NK}\sum_{k'} VK(x,k'-k)f^f(x,k')$$

(for $k > 0$; upwind differencing used for spatial gradient)

USING AN IMPLICIT NUMERICAL METHOD LEADS TO A LARGE SYSTEM OF LINEAR EQUATIONS FOR f^f (FOR THE CASE WITHOUT SELF-CONSISTENCY) :

$$[\underline{M}]_{NX \cdot NK}\, \underline{f}^f = \underline{RHS}$$

SPARSE MATRIX TECHNIQUES ARE USED TO SOLVE THIS SYSTEM.

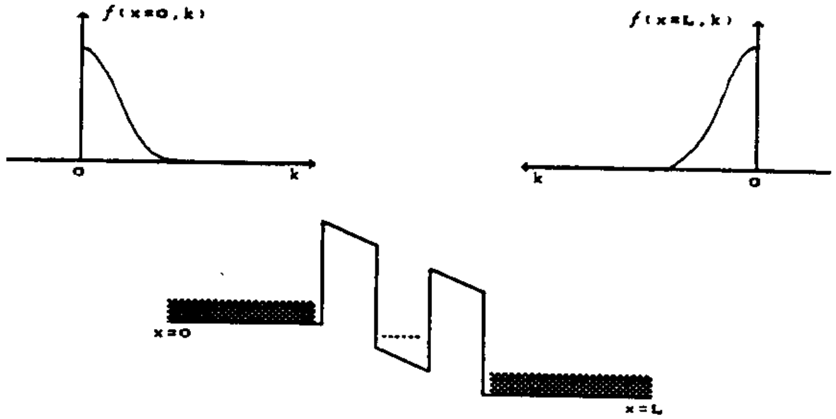

Values of f corresponding to states entering the boundaries are specified :

$$f(o,k) = F(k) \;,\quad k > o$$

$$f(L,k) = F(k) \;,\quad k < o$$

where F(k) is the equilibrium Fermi-Dirac distribution function (integrated over transverse momenta). $f(x,k)$ values at the boundaries for states leaving the device result from the simulation.

These boundary conditions introduce irreversibility into the device + reservoir combination and allow stable, steady-state solutions to be obtained.

METHOD OF SOLVING EQUATIONS

1). Setting $\frac{\partial f}{\partial t} = 0$ yields dc solution (operating point on I-V curve).

2). Including $\frac{\partial f}{\partial t} \neq 0$ yields transient solution starting from some initial state. Switching transients may be calculated ; also, large-signal simulations may be carried out.

3). Expanding f in dc + small-signal parts allows determination of the small-signal equivalent circuit of the device.

B = 28.2Å, W = 45.2Å,
VB = .28eV, T = 300ºK,
V = 0. (GaAs-GaAlAs).

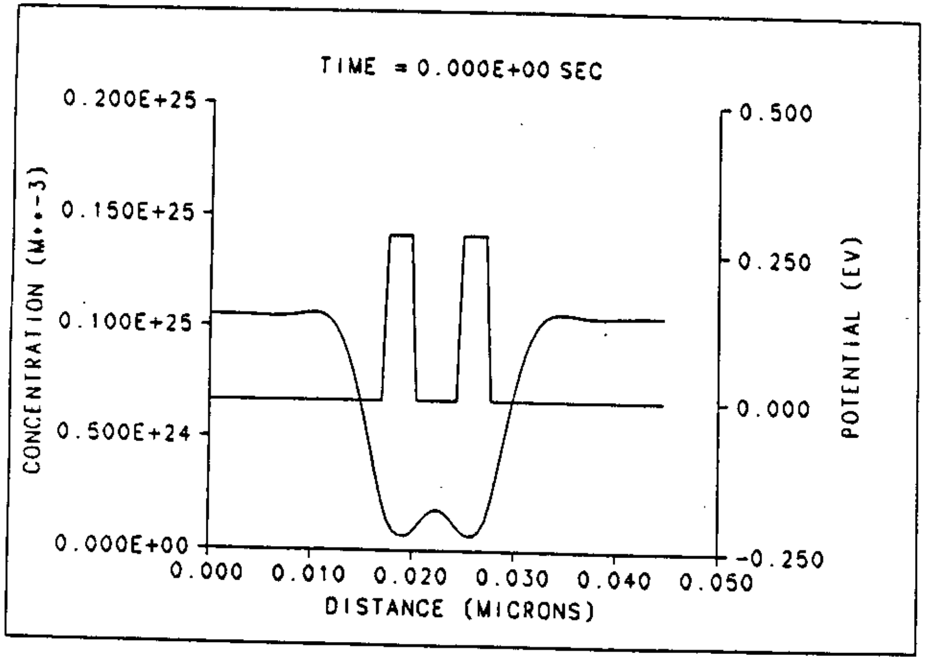

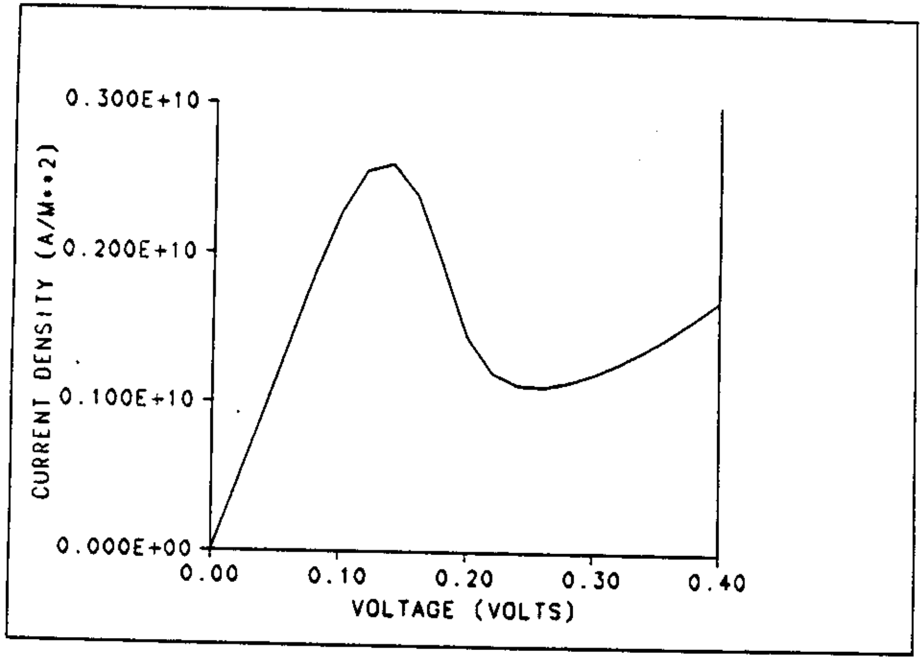

V = -.14 volts

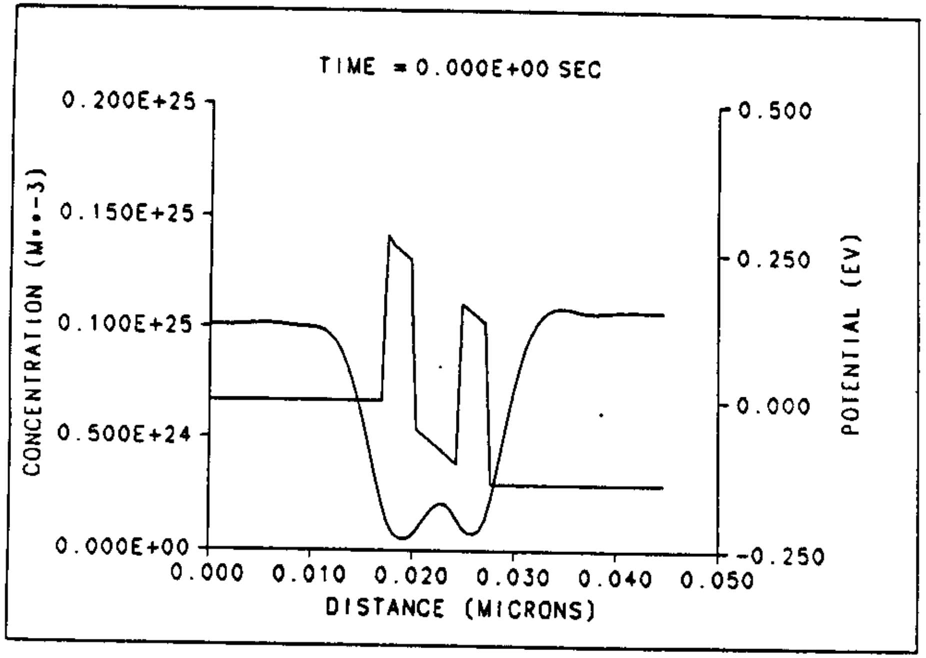

INCLUDING PHONON SCATTERING IN EQUATIONS

Scattering term similar in form to the term appearing in the Boltzmann transport equation is used :

$$\left\{\frac{\partial f(x,k)}{\partial t}\right\}_C = -S_{out}(k)f(x,k) + \sum_{k'} S_{in}(k',k)f(x,k')$$

Including phonon scattering in this way does not change the structure of the matrix; additional coupling among different $f(x,k)$ values in k-space is introduced. Acoustic and polar optic phonons have so far been included.

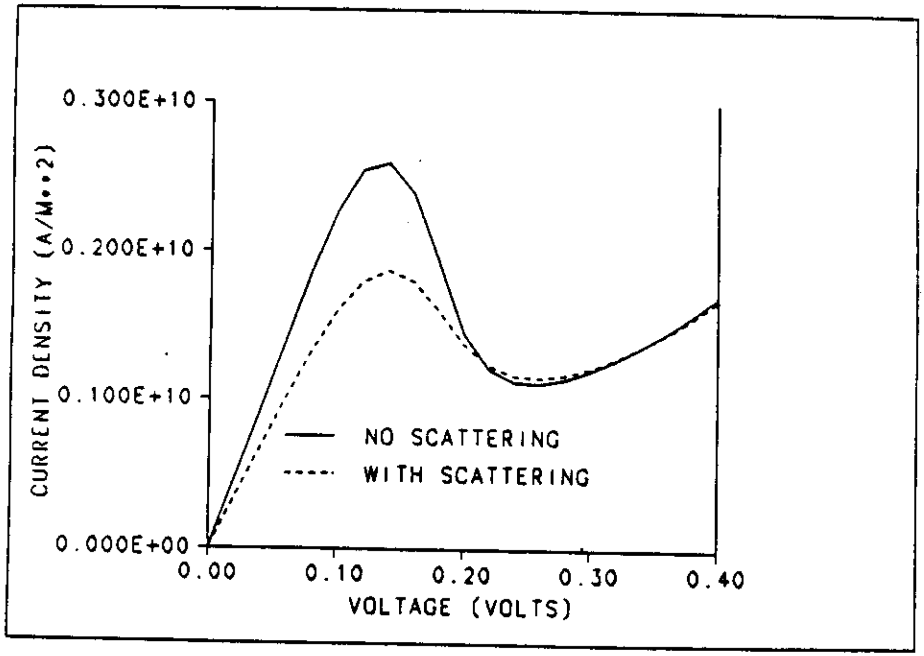

INCLUDING SELF-CONSISTENT POTENTIAL

1). Problem becomes non-linear, since $V(x)$ now depends on carrier density, which is a function of $f(x,k)$.

2). Self-consistent potential equations must be coupled to previous set of $\partial f/\partial t$ equations; the Newton-Raphson iterative method is used to solve the equations.

3). Results show accumulation and depletion regions next to the barriers under applied bias.

4). About half the applied voltage actually appears across the double barrier structure; the remaining voltage appears across the accumulation/depletion regions.

5). Effects of self-consistent potential on I-V curves and small-signal equivalent circuit are currently being studied.

SELF-CONSISTENT POTENTIAL EQUATIONS

1. POTENTIAL EQUATIONS

($V = \int \mathcal{E} dx$, where V = electron potential) :

$$V_{NX} - V_{NX-1} = \frac{1}{2}(\mathcal{E}_{NX-1} + \mathcal{E}_{NX}) \cdot \Delta x + \overline{V}_{NX} - \overline{V}_{NX-1}$$

•

•

•

$$V_2 - V_1 = \frac{1}{2}(\mathcal{E}_1 + \mathcal{E}_2) \cdot \Delta x + \overline{V}_2 - \overline{V}_1$$

$$V_1 = \overline{V}_1$$

2. ELECTRIC FIELD EQUATIONS

$\left(\frac{\partial \mathcal{E}}{\partial x} = \frac{\rho}{\epsilon}\right)$:

$$\mathcal{E}_{NX} - \mathcal{E}_{NX-1} = \frac{q\Delta x}{2\epsilon}\left[N_{NX} + N_{NX-1} - \Delta k \sum_{i=1}^{NK} (f(NX,i) + f(NX-1,i\right.$$

•

•

•

$$\mathcal{E}_2 - \mathcal{E}_1 = \frac{q\Delta x}{2\epsilon}\left[N_2 + N_1 - \Delta k \sum_{i=1}^{NK} (f(2,i) + f(1,i))\right]$$

$$[.5\mathcal{E}_1 + \mathcal{E}_2 + \ldots + \mathcal{E}_{NX-1} + .5\mathcal{E}_{NX}] \cdot \Delta x = V_{applied} + \overline{V}_1 - \overline{V}_{NX}$$

3. CONDITIONS ON k_{0L}, k_{0R}

(shifts of equilibrium distributions at contacts) :

$$\frac{\hbar k_{0L}}{m^*} = \mu \mathcal{E}_1$$

$$\frac{\hbar k_{0R}}{m^*} = \mu \mathcal{E}_{NX}$$

(μ = low-field mobility)

T = 300°K, V = 0.,
with scattering and
self-consistency.

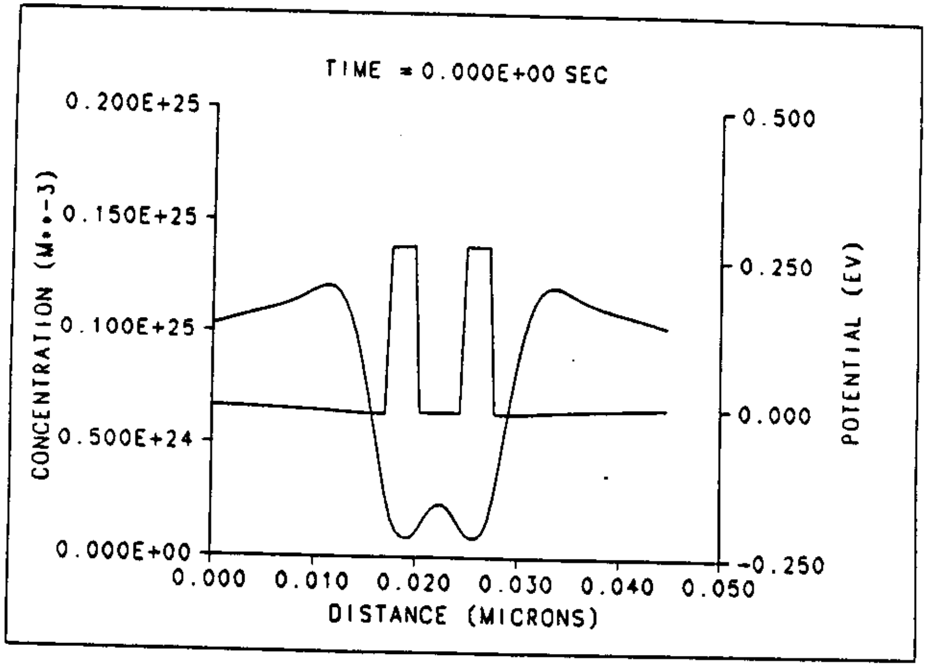

V = -0.28 volts, with scattering and self-consistency

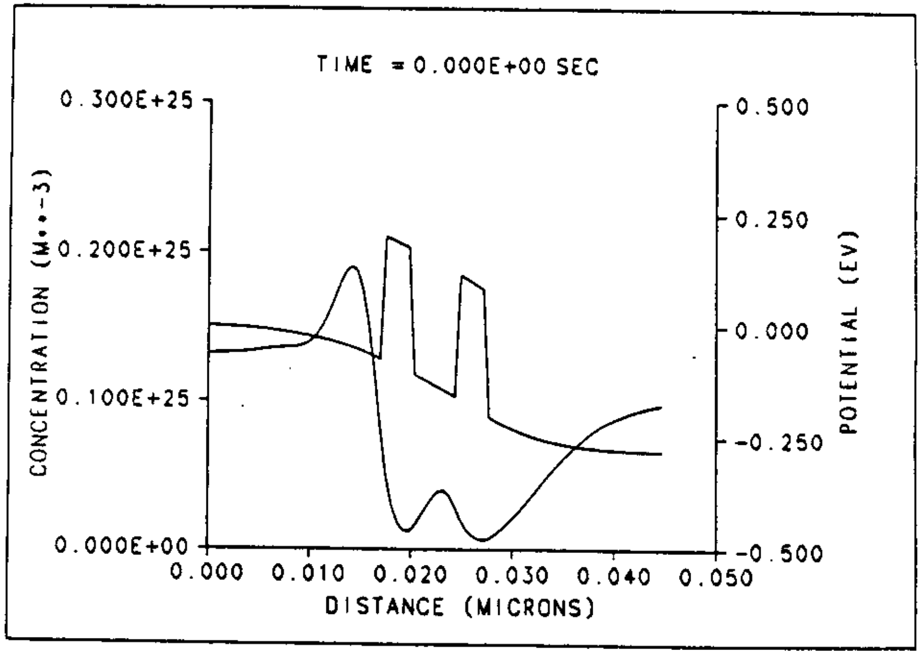

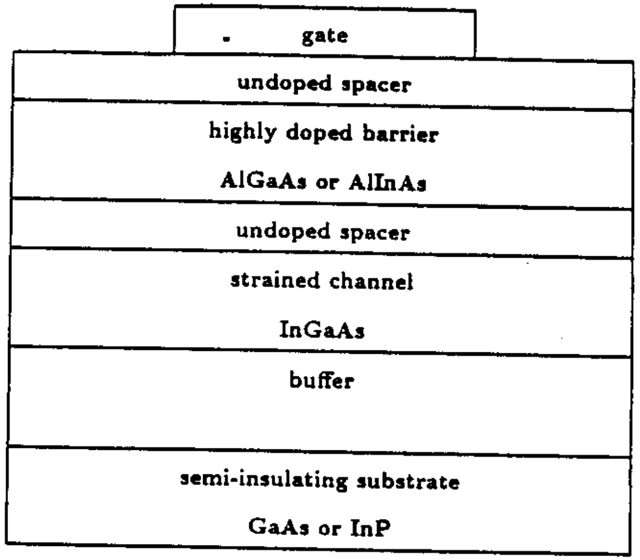

General structure of the pseudomorphic MODFET.

Why study strained MODFETs?

- Selective straining a semiconductor allows a degree of band tailorability to create materials with properties not readily available in lattice matched materials systems.
- Expected improvements in pseudomorphic MODFET performance over lattice matched MODFET performance may come in the following areas:
  - Higher band discontinuities at heterojunctions.
  - Better carrier confinement.
  - Higher mobility - lower access resistance.
- Strained MODFETs are a good tool to study carrier transport in a strained environment.

n-MODFET	p-MODFET
Strained channel material properties (electron masses) via a tight binding formalism	Deformation potential theory and the Kohn Luttinger hamiltonian
⇓	⇓
Schrödinger equation for the one band electron states solved self consistently with the Poisson equation	Four band Schrödinger equation for hole states solved self consistently with the Poisson equation
⇓	⇓
Subband levels, carrier density, and subband occupation	Subband levels, hole masses, carrier density, and band occupation.

Flow chart of modeling procedure for n- and p-type pseudomorphic MODFETs.

The Schrödinger Equation for Electrons

$$-\frac{\hbar^2}{2\overline{m}^*}\nabla^2\Psi_n(\mathbf{k}_\|, z) + V(z)\Psi_n(\mathbf{k}_\|, z) = E_n\Psi_n(\mathbf{k}_\|, z)$$

$$\Psi^n_{electron}(\mathbf{k}_\|, z) = \Psi_n(z)u_o(r)e^{i\mathbf{k}_\|\cdot\rho}$$

The Schrödinger Equation for Holes

$$\begin{bmatrix} H_{hh} & c & b & 0 \\ c^* & H_{lh} & 0 & -b \\ b^* & 0 & H_{lh} & c \\ 0 & -b^* & c^* & H_{hh} \end{bmatrix} \begin{bmatrix} \Phi_{\frac{3}{2}\frac{3}{2}} \\ \Phi_{\frac{3}{2}\frac{1}{2}} \\ \Phi_{\frac{3}{2}\frac{-1}{2}} \\ \Phi_{\frac{3}{2}\frac{-3}{2}} \end{bmatrix} = E \begin{bmatrix} \Phi_{\frac{3}{2}\frac{3}{2}} \\ \Phi_{\frac{3}{2}\frac{1}{2}} \\ \Phi_{\frac{3}{2}\frac{-1}{2}} \\ \Phi_{\frac{3}{2}\frac{-3}{2}} \end{bmatrix}$$

$$\begin{aligned}
H_{hh} &= -\frac{\hbar^2}{2m_o}\left[(k_x^2 + k_y^2)(\gamma_1 + \gamma_2) \; - \; (\gamma_1 - 2\gamma_2)\frac{\partial^2}{\partial^2 z}\right] + V(z) + \frac{1}{2}\delta_{sh} \\
H_{lh} &= -\frac{\hbar^2}{2m_o}\left[(k_x^2 + k_y^2)(\gamma_1 - \gamma_2) \; - \; (\gamma_1 + 2\gamma_2)\frac{\partial^2}{\partial^2 z}\right] + V(z) - \frac{1}{2}\delta_{sh} \\
c &= \frac{\sqrt{3}\hbar^2}{2m_o}\left[\gamma_2(k_x^2 - k_y^2) \; - \; 2i\gamma_3 k_x k_y\right] \\
b &= \frac{\sqrt{3}\hbar^2}{m_o}(-k_y - ik_x)\gamma_3\frac{\partial}{\partial z}
\end{aligned}$$

$$\Psi^n_{hole} = \sum_\nu \phi^\nu_n(\mathbf{k}_\|, z)u^\nu_o(r)e^{i\mathbf{k}_\|\cdot\rho}$$

The Charge Control Model

Poisson + Schrödinger

$$\nabla^2 V(z) = -\frac{\rho(z)}{\epsilon(z)}$$

$$\rho(z) = N_d(z) - N_a(z) - n_{free}(z) + p_{free}(z) - \sum_i n_i\phi_i^*(z)\phi_i(z)$$

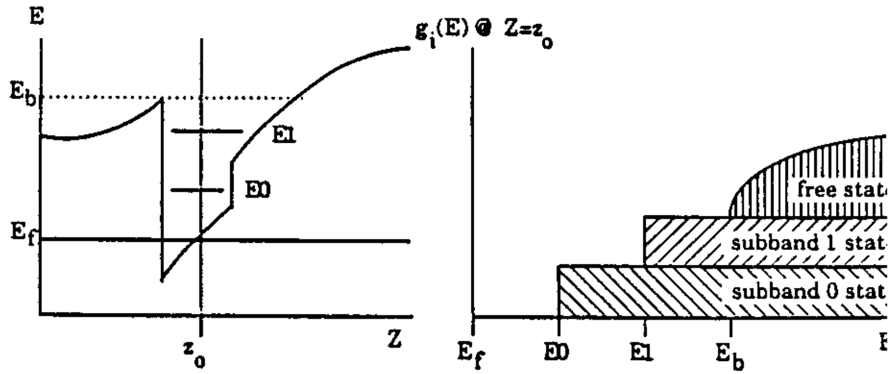

Simulation # 1	Simulation # 2
0.8V Schottky contact	0.8V Schottky contact
100 Å undoped $In_{0.52}Al_{0.48}As$	100 Å undoped $Al_{0.30}Ga_{0.70}As$
200 Å doped 2x10[18] $In_{0.52}Al_{0.48}As$	200 Å doped 2x10[18] $Al_{0.30}Ga_{0.70}As$
100 Å undoped $In_{0.52}Al_{0.48}As$	100 Å undoped $Al_{0.30}Ga_{0.70}As$
100 Å undoped $In_{0.53+x}Ga_{0.47-x}As$	100 Å undoped $In_xGa_{1-x}As$
400 Å undoped $In_{0.53}Ga_{0.47}As$	400 Å undoped GaAs
undoped $In_{0.52}Al_{0.48}As$	undoped $Al_{0.30}Ga_{0.70}As$
InP substrate	GaAs substrate

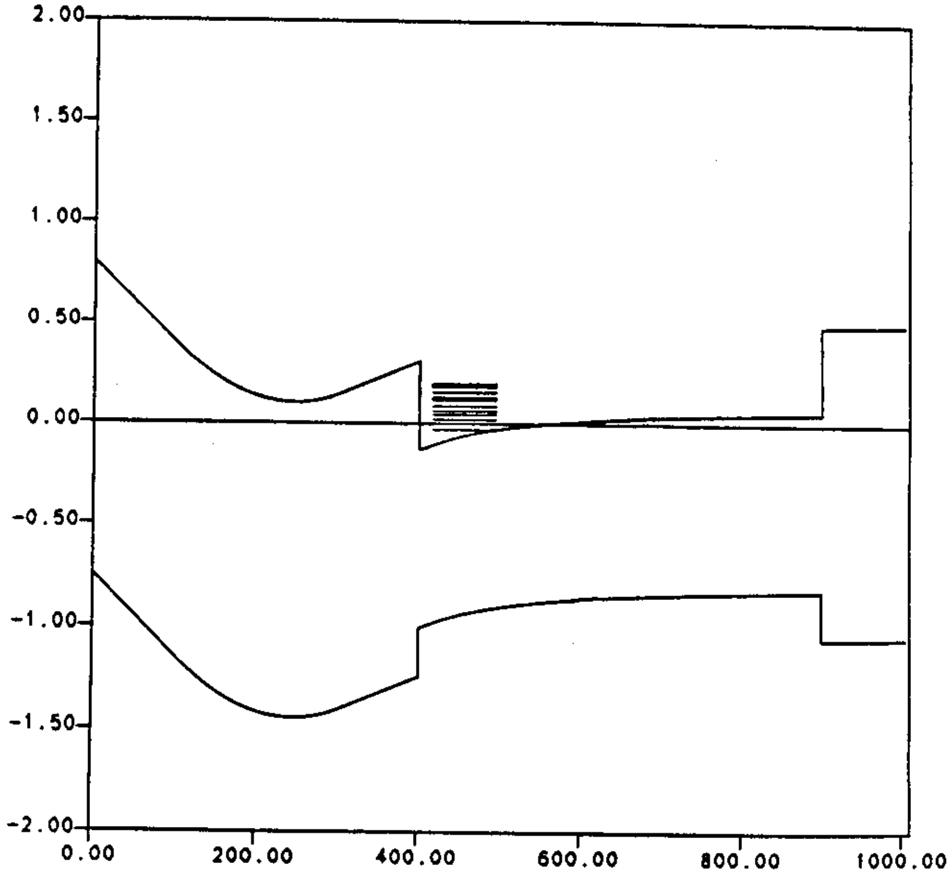

Conduction and valence bands and two dimensionally confined electron subbands in a $In_{0.52}Al_{0.48}As$ / $In_{0.53}Ga_{0.47}As$ / InP lattice matched MODFET.

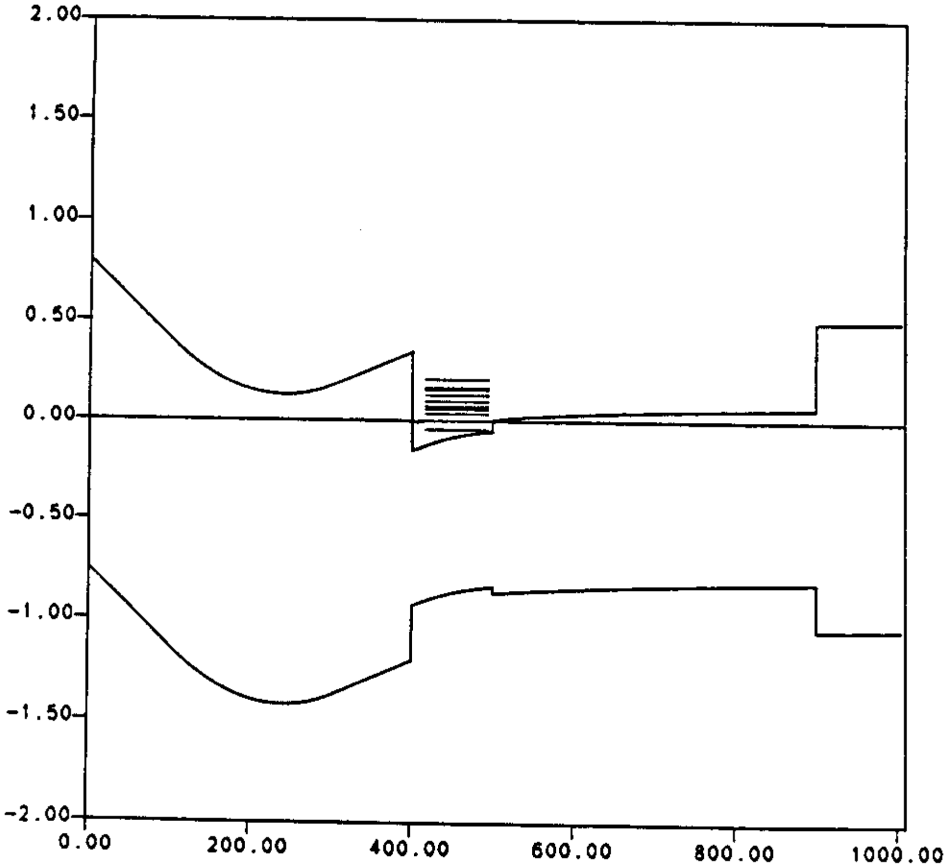

Conduction and valence bands and two dimensionally confined electron subbands in a $In_{0.52}Al_{0.48}As$ / $In_{0.65}Ga_{0.35}As$ / $In_{0.53}Ga_{0.47}As$ / InP pseudomorphic MODFET.

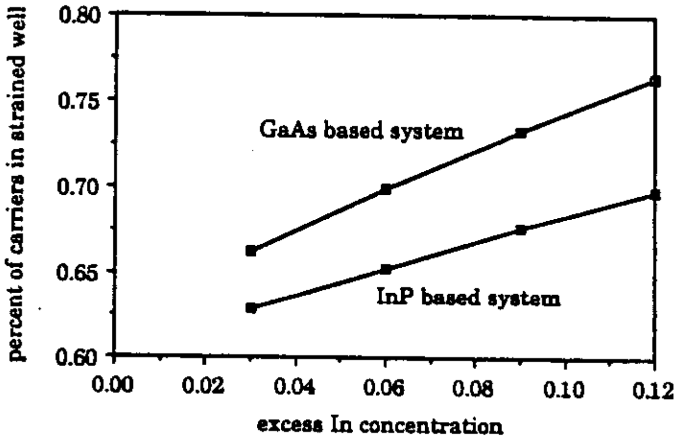

Spatial confinement in a strained well increases with added In.

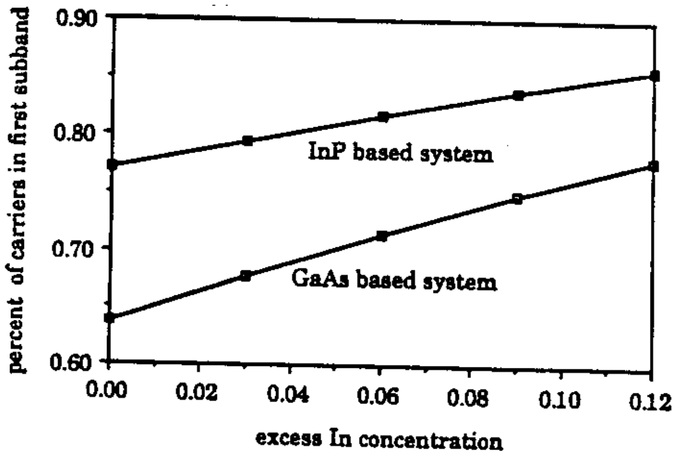

Confinement of carriers into the lowest energy subband also improves with added In in the channel region.

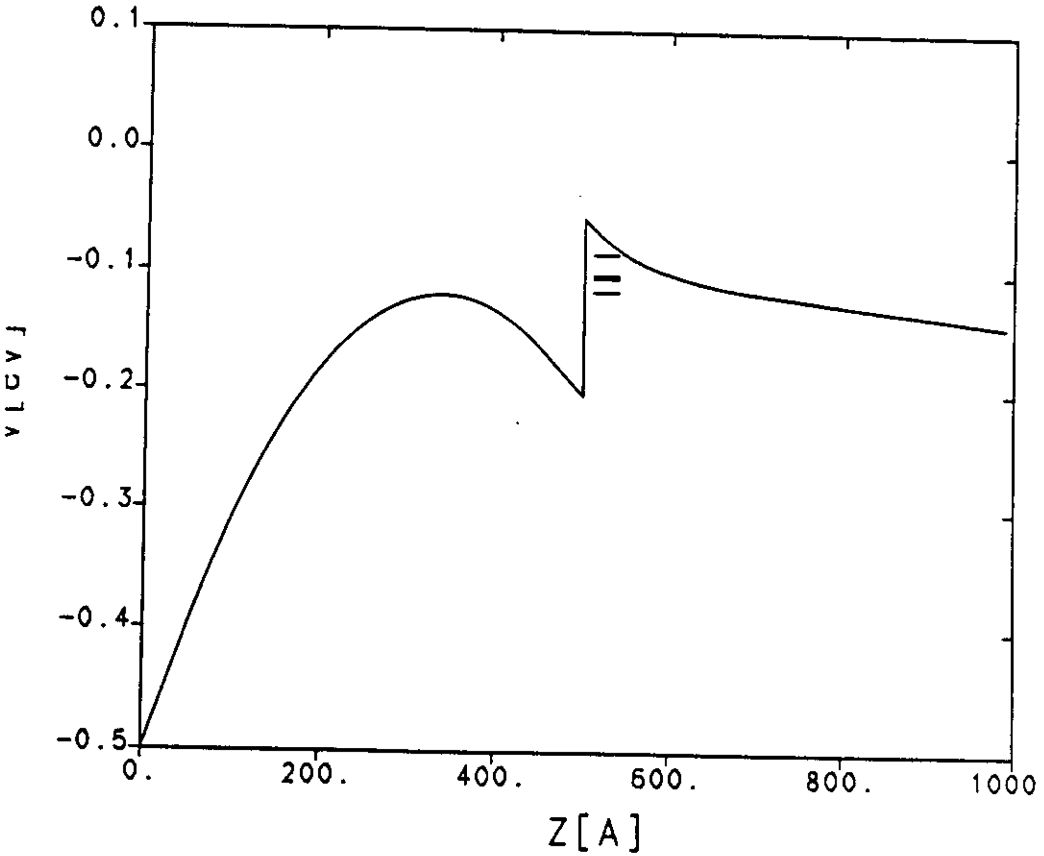

Valence band profile of a lattice matched p-type MODFET.

5m LM

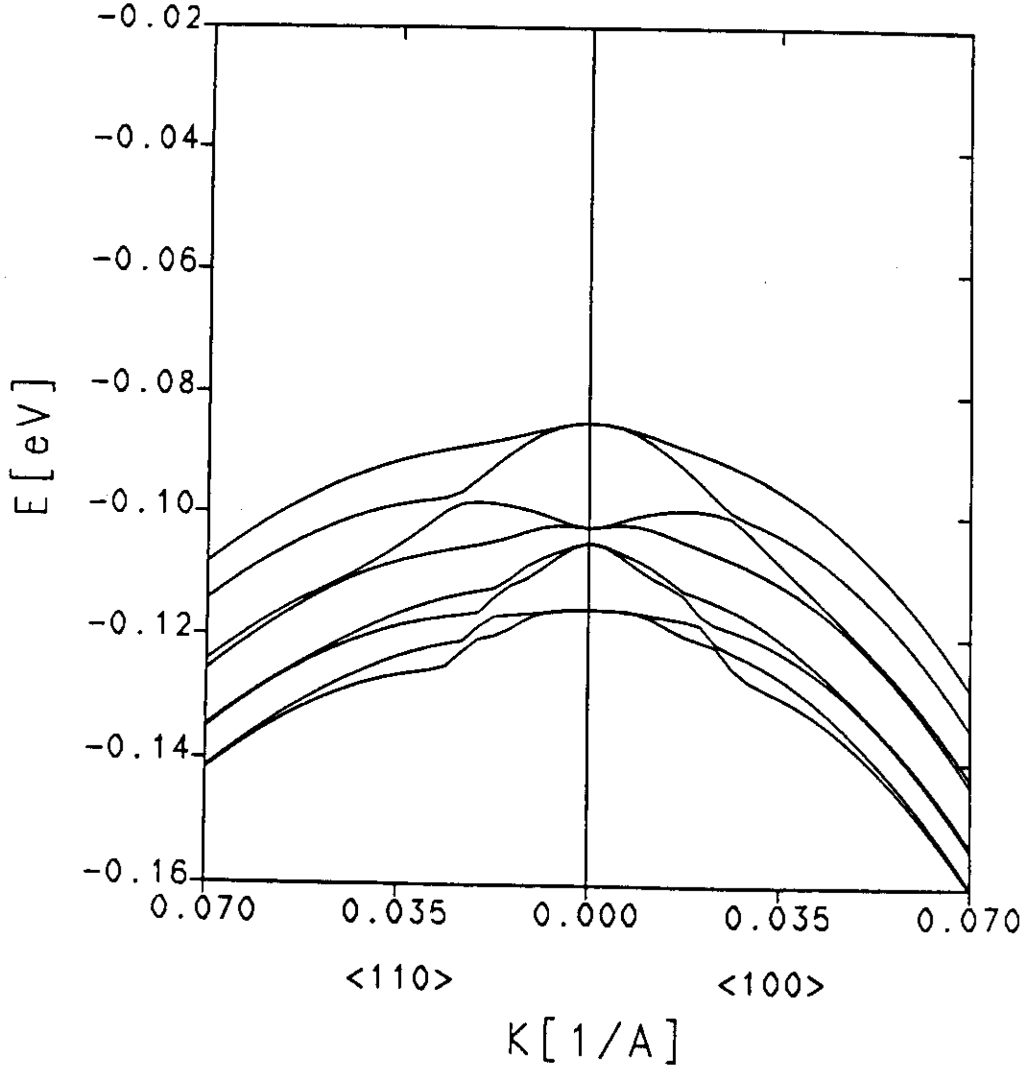

Hole band dispersion relationships in a lattice matched p-type MODFET.

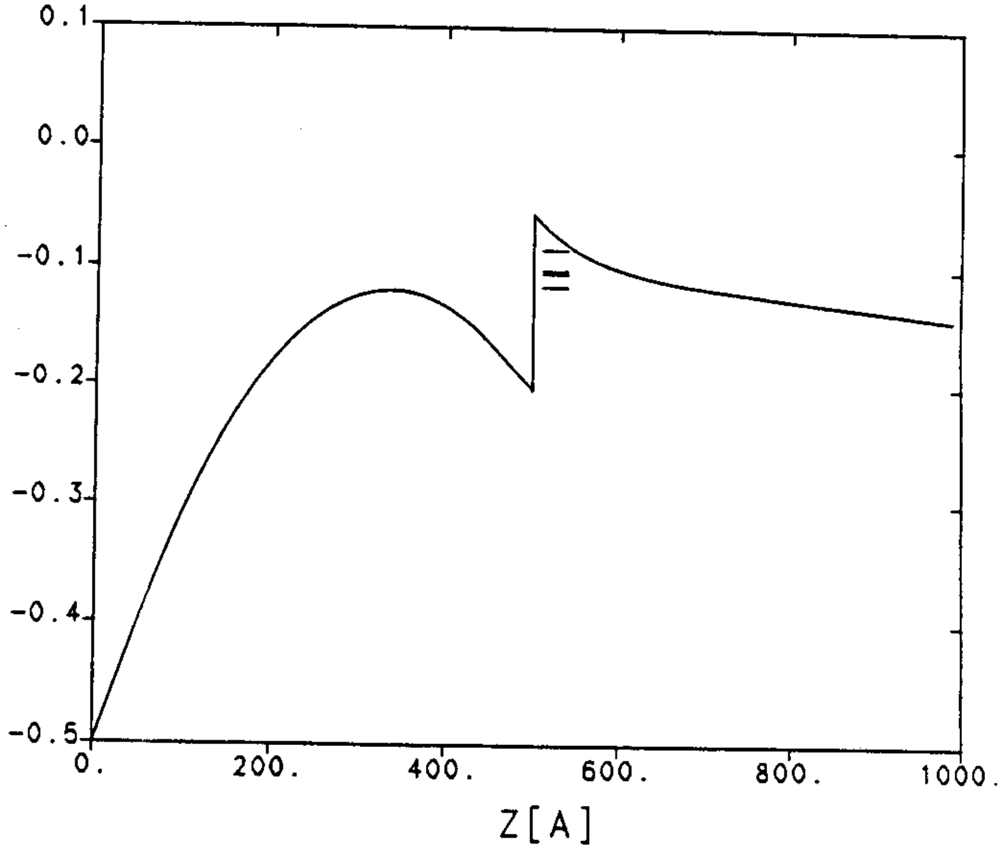

Valence band profile of a lattice matched p-type MODFET.

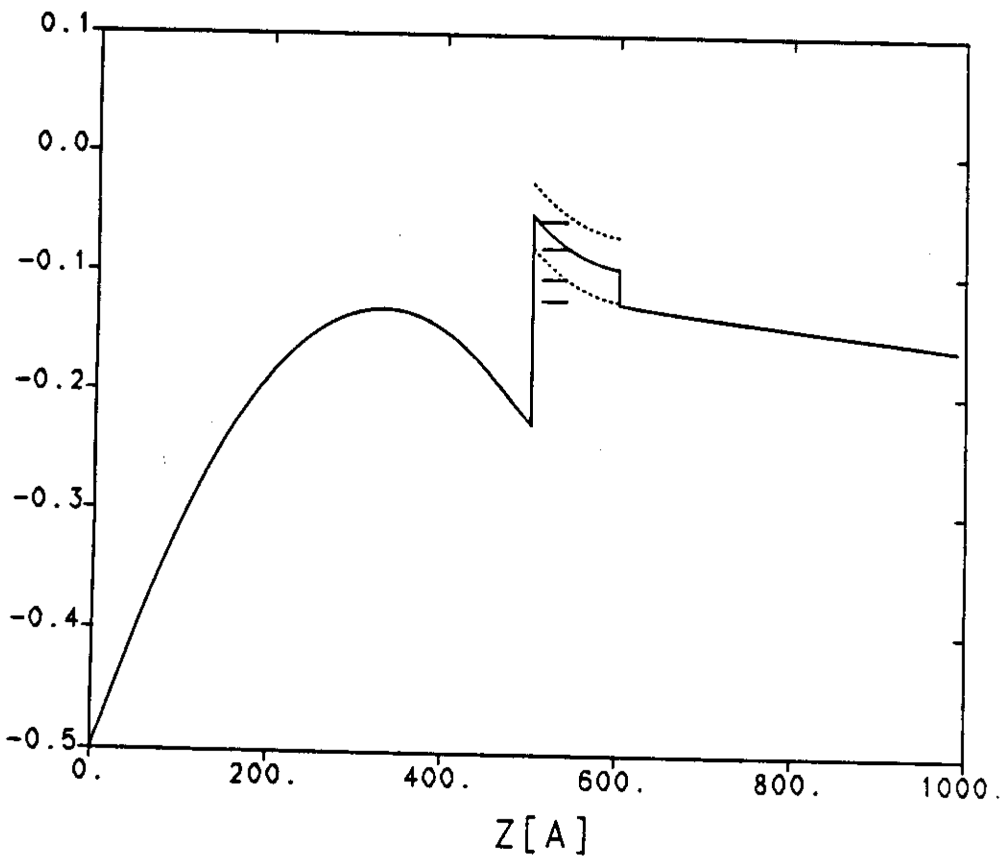

Valence band profile of a pseudomorphic p-type MODFET. Strain has altered the bandgap and split the light and the heavy hole bands.

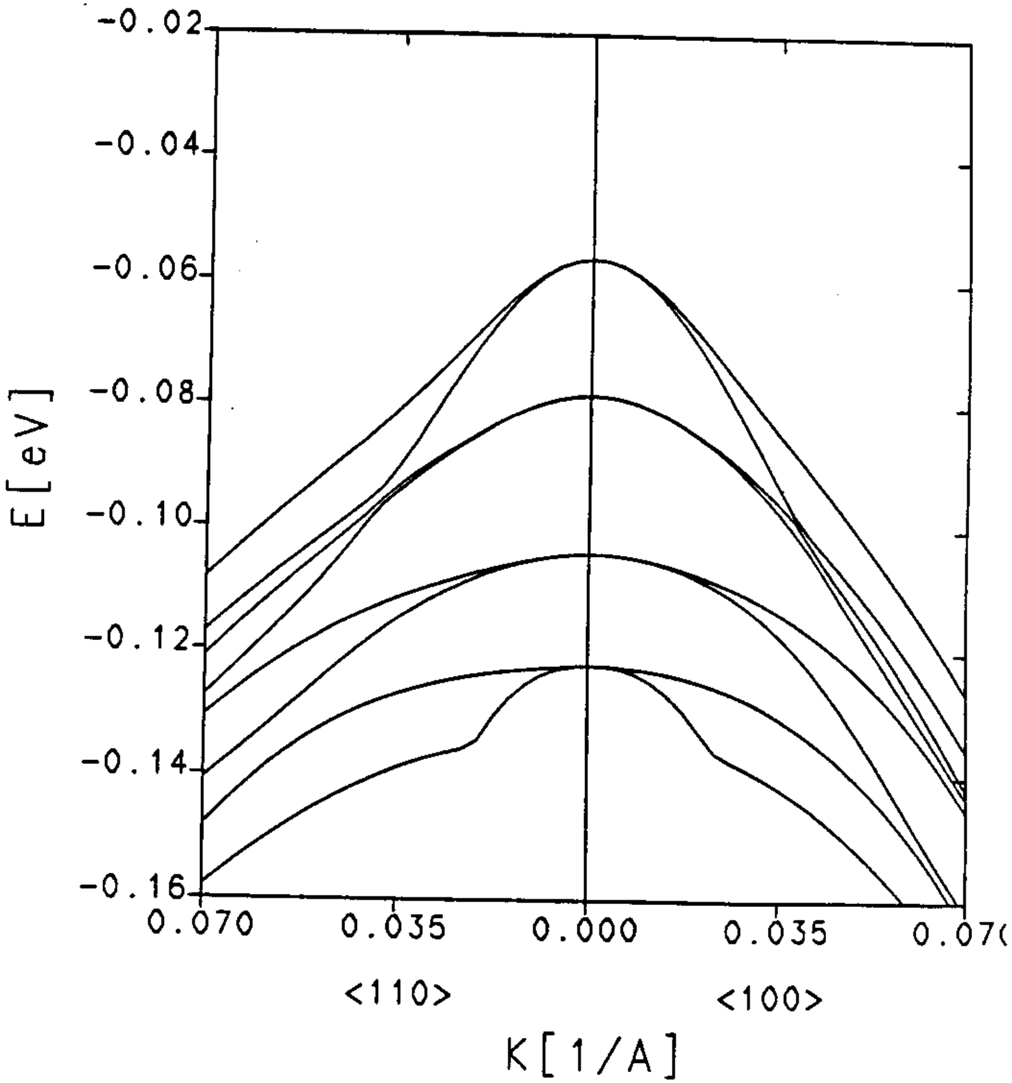

Hole band dispersion relationships in a pseudomorphic p-type MODFET. Strain has decreases the interaction between the light and the heavy hole states dramatically reducing the effective mass of the uppermost hole bands.

Summary:

- One dimensional charge control simulation can show many important features of both n- and p-type MODFETs.
- Pseudomorphic n-type MODFETs appear to be advantageous because of higher channel mobility resulting from better carrier confinement and lower carrier effective mass.
- Pseudomorphic p-type MODFETs appear to be advantageous because of the strain induced splitting of the light and the heavy hole subbands which significantly lowers the effective mass.

Figures of Merit for Device Performance

(1) $f_T=(g_{m,ext})/(2\pi C_{gs})$

Maximize f_T by $g_{m,ext}\uparrow$, $C_{gs}\downarrow$
while considering C_{dg}, R_i

(2) $g_{m,ext}=(g_{m,int})/(1+R_s g_{m,int})$

For high $g_{m,ext}$, it is necessary to:
$g_{m,int}\uparrow$, $R_s\downarrow$.

(3) Mobility and Velocity enchancement for devices to operate at mm-wavelenths.

(4) Sheet density increase for high-current, high power devices.

v

Motivation for Pseudomorphic Devices

(A) $Al_xGa_{1-x}As/GaAs$ MODFET

Advantages: Decreased ionized-impurity scattering
--> higher low field mobility and saturation velocity.

Performance: L_g=0.25μm, T=300K
g_m=430mS/mm, f_T=80GHz, f_{max}=120GHz
Noise Figure=2.7dB(associated gain 3.8dB)@62GHz

Disadvantages: High Al %
--> Persistent Photoconductivity Effect (PPC) and Uncontrolled Threshold (V_T) Shifts at cryogenic T.

(2) $Al_{0.15}Ga_{0.85}As/In_{0.15}Ga_{0.85}As$ Pseudomorphic MODFET

Advantages:
(a) Small Al % fraction <u>BUT</u> similar ΔE_C.
(b) Higher doping density due to reduced donor compensation (small Al %)
(c) Higher V_{sat}. (InGaAs vs. GaAs)

Perfromance: L_g=0.25μm, T=300K
g_m=495mS/mm, f_{max}=250GHz
Noise Figure=2.4dB(associated gain 4.4dB)@62GHz

Disadvantages: Low InAs mole fraction thus no full advantage of InGaAs.

(3) $In_{0.52}Al_{0.48}As/In_{0.53}Ga_{0.47}As$ MODFET

<u>(Lattice Matched to InP)</u>

Advantages: Increase InAs mole fraction thus exploit the superior transport properties of InGaAs.

- $\Delta E_C \uparrow$ and $n_s \uparrow$.
- $\mu \uparrow$.
- $V_{peak} \uparrow$.
- Γ-L separation↑.
- Reduced PPC and uncontrolled V_T shift.
- Better carrier confinement.
- Compatible with photonic devices(1.3-1.5μm).

Performance: L_g=1μm
$g_{m,ext}$(T=300K)=440mS/mm
$g_{m,ext}$(T=77K)=700mS/mm
Expected f_T=100GHz for submicron devices

(4) $In_{0.52}Al_{0.48}As/In_{0.53+x}Ga_{0.47-x}As$ MODFET

(Strained Channel)

Advantages: Increased InAs mole fraction → better electron transport properties than with 53% In.

Performance: L_g=1.6μm, $g_{m,ext}$=271mS/mm, f_T=23.5GHz

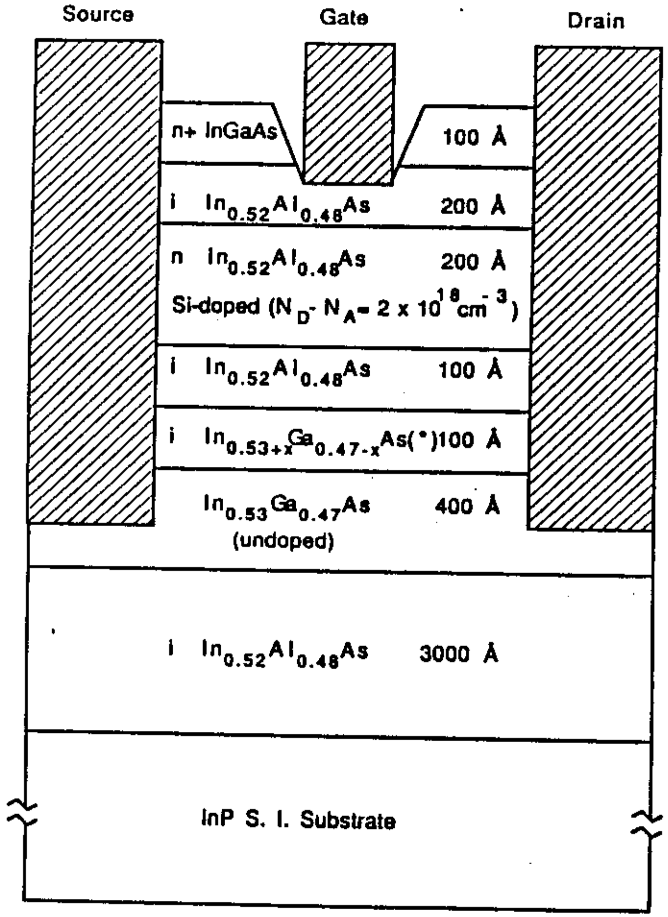

(*) 453 : x = 0
454 : x = 0.07
455 : x = 0.12

Device Optimization

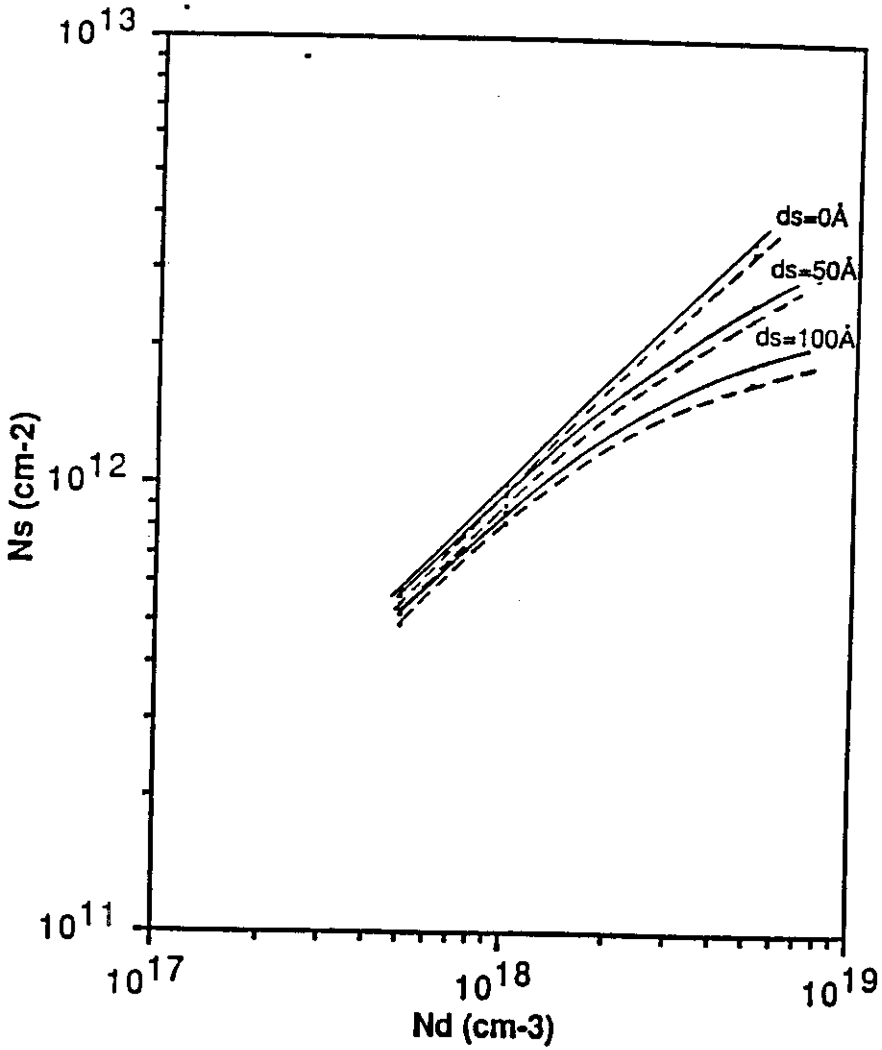

Total sheet density (n_s) in the well as a function of doping N_d for various spacers (d_s). (— strained, - - - lattice-matched)

(Donor layer thickness chosen for no-parasitic conduction)

- N_s depends primarily on N_d, d_{spacer}
- Strain has no major influence on N_s

Sheet density Ns and % $\frac{\text{carriers in strained channel}}{\text{total number of carriers in well}}$

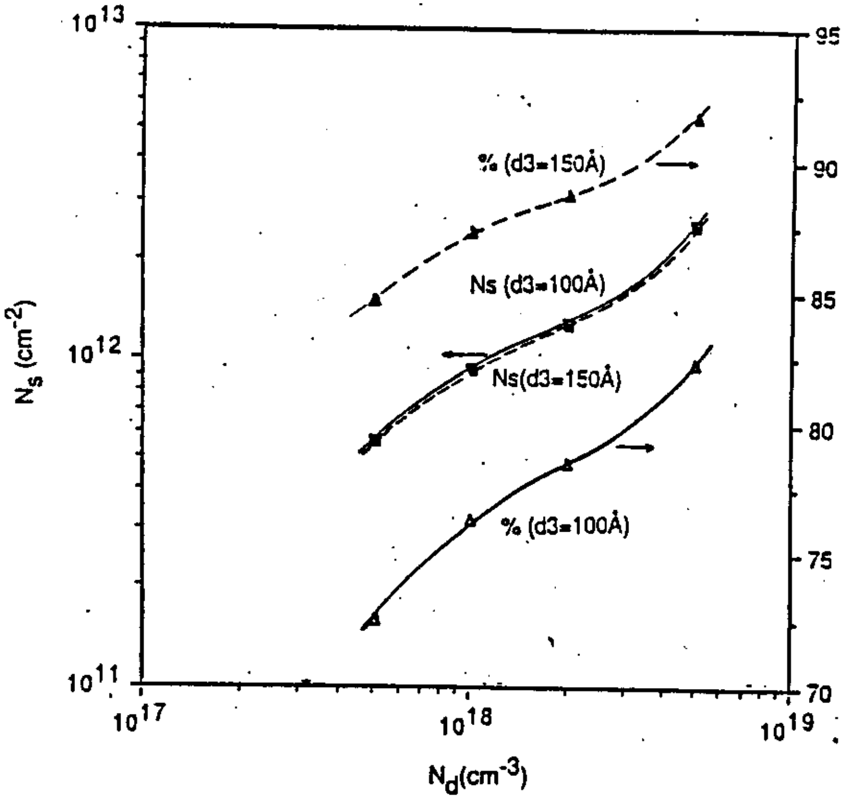

- Strained channel thickness (d_3) does not influence Ns
- Strained channel thickness (d_3) influences % of carriers in high InAs region

--> Improved mobility by <u>strained</u>, <u>thick</u> channels

Percentage of first subband occupation in the well (d_3+d_4) under lattice-matched and strained conditions for 100Å and 150Å strained channel thickness

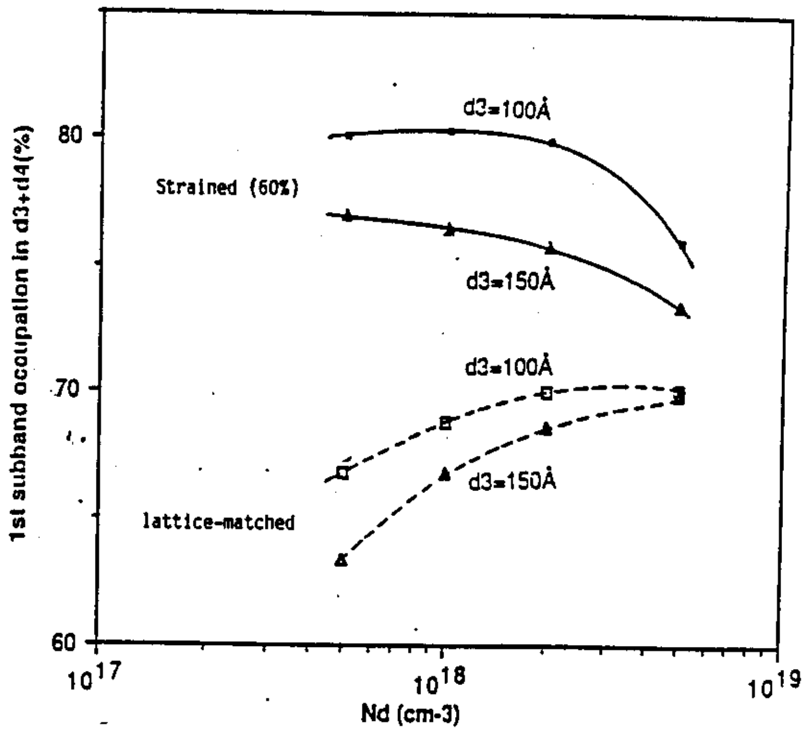

- Higher occupation with strain
- First subband occupation better with thin (100Å) channels (pronounced band splitting)

  --> Better confinement and thus R_{ds}, g_m improvement by <u>strained</u>, <u>thin</u> channels

Note: COMPROMISE <u>in strained channel thickness choices</u> for good μ, R_{ds}, g_m.

Cross sectioin of New Design for Lattice-Matched and Strained InAlAs/InGaAs MODFETs

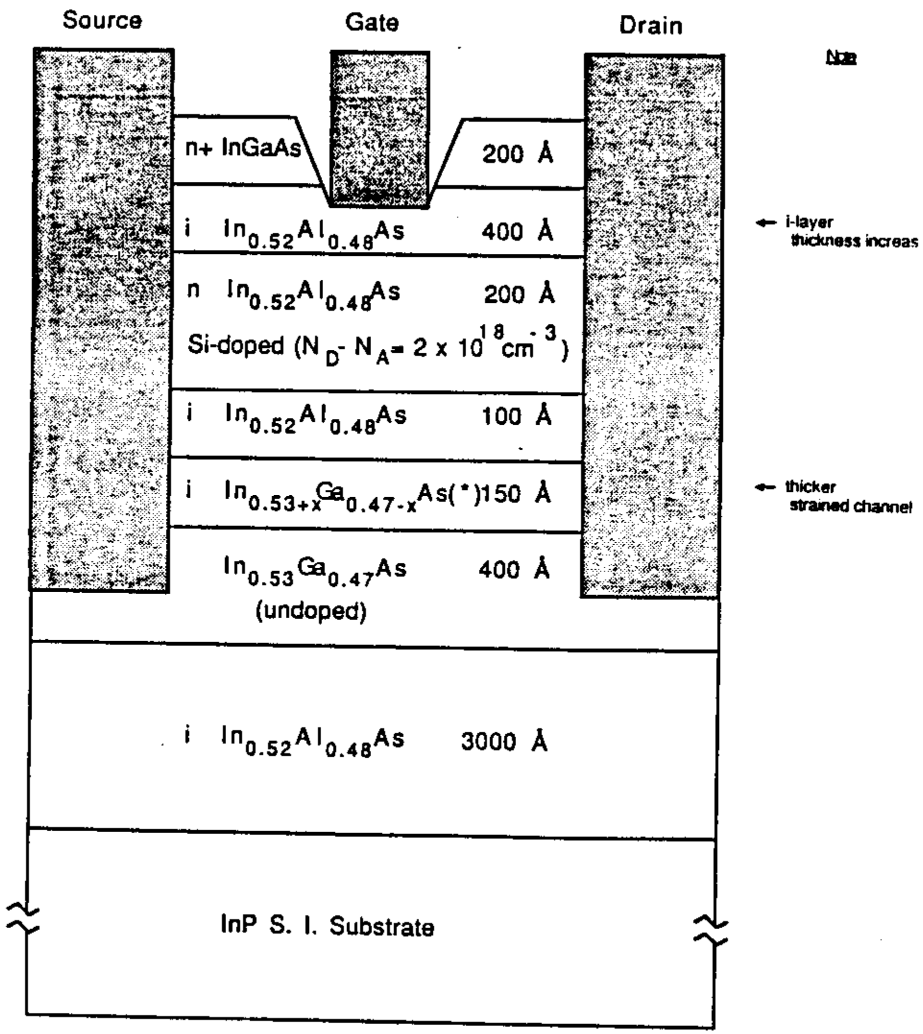

(*) 1058 : x = 0
1062 : x = 0.07
1063 : x = 0.12

Enhanced Low-Field Mobility With Strained N-Channels

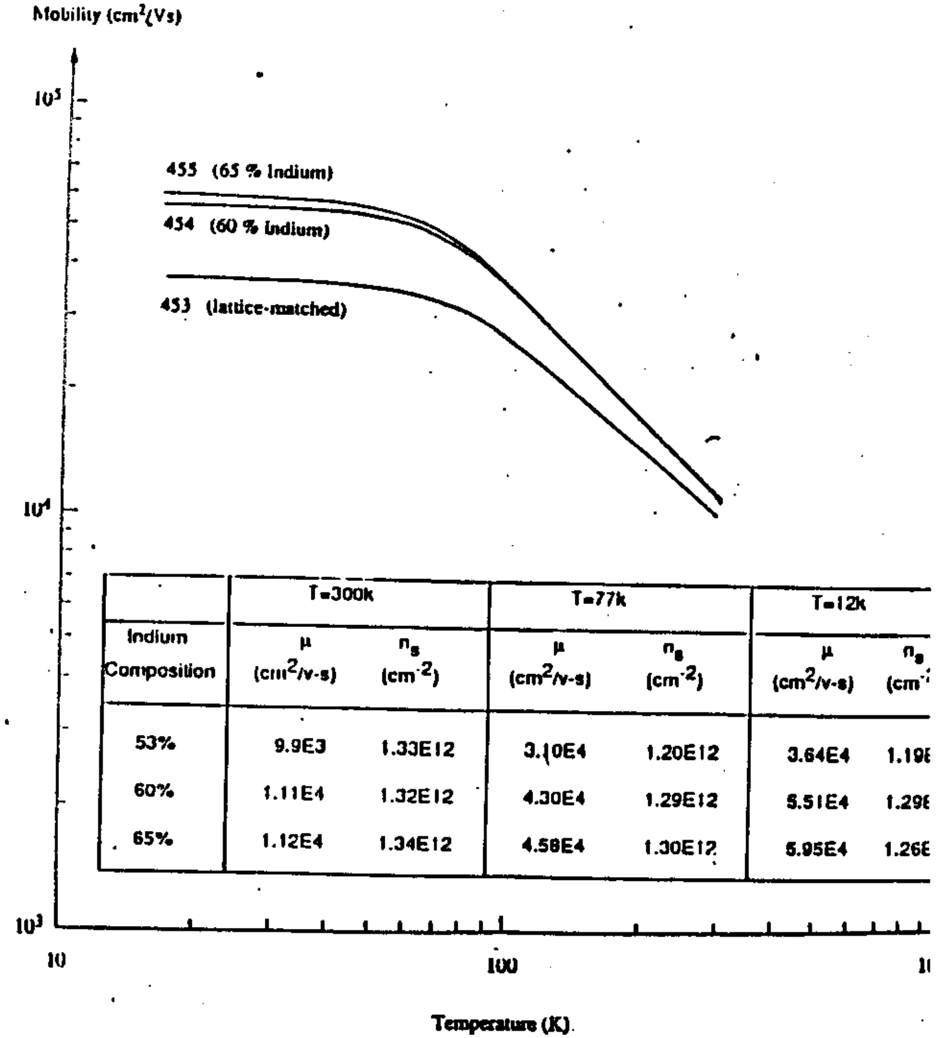

	T=300k		T=77k		T=12k	
Indium Composition	μ (cm²/v-s)	n_s (cm^{-2})	μ (cm²/v-s)	n_s (cm^{-2})	μ (cm²/v-s)	n_s (cm
53%	9.9E3	1.33E12	3.10E4	1.20E12	3.64E4	1.19E
60%	1.11E4	1.32E12	4.30E4	1.29E12	5.51E4	1.29E
65%	1.12E4	1.34E12	4.58E4	1.30E12	5.95E4	1.26E

Improving Maximum Transconductance with Strain
(L_g=1.5μm, V_{ds}=2.5v, T=300K)

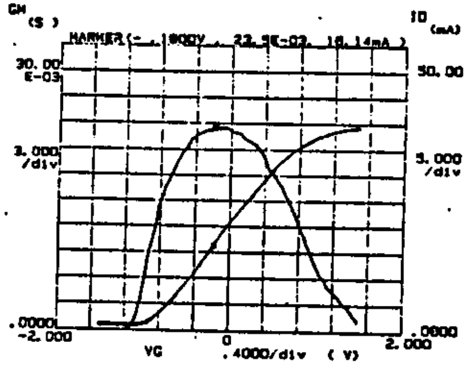

53% In
$g_{m,ext}|_{max}$=157 mS/mm

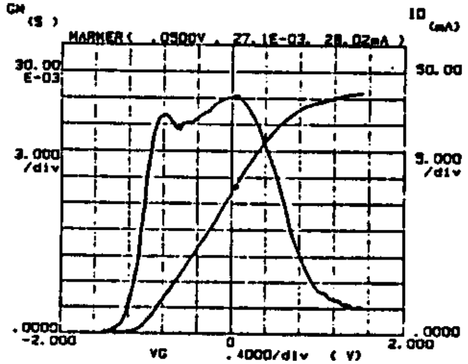

60% In
$g_{m,ext}|_{max}$=180 mS/mm

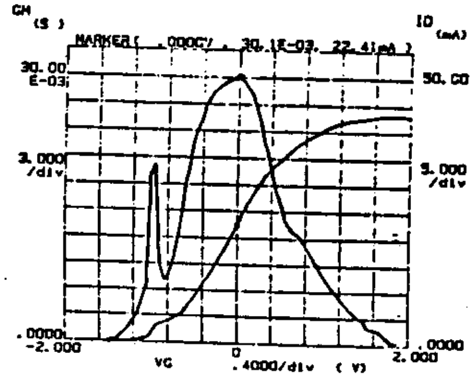

65% In
$g_{m,ext}|_{max}$=201 mS/mm

Performance of N-channel InAlAs/InGaAs MODFET with and without strain (tests on 1.5x150μm devices)

53% Indium

V_T= -1.0 V
At V_{gs}= -0.2 v, $g_{m,int}$(max) =191 mS/mm
I_{ds} =108 mA/mm

60% Indium

V_T= -1.2 V
At V_{gs}= 0.0 V, $g_{m,int}$(max) =321 mS/mm (40% Improvement)
I_{ds} =187 mA/mm

65% Indium

V_T= -1.2 V
At V_{gs}= -1.2 V, $g_{m,int}$(max) =359 mS/mm (47% Improvement)
I_{ds} =149 mA/mm

Transconductance (G_m) versue V_{ds} at different gate bias
For Lattice-Matched (53% In) and Strained (60% In) MODFETS

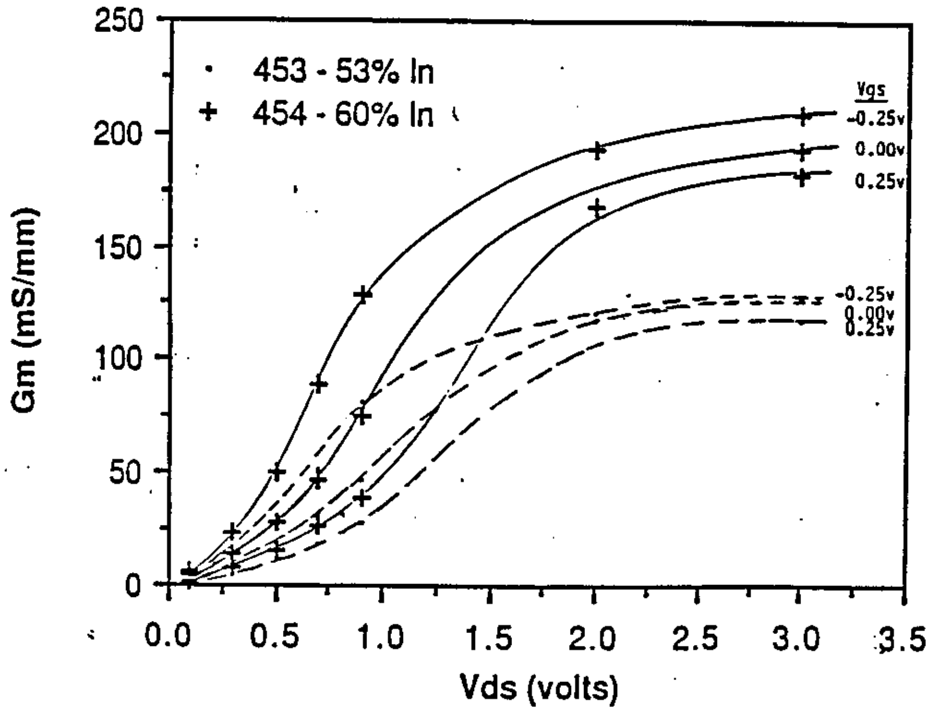

- Improved electron mobility and peak velocity by introducing strain

Channel Conductance versus V_{ds} at V_{gs}=0.5 V for
Lattice-Matched (53% In) and Strained (60% In) MODFETS

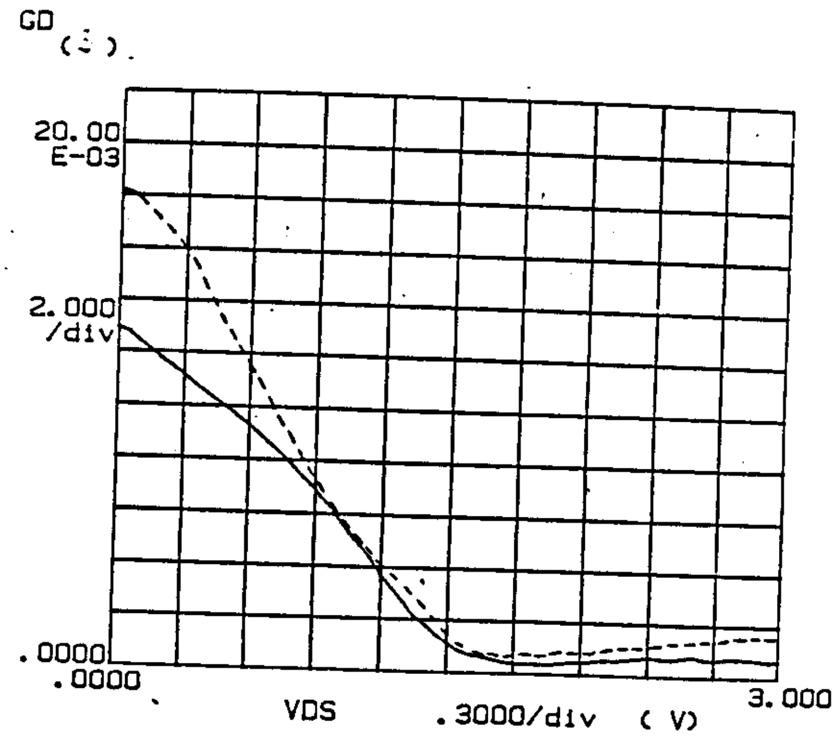

- Higher channel conductance at low-field
  BUT
- No large variations at high fields (Ec - band diagram)

CONCLUSIONS

1. The effect of strain on InAlAs/InGaAs MODFET characteristics is analyzed using 7% and 12% excess indium.

2. By increasing the indium composition, one obtains:

   (a) A marginal increase of sheet density.

   (b) A small reduction of effective mass and much better carrier confinement ==> mobility enhancement.

   (c) A small influence of spacer thickness on 2-DEG sheet density as compared to AlGaAs/GaAs system due to the higher conduction band discontinuity.

   (d) A need to compromise strained channel thickness for increase mobility (wider channel) and large output reistance or transconductance (thinner channel).

3. For of 1.5 µm gate length at 300K, intrinsic transconductance improvement is: 40% (321 mS/mm) for 60% In
   47% (359 mS/mm) for 65% In

4. Cut-off frequency improvement is primarily due to transconductance enhancement ;
   Output resistance is not substantially influenced by strain.

5. First characterizatiions showed that strained InAlAs/InGaAs MODFETs are good candidates for high-speed and high-frequency applications.

PHOTODETECTORS

Requirements

- High quantum efficiency
- Low dark current
- Low capacitance
- Low noise

Bandwidth and Gain are fundamental physical tradeoffs.

Bit Rate of application can determine which photodetector is the best choice.

CONTENTS

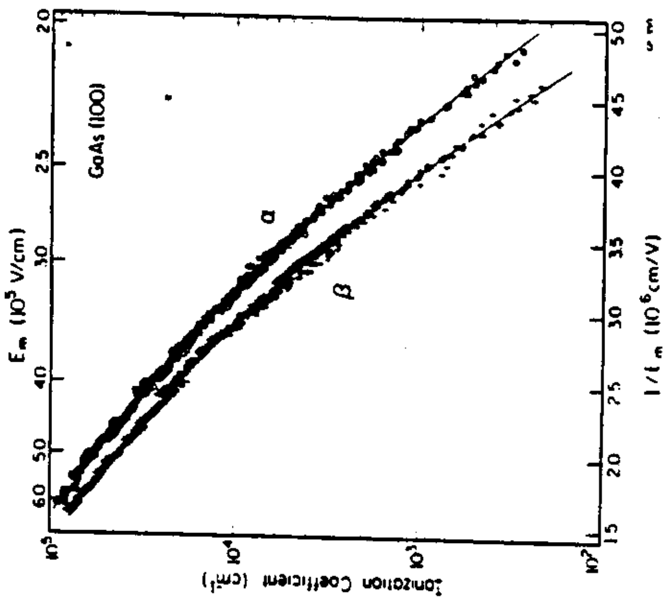

Problem: $\alpha/\beta \simeq 1$

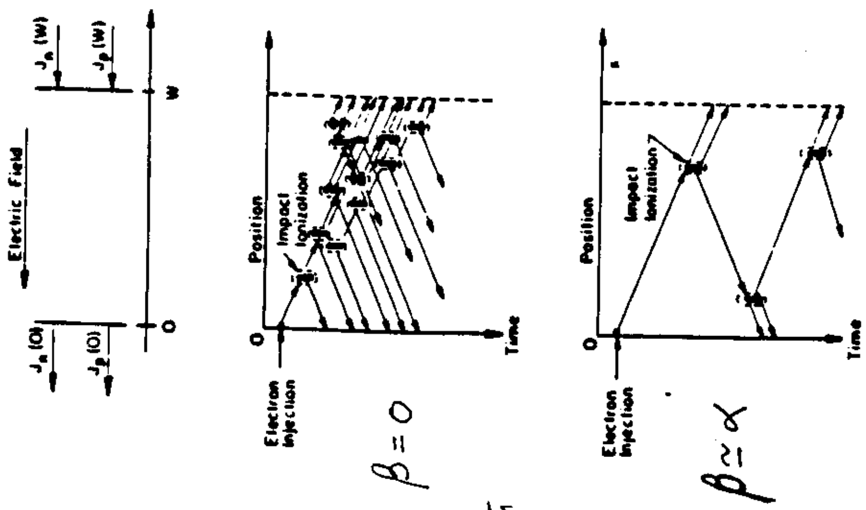

TYPES OF AVALANCHING MATERIALS

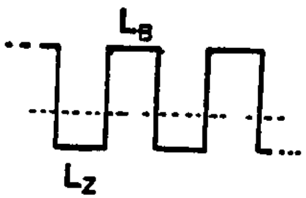

	L_B(Å)	L_Z(Å)
i)	56	34
ii)	154	33
iii)	145	87
iv)	145	174
v)	570	424

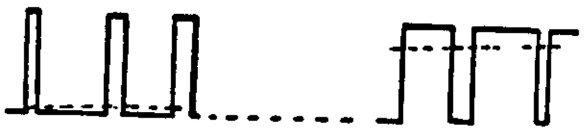

vi) GRADED BANDGAP

L_B = 10 Å - 110 Å

L_Z = 110 Å - 10 Å

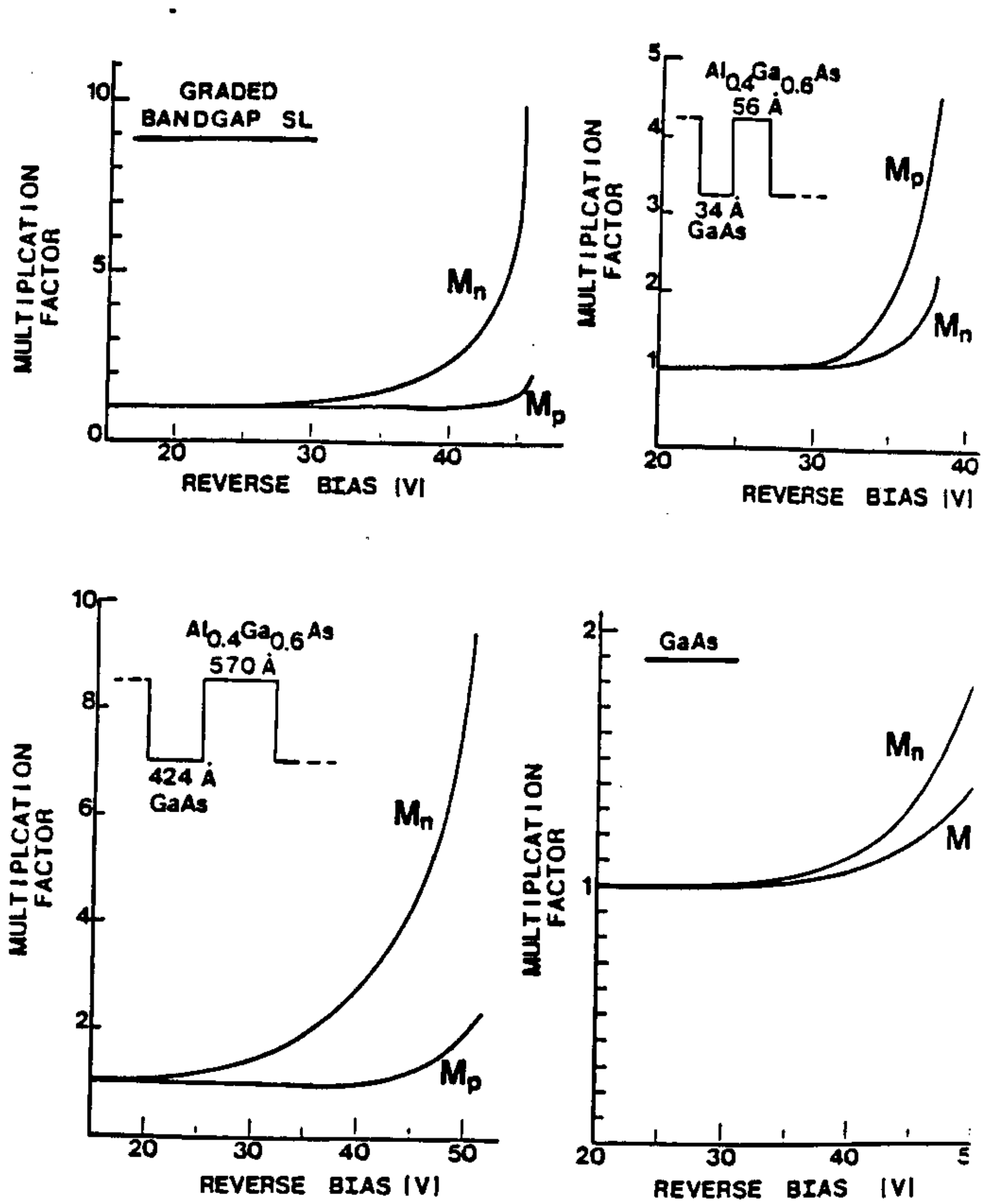

ENHANCEMENT OF α/β IN MQW AND SUPERLATTICES

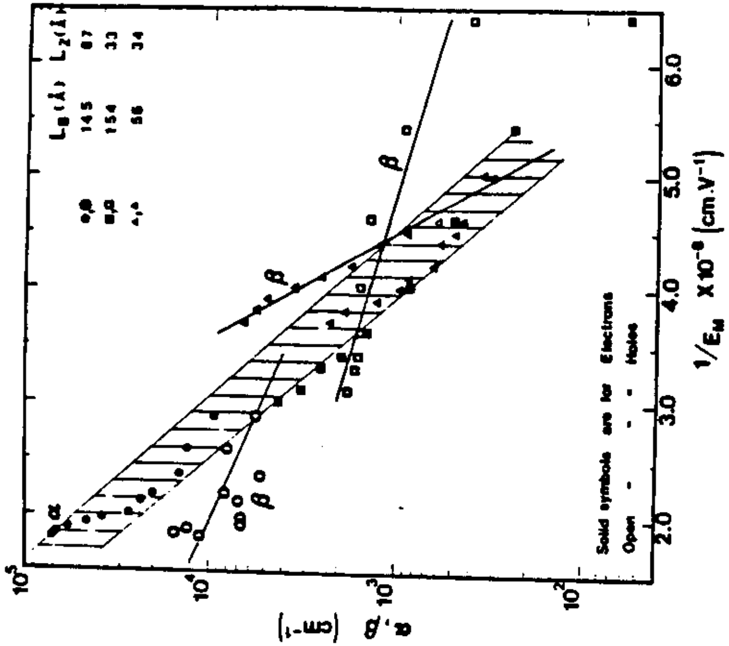

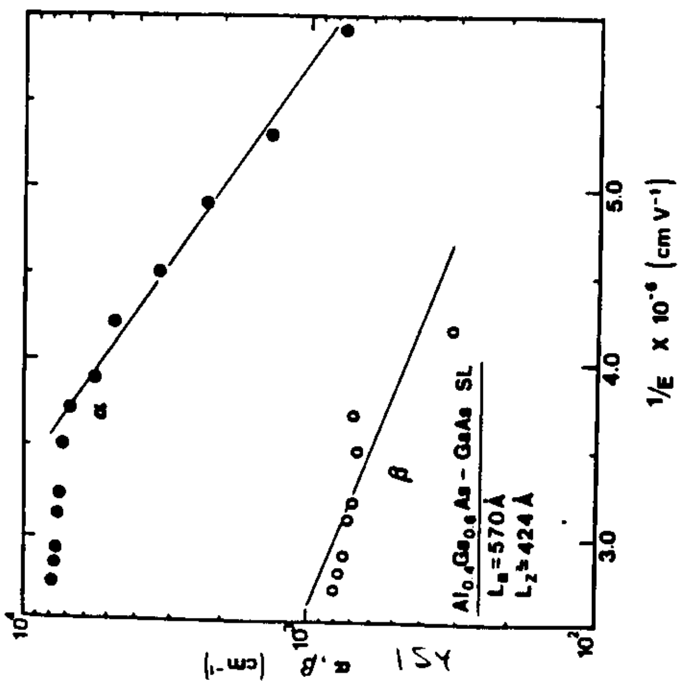

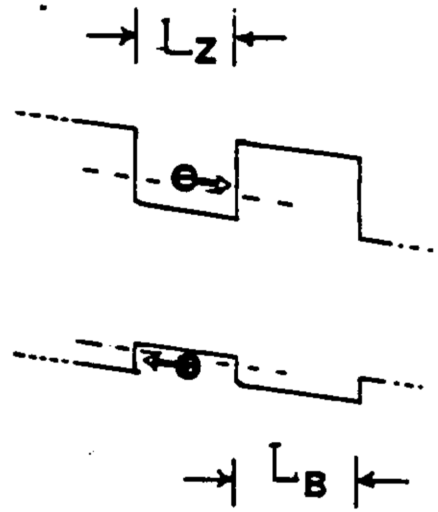

1) Increasing well size increases carrier confinement an scattering, predominantly for holes. Thereby β change

2) In graded bandgap APD, decrease of β may be due to:

   (i) Quasi-field opposing holes.

   (ii) Large wells in the GaAs side coupled with small barriers.

3) For very large wells and barriers, β is similar to that in GaAs, α is greatly enhanced.

Key Results from Monte Carlo Simulations:

- High (low) values of $\Delta E_c / \Delta E_v$ can produce high (low) α/β ratio.

- Dispersive barrier can significantly alter the impact ionization rates.

- High α/β (or β/α) ratio can be produced by choosing barriers which are selectively dissipative for holes (or electrons).

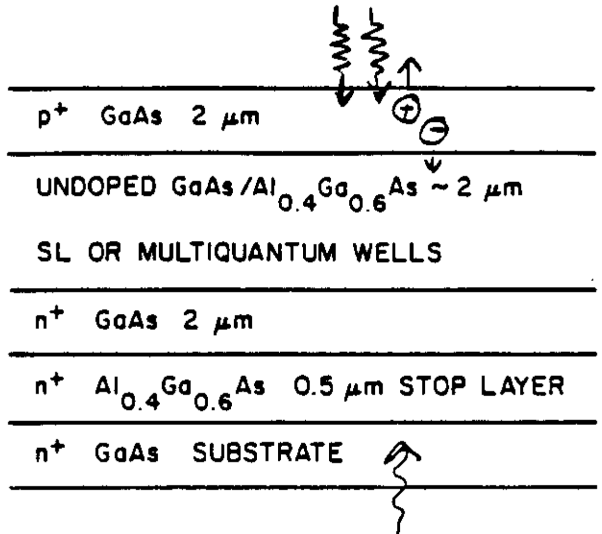

(a)

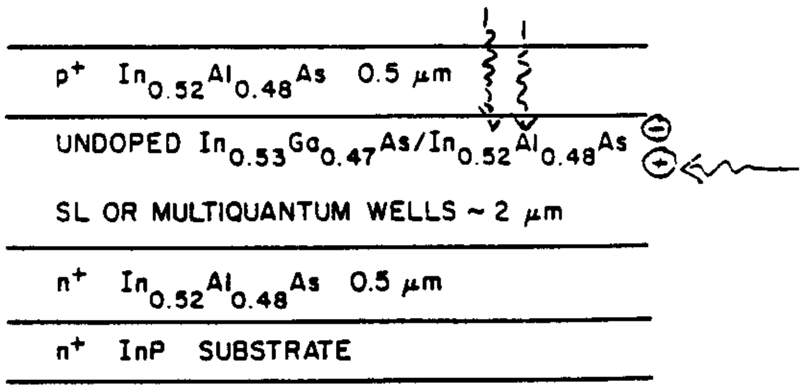

(b)

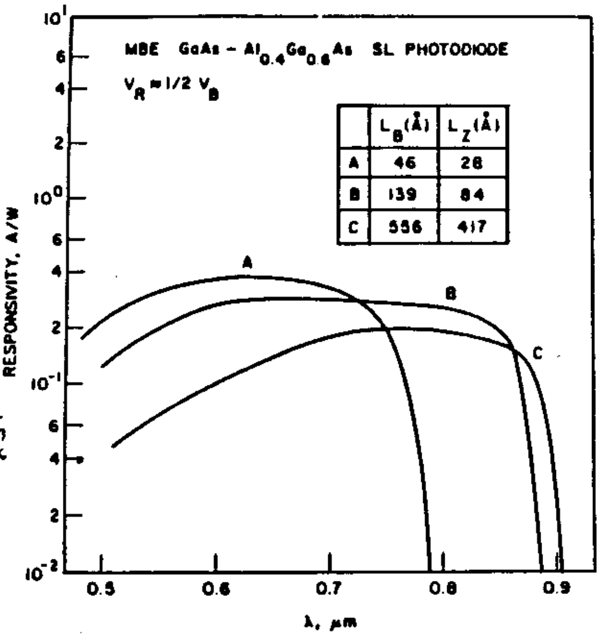

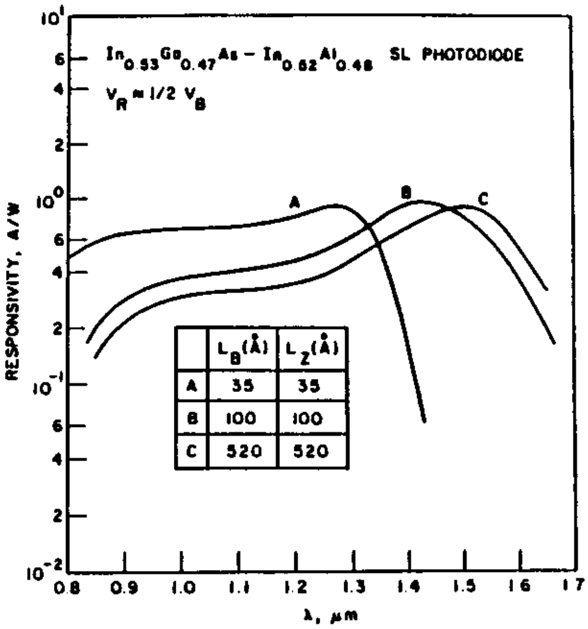

GAIN AND BANDWIDTH OF SL APD

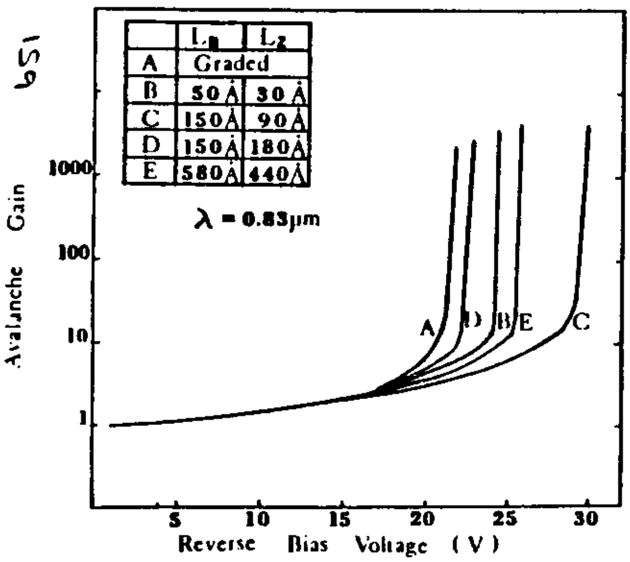

3dB roll-off ~ 12 GHz.

CONTENTS

Cation	Anion
Impingement from vapor	Impingement
⇓	⇓
Chemisorption	Physisorption
⇓	⇓
Surface evaporation	Surface migration/evaporation
⇓	⇓
Surface migration	Dissociative chemisorption
(in-plane; inter-plane)	⇓
⇓	Surface migration/evaporation
Incorporation	⇓
	Incorporation

Table 1: Conceptual Picture of MBE Growth

3

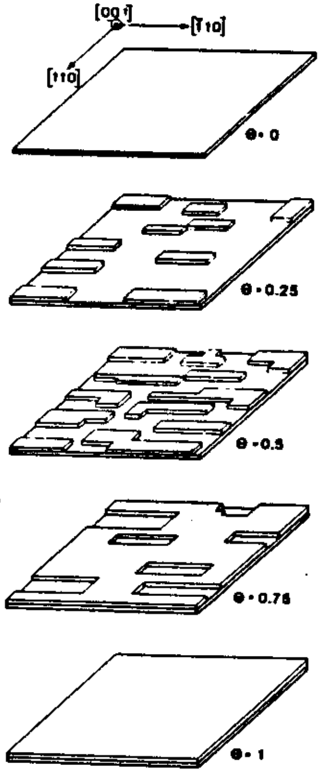
θ = 0
θ = 0.25
θ = 0.5
θ = 0.75
θ = 1

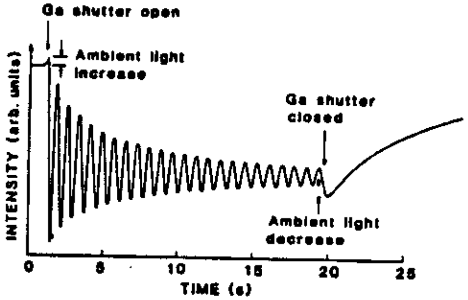
Ga shutter open
Ambient light increase
Ga shutter closed
Ambient light decrease
INTENSITY (arb. units)
TIME (s)
0
5
10
15
20
25

162

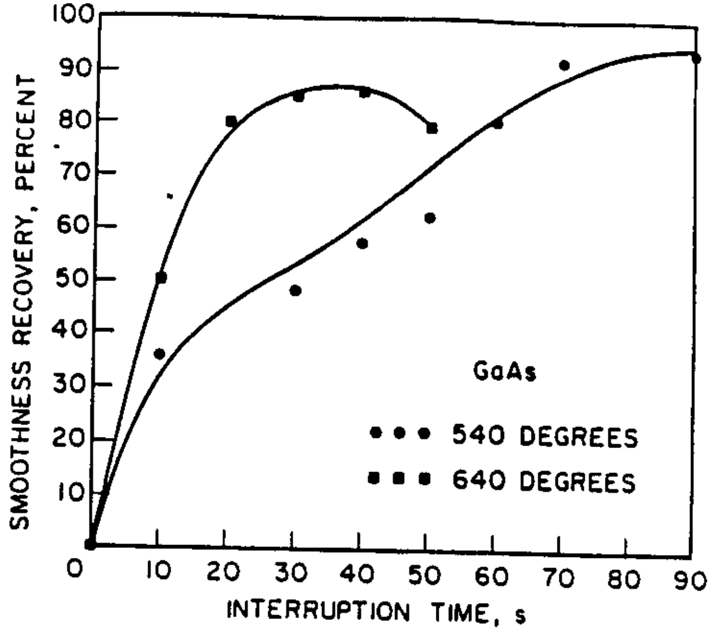
SMOOTHNESS RECOVERY, PERCENT
INTERRUPTION TIME, s
GaAs
540 DEGREES
640 DEGREES
0
10
20
30
40
50
60
70
80
90
100

(a)

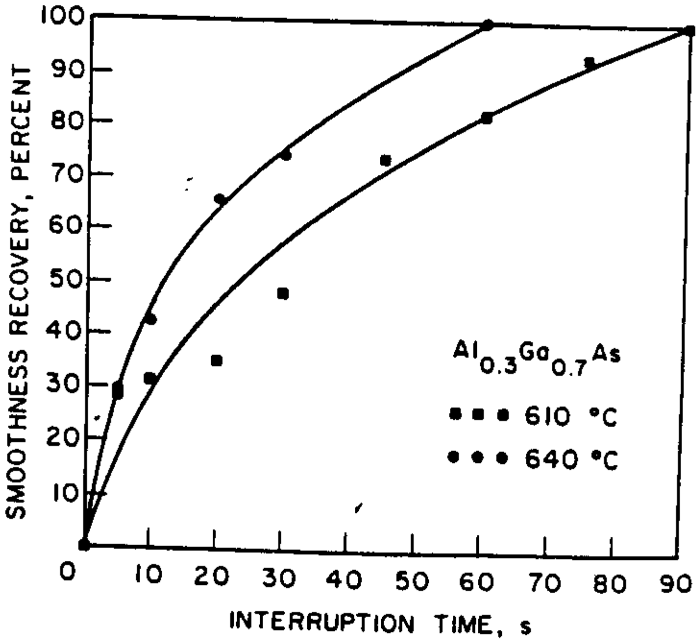
SMOOTHNESS RECOVERY, PERCENT
INTERRUPTION TIME, s
Al0.3Ga0.7As
610 °C
640 °C
0
10
20
30
40
50
60
70
80
90
100

163

(b)

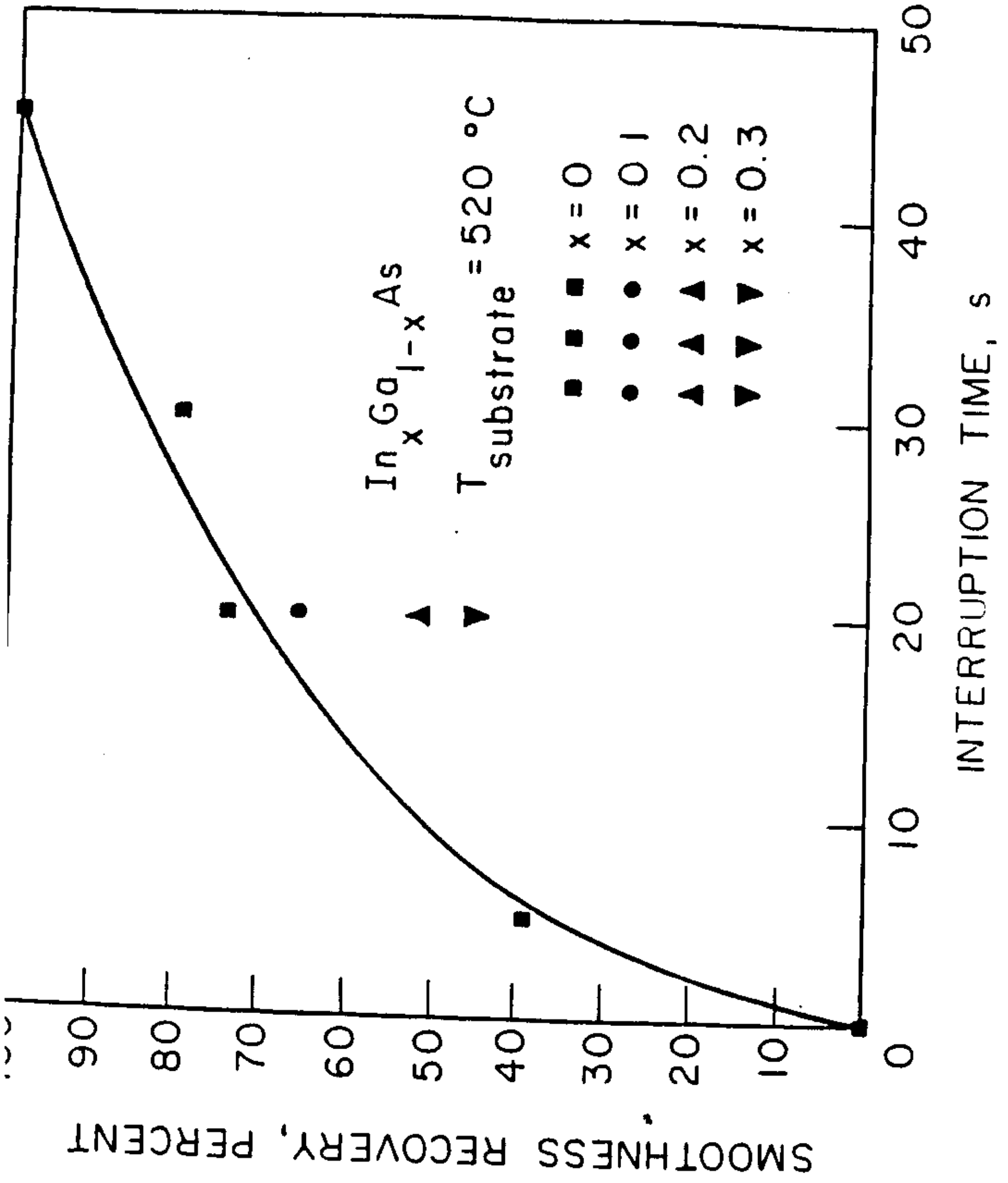

I. **OPTOELECTRONIC DEVICE REQUIREMENTS**

A. NARROW LINEWIDTH

B. HIGH INTENSITY

II. **MBE GROWTH**

A. GOOD OPTICAL AND ELECTRICAL MATERIAL QUALITY

B. ATOMICALLY SMOOTH AND ABRUPT INTERFACE

ACTIVE LAYER THICKNESS REQUIRED TO OBTAIN DESIRED MODULATION

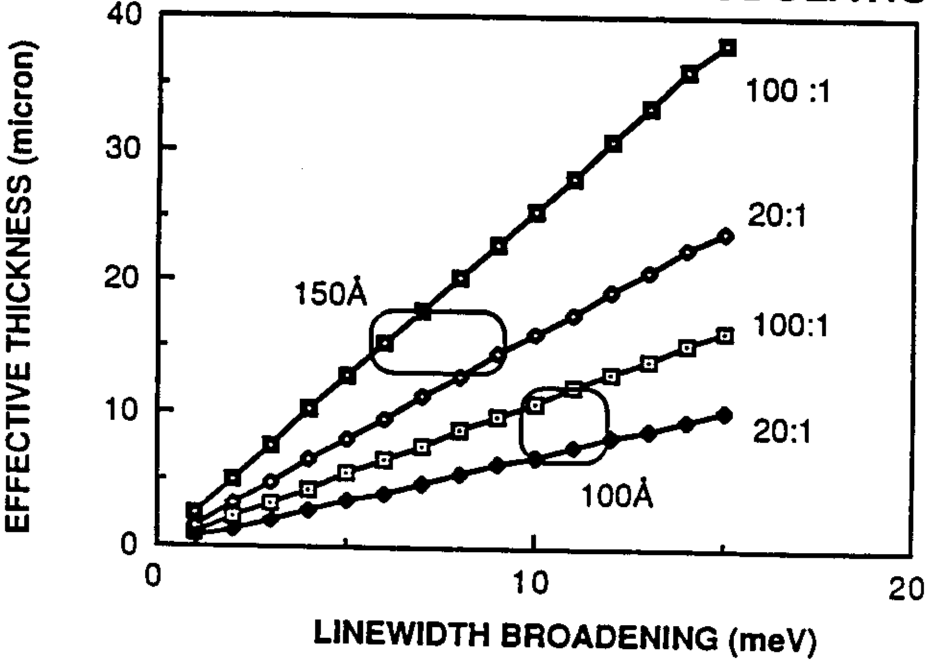

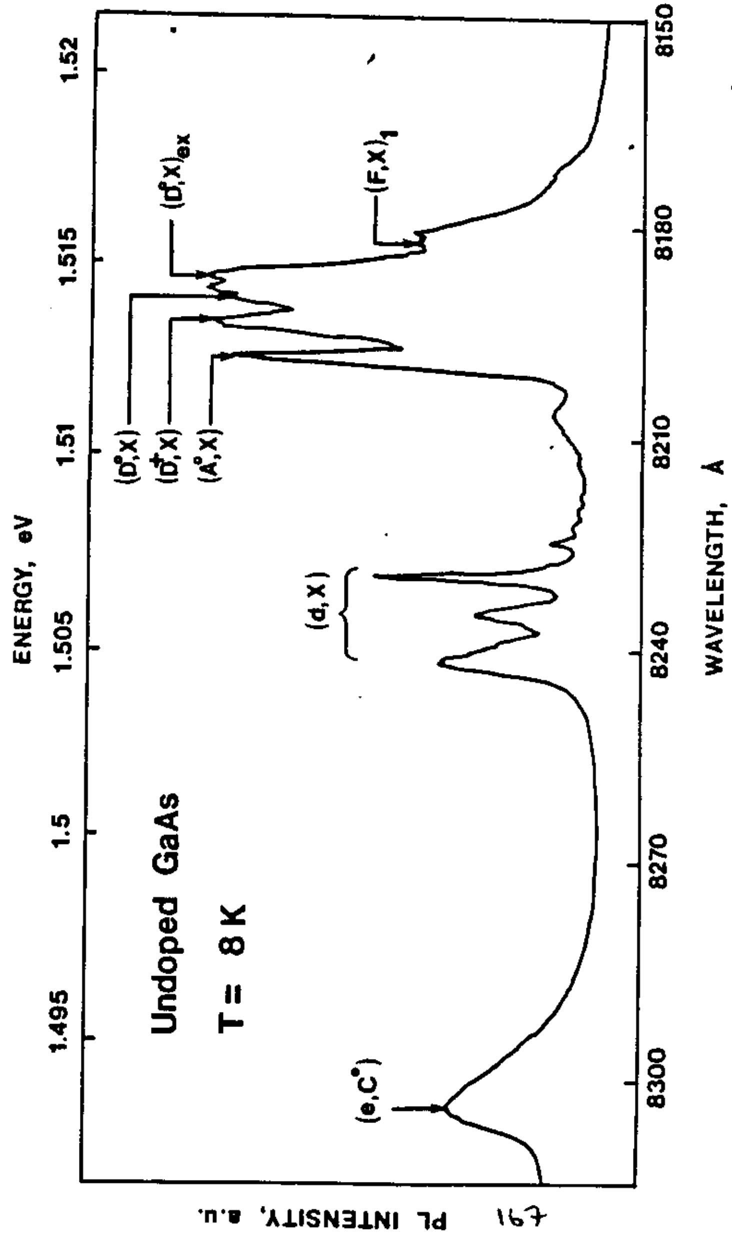

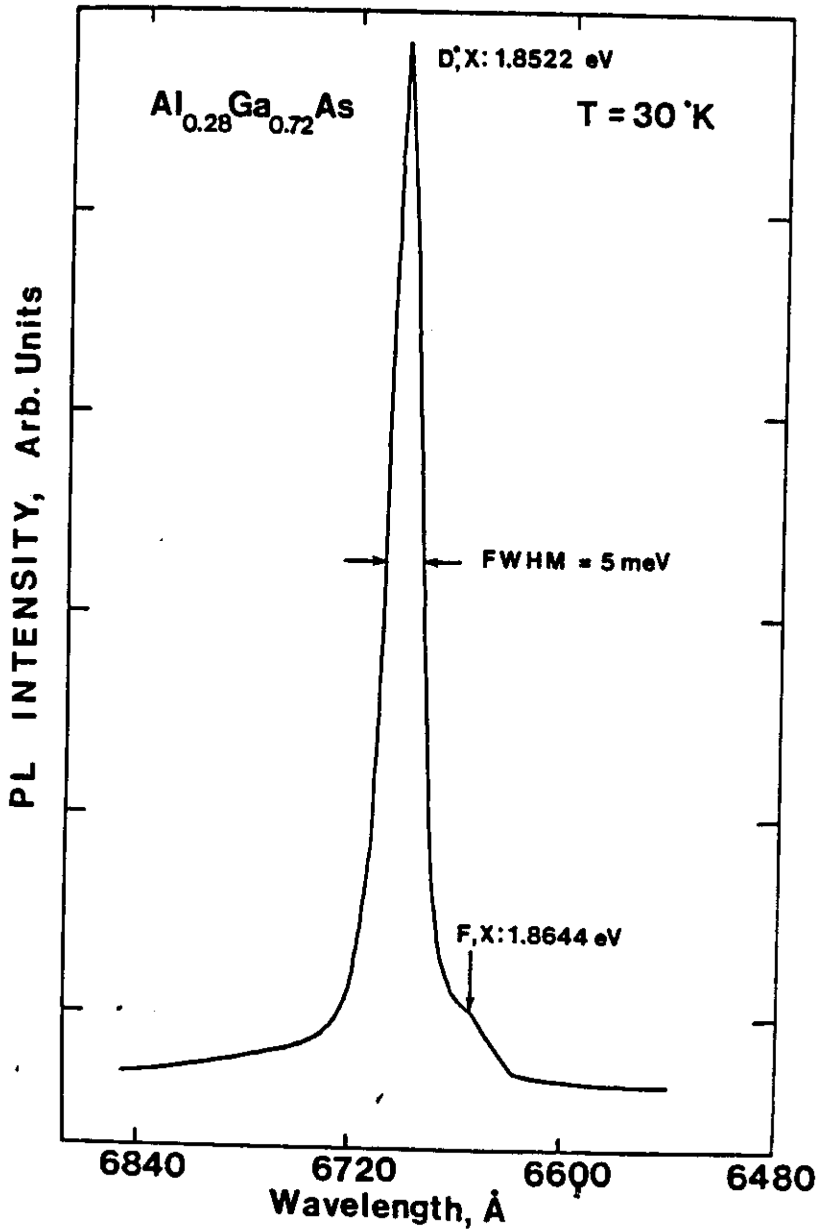

APPLICATIONS AND MOTIVATIONS FOR STUDYING THE InGaAs / InAlAs SYSTEM

TECHNOLOGICAL ISSUES

- High speed devices
- Tuned lasers for special applications
- Optical modulators → higher control due to greater confinement

PHYSICAL ISSUES

- Structural issues for interface formation
- Alloy clustering in far-from-equilibrium growth - generic information of fabrication of high quality immiscible systems
- Studies of strained structures - start with lattice-matched and move away on either side
- An important system to test theories of quasi-2D systems
- Impurity incorporation-doping

KINETICS OF GaAs, InAs AND AlAs GROWING SURFACE

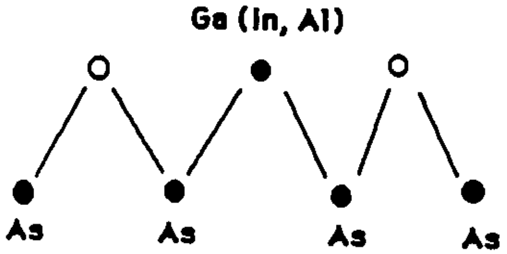

HOPPING RATE OF CATION (Ga, In, Al)

$$R = R_0 \exp[-(E^i - E^0/2)/K_BT] \quad (S^{-1})$$

E^i : ACTIVATION BARRIER (i=0,1,2,3)

	i	0	1	2	3
<u>InAlAs</u> T =480°C (K_BT=65meV)	In	4.5E3	457	45	4.5
	Al	7.5	0.3	0.01	0.005
<u>AlGaAs</u> T =650°C (K_BT=80meV)	Ga	3.3E4	1.0E4	4.5E3	610
	Al	312	21.7	1.[illegible]1	0.1

- <u>InAlAs</u> GROWTH FRONT IS EXPECTED TO BE ROUGHER THAN <u>AlGaAs</u> GROWTH FRONT.
- LARGE DIFFERENCE OF <u>In</u> AND <u>Al</u> HOPPING RATES COULD CAUSE <u>ALLOY CLUSTERING</u>.

CONSEQUENCES OF ALLOY CLUSTERING IN OPTICAL AND TRANSPORT PROPERTIES

$$\sigma_0 = 2 \cdot \left(\frac{1.4\, C_A^0\, C_B^0\, r_C^3}{R_{ex}^3}\right)^{1/2} \cdot (0.327)\, \Delta_1$$

$$\mu_0^{alloy} = \frac{32\sqrt{2}\, e\, \hbar^4}{9\,\pi^{3/2}\,(m^*)^{5/2}\, V_a\, C_A^0\, C_B^0\, \Delta E^2\, (kT)^{1/2}}$$

C_A^0, C_B^0: mean compositions of InAs & AlAs

Without clustering (Random alloy)

$$C_A^0 = 0.52, \quad C_B^0 = 0.48, \quad R_{ex} \approx 200\text{Å}$$

$$r_C = r_0 = 2.5\text{Å}$$

With clustering

$$r_C \longrightarrow n_C\, r_0 = 2.5\, n_C$$

$$\Delta_1 \longrightarrow \Delta_1\, |C_A^1 - C_A^2| = \Delta_1\, |C_B^1 - C_B^2|$$

$$\sigma = \sigma_0\, n_C^{3/2}\, |C_A^1 - C_A^2|$$

$$\mu = \mu_0^{alloy} \cdot \frac{1}{n_C^3\, |C_A^1 - C_A^2|^2}$$

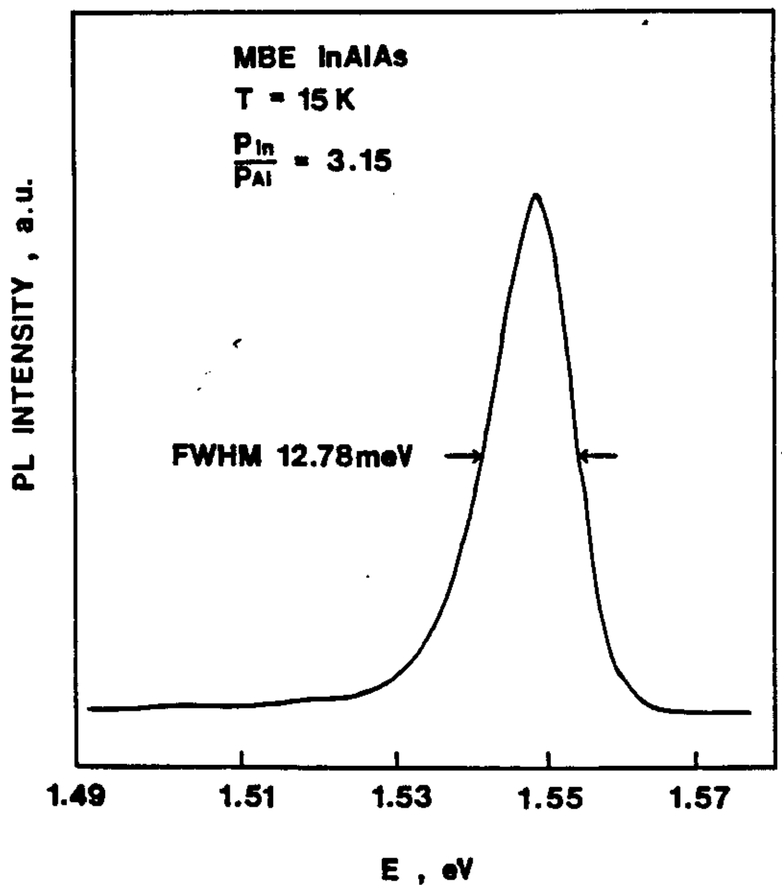
MBE InAlAs
T = 15 K
P In / P Al = 3.15
FWHM 12.78meV
PL INTENSITY , a.u.
1.49
1.51
1.53
1.55
1.57
E , eV

172

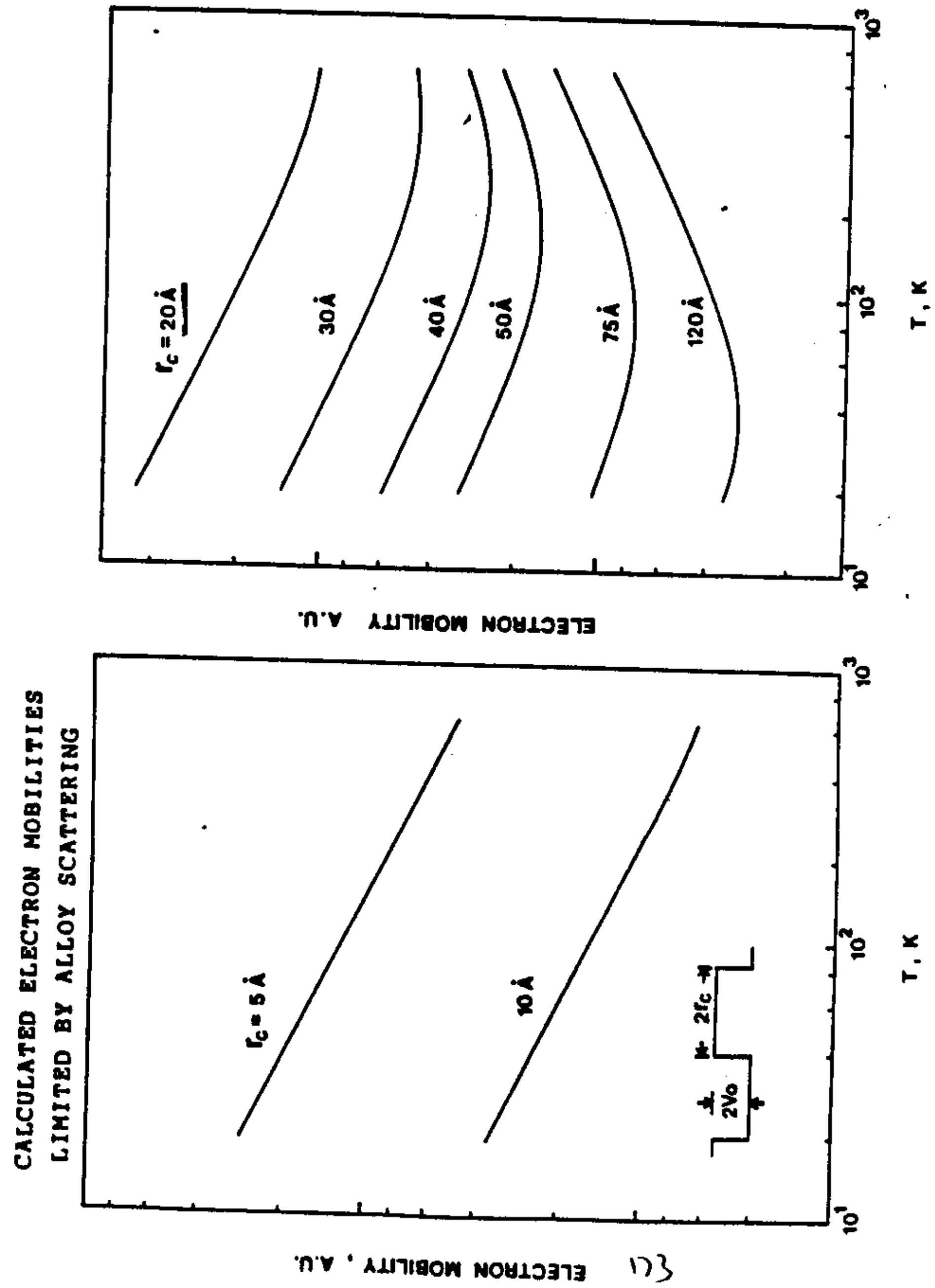
CALCULATED ELECTRON MOBILITIES
LIMITED BY ALLOY SCATTERING
ELECTRON MOBILITY A.U.
ELECTRON MOBILITY , A.U.
T , K
rc = 20 Å
30 Å
40 Å
50 Å
75 Å
120 Å
rc = 5 Å
10 Å
2Vo
2rc

173

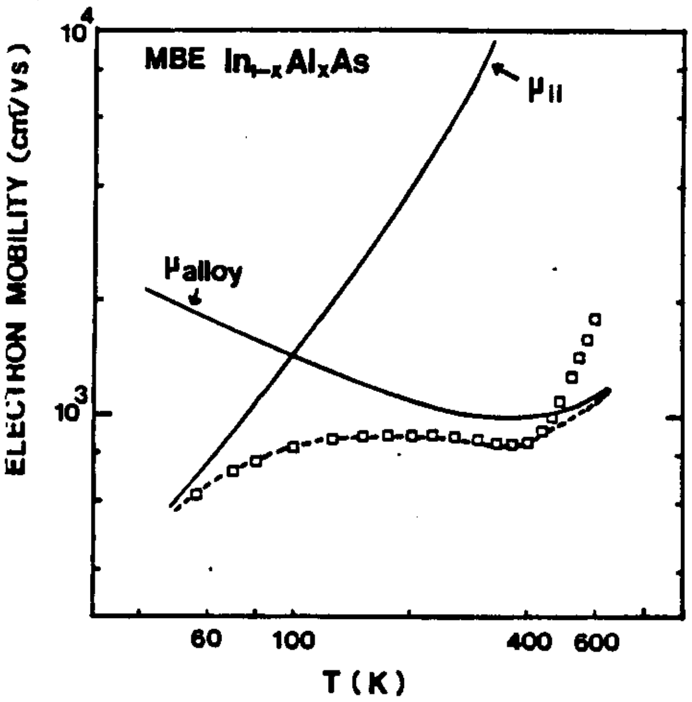

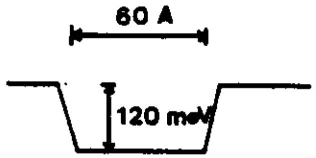

- Sharp rise in mobility beyond 450 K
- Sharp rise in carrier density beyond 480 K
  (Probably because of a deep donor)

Mobility fit with 33 Å clusters of composition x=0.46 and x=0.50 agrees well with data from 60 K to 400 K.

We expect that the screening effects due to increase in n_H beyond 480 K will lead to a better fit at higher temperatures

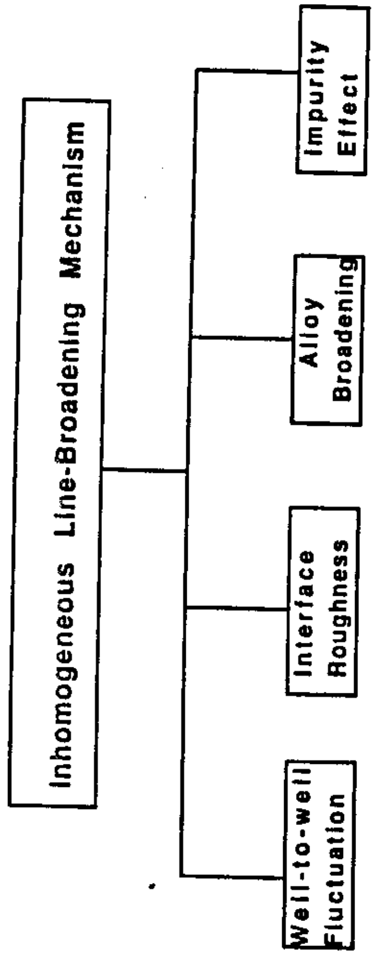

$$E = E_g + E_e + E_h - E_{exc} - E_b$$

A. Well-to-Well Fluctuation

$$E = \frac{\hbar^2\pi^2}{m^* L_z^2}$$

$$\Delta E = \frac{\hbar^2\pi^2}{2m^* L_z^3}\Delta L_z$$

ΔL_z is dependent on

(1) the growth rate fluctuation

(2) the shutter opening/closing time

If $L_z = R{\cdot}t$

$$\Delta L_z = \Delta R \cdot t + \Delta t \cdot R$$

Assume that $\Delta t \simeq 0$

$$\Delta E = \frac{\hbar^2\pi^2}{2m^* L_z^2}\frac{\Delta R}{R}$$

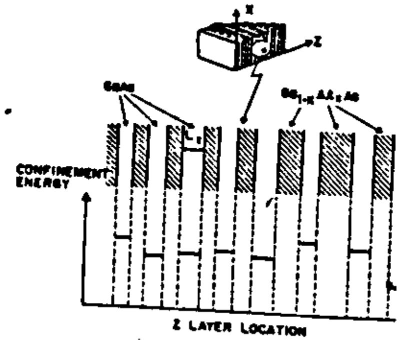

B. Interface Roughness

(1) $\delta_2 < d_{exc}$

ref.: Singh, et al., *Appl. Phys. Lett.*, **44**(8), 805(1984)

(2) $\delta_2 \simeq d_{exc}$

ref.: Bastard, et al., *Phys. Rev. B*, **29**(12),7042(1984)

(3) $\delta_2 \gg d_{exc}$

Splitted Excitonic emission peaks (fine structure)

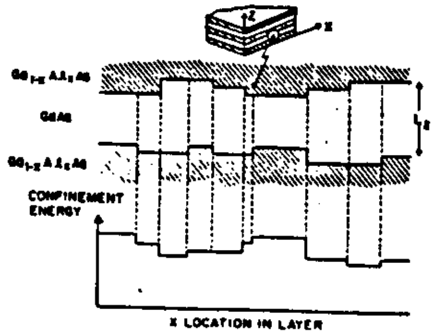

18

THEORETICAL PL HWHM DUE TO INTERFACE ROUGHNESS AS A FUNCTION OF WELL SIZE

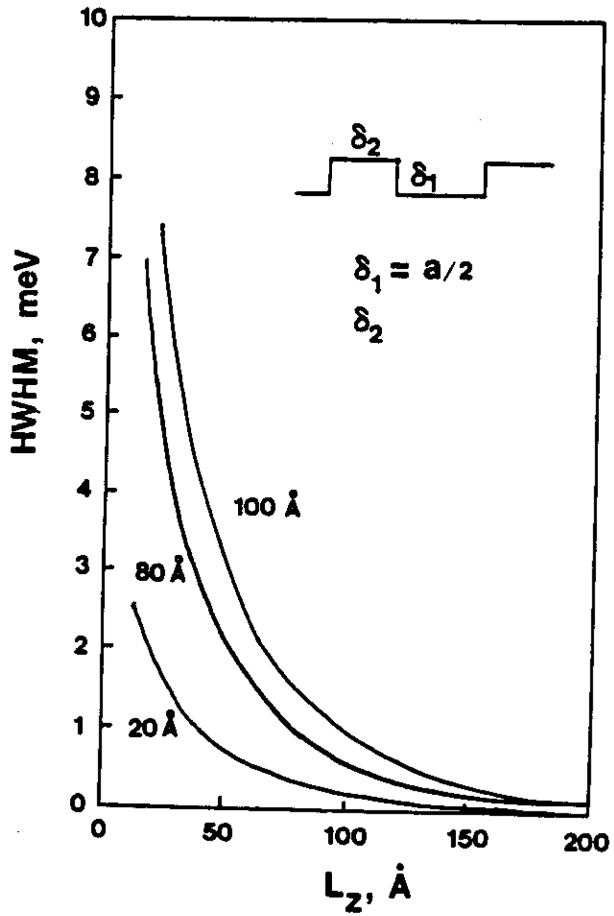

177

19

$GaAs/Al_{0.3}Ga_{0.7}As$ MQW

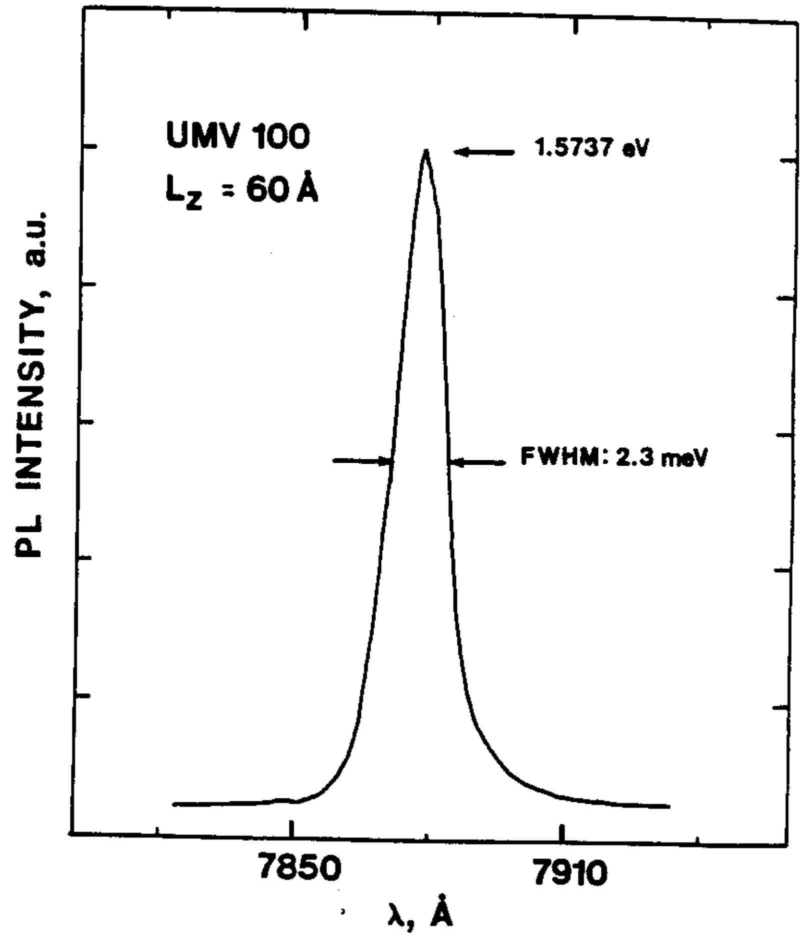

179

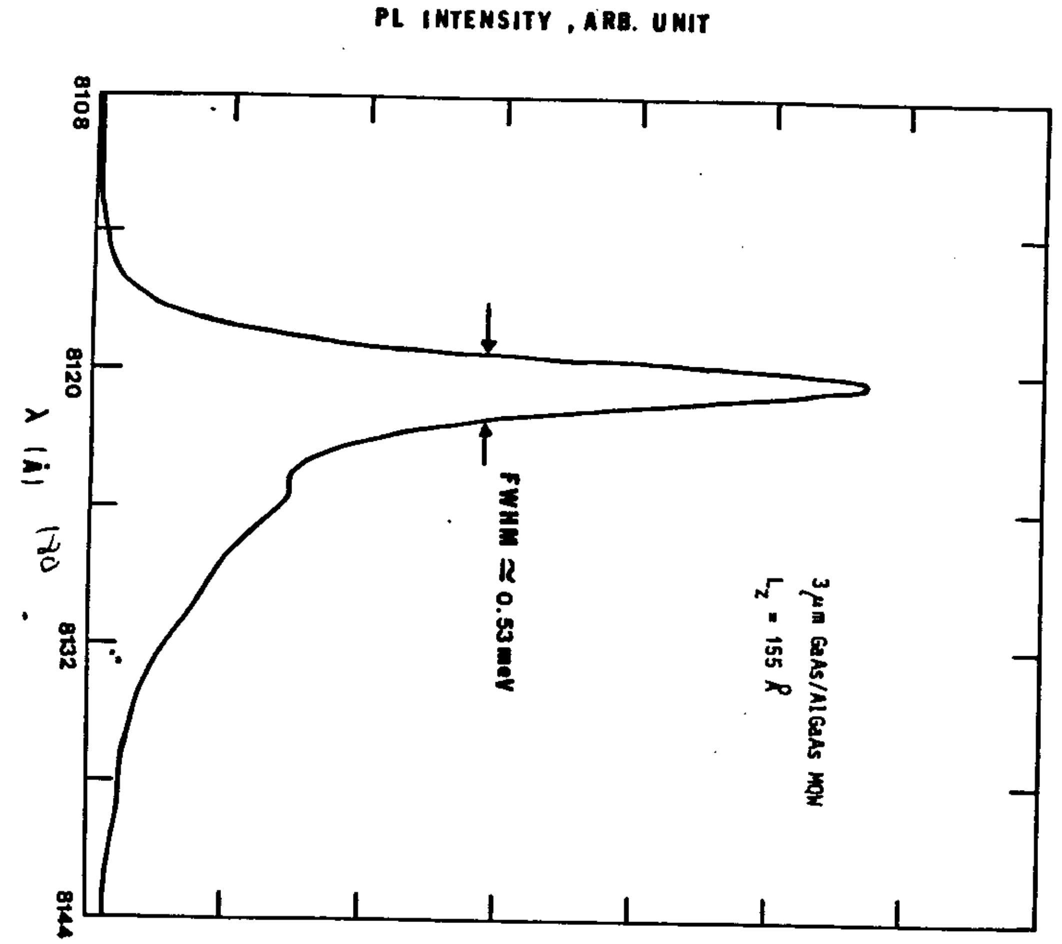

$Al_{0.4}Ga_{0.6}As/AlAs$ MQW's

1) Possible Maximum Oscillator Strength
2) Visible Light Range

Problem

Alloy Broadening

Solution

Use a novel growth technique
==> Monolayer Superlattice (ML-SL)

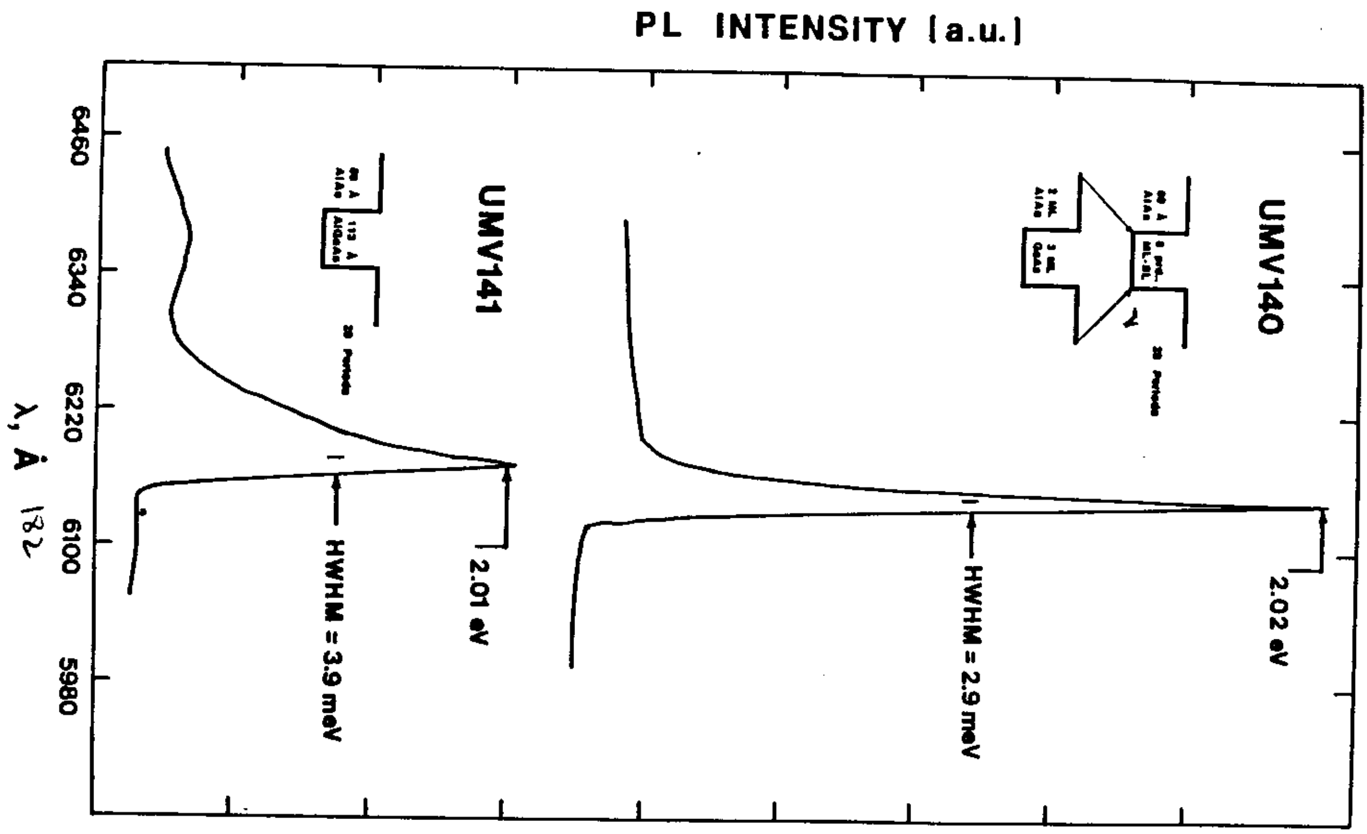

<u>SUMMARY</u>

1. Present-day Opto-Electronic Device place stringent requirements on materials and heterostructure quality; extremely high-quality MBE and novel growth approaches are necessary.

2. Optimized Growth Conditions for MQW's

   Low Background Species
   Low Growth Rates
   Low V/III Ratio
   Optimized Growth Interruption Time